Università degli studi di Genova
Dipartimento di Informatica, Bioingegneria,
Robotica ed Ingegneria dei Sistemi

Optimization of Electric-Vehicle Charging: scheduling and planning problems

by

Luca Parodi

Thesis Series **DIBRIS-TH-2023-**

DIBRIS, Università di Genova

Via Opera Pia, 13 16145 Genova Italy http://www.dibris.unige.it/

Università degli studi di Genova

Dipartimento di Informatica, Bioingegneria,
Robotica ed Ingegneria dei Sistemi

Ph.D. Thesis in Computer Science and Systems Engineering
Systems Engineering Curriculum

Optimization of Electric-Vehicle Charging: scheduling and planning problems

by

Luca Parodi

May, 2023

Dottorato di Ricerca in Informatica ed Ingegneria dei Sistemi
Indirizzo Informatica
Dipartimento di Informatica, Bioingegneria, Robotica ed Ingegneria dei Sistemi
Università degli Studi di Genova

DIBRIS, Università Degli Studi di Genova
Via Opera Pia, 13
I-16145 Genova, Italy
http://www.dibris.unige.it/

PhD Thesis in Computer Science and Systems Engineering
Systems Engineering Curriculum
(S.S.D. ING INF/04)

Submitted by Luca Parodi DIBRIS, Univ. di Genova

Date of submission: 07/05/2023

Title: Optimization of Electric-Vehicle Charging: scheduling and planning problems

Advisor: Prof. Michela Robba
Dipartimento di Informatica, Bioingegneria, Robotica ed Ingegneria dei Sistemi (DIBRIS)
Università di Genova

Advisor: Prof. Riccardo Minciardi.
Dipartimento di Informatica, Bioingegneria, Robotica ed Ingegneria dei Sistemi (DIBRIS)
Università di Genova

External Reviewers:

Prof. Enrique Personal Vazquez, University of Sevilla; epersonal@us.es;

Prof. Raffaele Carli, Polytechnic of Bari; raffaele.carli@poliba.it;

Acknowledgements

I want to thank all the people who have been close to me over the years. Starting of course with my family, thank you for being there and supporting me in all my decisions and difficulties.

I also thank my speakers for all the time they have given me and for the myriad of things they have allowed me to learn during this journey.

Sincere thanks also to my colleagues for being friends first, and then for helping me many moments.

Abstract

The progressive shift from traditional vehicles to Electric Vehicles (EVs) is considered one of the key measures to achieve the objective of a significant reduction in the emission of pollutants, especially in urban areas. EVs will be widely used in a not-so-futuristic vision, and new technologies will be present for charging stations, batteries, and vehicles. The number of EVs and Charging Stations (CSs) is increased in the last years, but, unfortunately, wide usage of EVs may cause technical problems to the electrical grid (i.e., instability due to intermittent distributed loads), inefficiencies in the charging process (i.e., lower power capacity and longer recharging times), long queues and bad use of CSs. Moreover, it is necessary to plan the CSs installation over the territory, the schedule of vehicles, and the optimal use of CSs.

This thesis focuses on applying optimization methods and approaches to energy systems in which EVs are present, with specific reference to planning and scheduling decision problems.

In particular, in smart grids, energy production, and storage systems are usually scheduled by an Energy Management System (EMS) to minimize costs, power losses, and CO2 emissions while satisfying energy demands. When CSs are connected to a smart grid, EVs served by CSs represent an additional load to the power system to be satisfied, and an additional storage system in the case of vehicle-to-grid (V2G) technology is enabled. However, the load generated by EVs is deferrable. It can be thought of as a process in which machines (CSs) serve customers/products (EVs) based on release time, due date, deadline, and energy request, as happens in manufacturing systems.

In this thesis, first, attention is focused on defining a discrete-time optimization problem in which fossil fuel production plants, storage systems, and renewables are considered to satisfy the grid's electrical load. The discrete-time formalization can use forecasting for renewables and loads without data elaboration. On the other side, many decision variables are present, making the optimization problem hard to solve through commercial optimization tools. For this reason, an alternative method for the optimal schedule of EVs characterized by a discrete event formalization is presented. This new approach can diminish the number of variables by considering the time intervals as variables themselves. Of course, the solution's optimality is not guaranteed since some assumptions are necessary.

Moreover, the last chapter proposes a novel approach for the optimal location and line assignment for electric bus charging stations. In particular, the model provides the siting and sizing of some CSs to maintain a minimum service frequency over public transportation lines.

Table of Contents

Acronyms

DSM	Demand Side Management
EB	Electric Buses
EC	Energy Community
EMS	Energy Management System
EV	Electric Vehicle
EVA	Electric Vehicles Aggregators
G2V	Grid-to-Vehicle
H2V	Home-to-Vehicle
HVAC	Heating, Ventilation, and Air Conditioning
P2P	Peer-to-Peer
SC	Smart Charging
SOC	State-Of-Charge
SOH	State-Of-Health
TSO	Transmission System Operator
V2B	Vehicle-to-Building
V2G	Vehicle-to-Grid
V2H	Vehicle-to-Home
V2X	Vehicle-to-Everything

Chapter 1
Introduction and Motivation

Sustainability is one of the most widespread words in recent years. It can be considered in different frameworks as economic, social, or environmental one. Deepening the latter one, it is necessary to focus on pollution. Among the numerous sources of pollution, transportation represents a considerable contribution. Through an improvement in this field, it is possible to affect global pollution positively. One of the most promising technologies is Electric Vehicles (EVs) for private and public (usually Electric Buses, EBs) transportation. According to many studies, they both are able to reduce the emissions, especially when integrated with renewable plants, typically photovoltaic (PV) ones.

The introduction of these kind of vehicles, carries many drawbacks to be faced. In particular,the main issues for the transition to EVs from traditional ones are, on the users' side, the high purchasing costs and the duration of the charging process; on the grid side, the impact of such large loads on the present infrastructure.

The first issues can be addressed with researches on new technologies for the batteries, which is nowadays the most expensive component of the EVs. Instead, the increase of the maximum charging power can reduce by far the duration of the charging process. This last consideration is strictly linked with the issues relevant to the power grid. In fact, the EVs' charging process can represent a significant load that, especially increasing the number of EVs, can lead to malfunctions of the power network. To address this issue, it is necessary to focus on the charging process, and to find new approaches well suited to real applications to define the optimal schedule under specific constraints as well as the optimal planning of the CSs

In this thesis, both these aspects related to EVs will be considered; in particular, two approaches based on a discrete time model and a discrete events one will be presented for the charging scheduling..

1.1 Main Contributions

The main contribution of this Ph.D. thesis can be summarized as:

- Development of a discrete event optimization model for the optimal scheduling of some EVs in a smart grid.
- Development of a multistep approach for determining the actual power flows as continuous functions starting from the discrete event model.
- Comparison between the two proposed approaches in order to highlight the advantages and disadvantages of both the models.
- Development of a new model for the optimal location and line assignment for electric bus charging stations.

1.2 Thesis organization

This thesis is the collection of several research works. The chapters are based on lecture notes, journal or conference papers, and book chapters, which are either published or currently under review that is reported at the beginning of each Chapter. This thesis consists of six Chapters, namely:

- Chapter 2 presents the introduction about the EVs framework focusing on their main characteristics and highlighting the possible application that would benefit from the introduction of the EVs as well as the many issues linked to this new actor in the modern grid architecture.
- Chapter 3 is mainly voted to the analysis of the state of the art regarding the EVs modeling, in particular the focus is on the batteries and the charging process in the smart grids framework.
- Chapter 4 consists of a discrete time model for the optimal scheduling of the charging processes in a smart grid.
- Chapter 5 presents the discrete event optimization model for the optimal charging of EVs in a smart grid. In particular, the new approach is described and a focus on the piecewise linear characteristic of the battery is presented. This chapter also includes two extensions of the model to the multi-socket case and the periodic one.
- Chapter 6 presents the optimal location and line assignment for electric bus charging stations.
- Chapter 7 includes the conclusions and some proposals for future developments.

1.3 List of Publication and editorial activity

The publications, special sessions organization, and open invited track list of Luca Parodi is hereafter reported. My indexes are

- H index Scopus 4, 38 citations
- H index Scholar 4, 50 citations

1.3.1 Journal Papers-Published

- G. Ferro, R. Minciardi, L. Parodi, M. Robba, and M. Rossi, "Optimal Control of Multiple Microgrids and Buildings by an Aggregator," *Energies*, vol. 13, no. 5, p. 1058, Feb. 2020.
- G. Ferro, R. Minciardi, L. Parodi, and M. Robba, "Discrete event optimization of a vehicle charging station with multiple sockets," *Discrete Event Dynamic Systems*, vol. 31, no. 2, pp. 219–249, 2021.
- V. Casella, D. Fernandez Valderrama, G. Ferro, R. Minciardi, M. Paolucci, L. Parodi, and M. Robba, "Towards the Integration of Sustainable Transportation and Smart Grids: A Review on Electric Vehicles' Management," *Energies*, vol. 15, no. 11, p. 4020, 2022.
- G. Ferro, R. Minciardi, L. Parodi, and M. Robba, "Optimal Planning of Charging Stations in Coupled Transportation and Power Networks Based on User Equilibrium Conditions," *IEEE Transactions on Automation Science and Engineering*, vol. 19, no. 1, pp. 48–59, Jan. 2022.

- M. Caliano, F. Delfino, M. Di Somma, G. Ferro, G. Graditi, L. Parodi, M. Robba, and M. Rossi, “An Energy Management System for microgrids including costs, exergy, and stress indexes,” *Sustainable Energy, Grids and Networks*, p. 100915, 2022.
- G. Ferro, R. Minciardi, L. Parodi and M. Robba, "Optimal Location and Line Assignment for Electric Bus Charging Stations," *IEEE Systems Journal*, pp. 1-12, 2023.

1.3.2 Conference Papers-Published

- G. Ferro, R. Minciardi, L. Parodi, M. Robba, and M. Rossi, “Optimal coordination of buildings and microgrids by an aggregator: A bi-level approach,” *IFAC-PapersOnLine*, vol. 53, no. 2, pp. 16587–16592, 2020.
- G. Ferro, R. Minciardi, L. Parodi, M. Robba, and M. Rossi, “A multi-objective and multi-decision maker approach for the balancing market in distribution grids in presence of aggregators,” in *2020 7th International Conference on Control, Decision and Information Technologies (CoDIT)*, 2020, vol. 1, pp. 784–789.
- G. Ferro, R. Minciardi, L. Parodi, and M. Robba, “A bi-level approach for the optimal planning of charging stations and electric vehicles traffic assignment,” in *2020 7th International Conference on Control, Decision and Information Technologies (CoDIT)*, 2020, vol. 1, pp. 533–538.
- G. Bianco, S. Bracco, F. Delfino, G. Ferro, L. Parodi, M. Robba, and M. Rossi, “A Demand Response Energy Management System (DR-EMS) for sustainable district,” in *2020 7th International Conference on Control, Decision and Information Technologies (CoDIT)*, 2020, vol. 1, pp. 551–556.
- G. Ferro, R. Minciardi, L. Parodi, and M. Robba, “Optimal planning of charging stations and electric vehicles traffic assignment: a bi-level approach,” in *21st IFAC World Congress, Germany*, 2020.
- V. Casella, G. Ferro, R. Minciardi, L. Parodi, and M. Robba, “Optimal charging of electric buses: a periodic discrete event approach,” in *2021 29th Mediterranean Conference on Control and Automation (MED)*, 2021, pp. 208–213.
- F. Delfino, G. Ferro, L. Parodi, M. Robba, M. Rossi, M. Caliano, M. Di Somma, and G. Graditi, “A multi-objective Energy Management System for microgrids: minimization of costs, exergy in input, and emissions,” in *2021 International Conference on Smart Energy Systems and Technologies (SEST)*, 2021, pp. 1–6.

1.3.3 Conference Papers-Submitted

- V. Casella, G. Ferro, R. Minciardi, L. Parodi, and M. Robba, “Optimization of electric buses charging station with multiple sockets: The case of Genoa Municipality,” *IFAC WC2023*.
- D. Fernandez Valderrama, G. Ferro, L. Parodi, and M. Robba, “A multilevel optimization model for a distribution power grid with the active participation of electric vehicles via aggregators,” *CoDIT2023*.

1.3.4 Book Chapter-Published

- G. Ferro, R. Minciardi, L. Parodi, and M. Robba, “Optimal Charging Management of Microgrid-Integrated Electric Vehicles,” in *Developing Charging Infrastructure and Technologies for Electric Vehicles*, IGI Global, 2022, pp. 133–155.

1.3.5 Authored Book-Submitted

- G. Ferro, R. Minciardi, L. Parodi, and M. Robba, “Optimization of Electric-Vehicle Charging: scheduling and planning problems,” Springer.

1.3.6 Special Session organization

- CODIT 2020 (International Conference on Control, Decision and Information Technologies) "Energy Management Systems for Sustainable Districts" Michela Robba, Giulio Ferro, Luca Parodi, Giovanni Bianco, Riccardo Minciardi (Università di Genova).

1.3.7 Open Invited Track organization

- IFAC WC 2023 (The 22nd World Congress of the International Federation of Automatic Control) "Sustainable Transportation and Energy Systems: Automation and Optimization” Luca Parod, Giulio Ferro, Massimo Paolucci, Michela Robba, Yassine Ennassiri (Università di Genova), Mariagrazia Dotoli (Politecnico di Bari), Yrjö Majanne (Tampere University).

1.4 Projects

During my Ph.D. activities I participated in the following projects:

- PICK UP - project funded by the Liguria Region Innovation Program (2018-2021). In collaboration with ABB, SIGLA Group, RULEX, MAPS, Flairbit, Stam, Algowatt. Activities: Definition and implementation of an energy management system for buildings connected to polygenerative microgrids. Role: participant. Project leader: Prof. Michela Robba.
- LIVING GRID - project funded by the National Energy Cluster (2020-2021). In collaboration with Terna, ENEL, Enea, RSE, CNR, Ensiel. Activities: Definition and implementation of a demand response platform for distribution networks and intentional isolation. Role: participant. Project leader: Prof. Michela Robba.
- RESTABILIZE 4.0 - project funded by the National Competence Center START 4.0 (Center of Competence for Security and Optimization of Strategic Infrastructures, https://www.start4-0.it/), as part of the competitive call (which included peer review) for industrial research and experimental development projects on enabling technologies 4.0 for critical infrastructure security (2020-2021). In collaboration with Flairbit, Algowatt and Camelot Biomedical Systems. Activity: Modeling study for resilience of electrical distribution networks with mitigation actions based on Demand response Role: participant. Project leader: Prof. Michela Robba.
- SAMPLE - project funded by the National Competence Center START 4.0 (Center of Competence for Security and Optimization of Strategic Infrastructure, https://www.start4-0.it/), as part of the competitive call (which included peer review) for industrial research and experimental development projects on Enabling Technologies 4.0 for Critical Infrastructure Security (2021). In collaboration with

MAPS, Algowatt, Acea production. Activity: Models for predictive maintenance of large-scale PV systems. Role: participant. Project leader: Prof. Michela Robba.

- PRELUDE - project funded by the European Union's Horizon 2020 research and innovation program under Grant Agreement No. 958345 (2020-2024). The project includes 24 partners across Europe, divided between universities and companies. Activity: Models for cost and comfort optimization in smart buildings. Role: participant. Project leader: Luigi Sechi.

Chapter 2
Introduction to Electric Mobility

In this chapter, an introduction about the electric mobility is presented. In particular, in Section 2.1 a general description about EVs' batteries and emissions is provided. Section 2.2 is relevant to the charging stations, the different charging modes and the available connnectors. Section 2.3 describes the role of EVs in the power network. The chapter ends with a discussion about the discrete event approach in Section 2.4.

2.1 EVs

Pure EVs are moved only by an electric motor, without the presence of an electric or mechanical power generator powered by an engine of another type. The general scheme of this type of vehicle (Fig. 2.1) can be represented by one or more electric motors and an energy storage system.

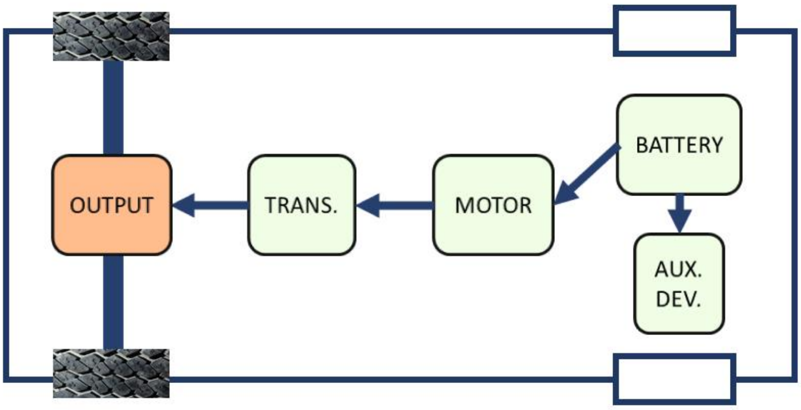

Fig. 2.1. Configuration of an EV.

Since not all the main technical characteristics of the EVs are necessary in the presentation of the thesis, the only component which is analyzed in the next sections is the battery.

2.1.1 EVs: Batteries

The whole commercial, marketing, and economic history of the EVs' production have been associated with the electric battery autonomy problems in terms of feasible distance and hours duration. They are used to store electrical energy that the electric motor uses to power the vehicle. Unfortunately, current battery systems tend to be heavy and costly, so the priority is to improve battery systems to make electrification as accessible as possible. In fact, the battery represents the most expensive component of an EV, since his cost is from 25% to 50% of the total, depending of which technology is used [1]–[3].

Battery improvements are moving fast in order to make EVs competitive with respect of internal combustion engine vehicles (ICEVs): for instance, production costs of the Li-Ion batteries was expected to reach 225$/kWh in 2025 [4], but according to [5] the price reached a minimum price of about 150$/kWh in 2022 and it is expected to decrease in the next years. In fact, the literature review shows that an increase in gravimetrical and volumetric density can be expected at both cell and pack level. This may help reduce the fear of low ranges in the future, making EVs more attractive for buyers.

Even if EVs are currently more expensive than ICEVs, the forecast shows that, from 2026, the parity with ICEV can be reached and EVs will be cheaper than other electrification solutions (such as plug-in hybrid EVs and fuel cells EVs). [3]

Several battery-manufacturing technologies are suitable to equip an EV. Technologies that today are widely accepted by the companies in the manufacturing industry are listed in Table 2.1 [6]:

Table 2.1 Battery Technologies

Battery technology	**Main advantages**	**Main disadvantages**
Lead-acid (Pb-acid)	Well-known technology; Cheap manifacturing;	Presence of Pb and acid substances; Low energy density;
Nickel-Cadmium (NiCd)	High lifespan	Presence of Cadmium which is limited by EU directives
Nickel-Metal-Hydride (NiMH)	Lack of memory effect	High costs; Problems of selfdischarge
Lithium-ion (Li-ion)	Large power storage capacity; High energy density	High costs; Potential for overheating; Limited life cycle
Lithium-ion Polymer	Highel life-span than Li-ion	High costs; Potential for overheating
Sodium Nickel Chloride (NaNiCl)	High stored energy density	Operational safety (between 270 and 350 °C)

Li-Ion batteries nowadays represent the most used technology in EVs [7], mainly due to their high energy density, allowing the development of some types of batteries with reduced weight and dimensions at competitive prices.

Lithium-ion batteries also have negative aspects: charging them at sub-zero degrees Celsius reduces battery life. The battery's cathode breaks down at extremely low temperatures, causing a short circuit. If the voltage is too low or the battery is overloaded, battery performance decreases. In addition, internal short circuits with potential security risks could occur. For example, extremely high voltage or excessive charge result in the production of a large amount of heat. Metallic lithium settles on the surface of the negative electrode, accelerating capacity reduction causing risky internal short circuits. Therefore, nowadays, the aim is to develop a new battery system capable of operating even in particularly unfavorable situations and equipping lithium-ion batteries with a management system to be controlled and managed effectively.

For safety and reliability to be guaranteed, this type of battery must operate within an operating range, but temperature and power voltage constraints limit it. If these constraints are not met, battery performance is generally quickly attenuated, even with safety issues.

Generally, the capacity and voltage of the cells used for EVs are relatively low. They are integrated into a module, and an EV's battery pack contains one or more modules depending on the requirements. The battery pack consists, therefore, of several individual cells. To handle such a large number of cells, a battery management system (BMS) is required, including sensors, actuators, and controllers in EVs.

The main tasks of the BMS in vehicles are: protect cells and battery packs from damage; run the batteries within the correct voltage and temperature ranges, ensure safety and extend battery life for as long as possible; make batteries operate in a state where the battery meets the vehicle's requirements.

Moreover, the battery is not symmetrical between the charge and discharge phases: this can be derived from the equivalent internal resistance having two different values depending on the current direction due to the different chemical reactions involved in the two different phases. Therefore, a battery discharged in a certain time will require more recharging. In addition, the maximum charging power can be quite low for certain types of batteries, as a result, it will take quite a long time (up to hours) to recharge the battery fully. This is inevitably a disadvantage compared to the traditional petrol and diesel vehicle, which instead has relatively low "recharge" times (to fill up the car takes one to two minutes at most). [8]

It is essential to consider that the capacity of a lithium-ion battery does not have a constant value but is reduced due to aging processes. The "end of life" (EOL) of a battery is defined as an 80% remaining capacity (or as a doubled internal resistance, depending on what occurs before).

The condition of the EOL is essential for sizing the battery capacity: there is, in fact, the necessity to consider a 20% bound as a reserve. The battery is used under strict constraints to limit and decelerate aging, and the "state of charge" (SOC) must fall within a predefined range. The lower threshold also referred to as the "safety limit", should never be exceeded to ensure battery reliability and performance stability. As soon as the SOC level drops below this threshold, the EV is recharged so that the battery is protected from excessive exhausting and a complete exhaustion does not stop the vehicle.

On the other hand, the upper limit is set by the maximum level of charge status compatible with full charging power. If this threshold is exceeded, the charging power is reduced. The fast-charging causes a further reduction in usable capacity due to voltage limits. At high values of the charging state, the current with which the vehicle is recharged must be reduced not to exceed the battery's upper voltage limit. This effect increases with the battery's aging due to the increase in internal resistance. Reducing the current increases the charging time, going against the concept of "fast charging". The upper region of the SOC cannot, therefore, be loaded too quickly. Even with all these measures, the degradation of the battery must be taken into account with an initial oversizing of the battery capacity itself.

In any case, the sizing of the battery is the result of a compromise between the required range and the weight and cost of the battery pack and, therefore, the EV.

2.1.2 EVs: Emissions

The present technologies used to build EVs (and battery packs) are complex, considering the length and structure of the production chain.

Besides, EVs have the advantage of not emitting harmful exhaust gases on site. For assessing greenhouse gas (GHG) emissions, however, it is necessary to consider the entire life cycle of the vehicle and all its phases, starting with the production and transport of electricity. Therefore, the emissions analysis integrates two phases [9], [10]:

- the assessment of the WTT (Well-to-Tank) provides the emissions during the extraction and distribution of fuel and the production and distribution of energy;
- the TTW (Tank-to-Wheel) evaluation, on the other hand, measures the emissions during the use of the vehicle and, therefore, those measured at the tailpipe.

Usually, it is common to talk about Well-to-Wheel (WTW) considering the combination of the WTT and the TTW. Of course, indirect emissions (WTT) depend on the primary source, the production method, and the distribution route. Furthermore, they are closely linked to the energy mix at the local level. In particular, if the energy mix is mainly based on producing energy from renewable sources, this type of emissions is very low.

In general, the assessment of direct emissions (TTW) is complex, and their extent depends on the type of vehicle (fuel used, abatement devices, etc.) and the context (driving conditions, traffic situation, use of auxiliaries, load profile, etc.) but, when considering a "pure electric" vehicle, this type of emissions is zero.

It can therefore be concluded that, if powered by a renewable source of electricity, "pure electric" vehicles are considered the ultimate solution to avoid greenhouse gas emissions in the road transport sector.

Authors in [11] compare conventional diesel buses (DBs) and EBs regarding polluting emissions and consumption of oil and fossil fuels. The fossil fuels considered in this analysis are coal, oil, and natural gas. They show how most of an EB's energy demand and emissions are passed upstream in the production phase. In all the speed and traffic conditions taken into consideration, EBs are advantageous from the point of view of both oil and fossil fuel consumption. Considering that the cost of primary energy sources is constantly growing, reducing such consumption would lead to significant savings in terms of operating costs.

Furthermore, they highlight how oil is reduced more than fossil fuels because there is still a significant consumption of coal for the production of upstream energy. Regarding carbon dioxide emissions, although EBs can be considered zero emissions in the TTW phase, thermoelectric power plants emit a significant amount of CO_2. As a result, EBs only reduce carbon dioxide emissions by 19-24% compared to DBs. Therefore, this highlights the need to increase the contribution of renewable sources to electricity production to make the penetration of EBs advantageous. In fact, many studies show how the use of renewables can lead to significative reductions in greenhouse gases emissions. In [12] the authors estimate an overall reduction (WTW) of about 30% for hybrid EVs and about 50% for battery EVs. This last value is also confirmed by [13] in the countries with a larger integration of renewables in the energy production sector. Another examble is given by [14], where the authors estimate that, considering hybrid EVs, the emission reductions regarding CO_2, CO, and NO_x are 21.6%, 31.3%, and 53.0%(Toronto), and 41.0%, 28.9%, and 68.5% (Beijing). Authors in [15] provide an accurate review about the emissions of ICEVs and EVs, confirming the great advantage brought by EVs in terms of WTW GHG emissions. Fig. 2.2 reports their main results

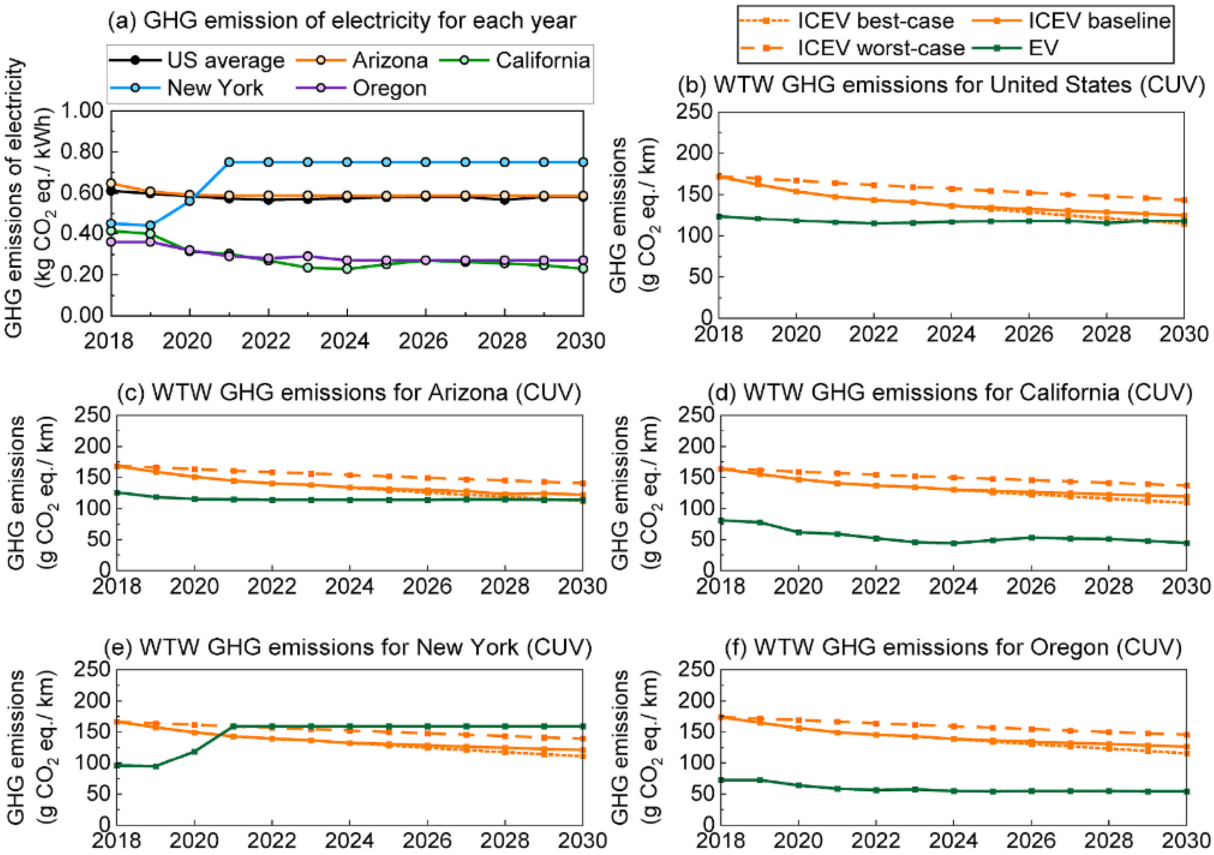

Fig. 2.2 GHG emissions of electricity in the different locations are shown in (a) Well-to-wheel GHG emissions of internal combustion engine and electric crossover utility vehicles (CUVs) are used in (b) the US, (c) Arizona, (d) California, (e) New York, and (f) Oregon, from 2018 to 2030 for the three scenarios-baseline, best-case, and worst-case for the internal combustion engine CUV. [15]

Another very useful charcteristic that must be taken into account is the Life Cycle Assessment (LCA). LCA can be used to assess the environmental impact of the relationship between input components (primary resources, energy, and materials) and output factors (emissions, trash). [16], [17]

The main takeaway from the LCA of batteries is that for each type of vehicle, the environmental effect and longevity of the vehicle rely on every stage of the production, use, and EOL of the vehicle.

An integral part of a comprehensive LCA is the recycling process. Valuable materials such as cobalt, nickel, manganese are recovered and sent to refining [18], [19]. Unfortunately, the lithium and rare earth elements go to the slag. Still, discussions on this issue highlight the need for continuous and further development of an efficient recycling process and an efficient material re-use strategy [20]–[22]

Despite the advantages from an environmental point of view, all EVs, present a series of criticalities. Among them, a critical point is the one related to the charging process which usually has to be carried out in specific infrastructures.

2.2 Charging Stations

Before presenting the technical characteristics of the charging station, it can be helpful a brief introduction on the main differences between the charging processes.

In general, there are four possible "speeds," namely:

- Slow charging.
- Fast charging.
- Rapid charging.
- Ultra-rapid charging.

Slow charging rates range between 2.3 kW and 3 kW, depending on the location. A full charge on a 3 kW unit will typically take around 10-14 hours, and for cars with a larger battery, it could take even longer. Slow charging is usually considered for overnight charging.

The fast-charging range is between 7 and 22 kW can be typically found in public areas such as parking lots. It is suitable for users who have few hours to charge the vehicle.

Rapid charging refers to those chargers that allow (AC or DC) charges at 43 kW and 50kW.

Ultra-rapid chargers can deliver 100kW, 150kW, or 350kW. These are only DC chargers.

The well-known company Tesla uses the 150kW ultra-rapid chargers, which have the infrastructure for charging EVs. This chapter does not focus on this particular case, but the common characteristics identified by the international standards will be described.

Describing the technical characteristics of the charging facilities, it is necessary to cite the IEC 62196 which is an international standard for a set of electrical connectors for EVs and is maintained by the International Electrotechnical Commission (IEC).

The standard is based on the IEC 61851 [23], in which general characteristics are established, including charging modes and connection configurations, safety requirements of EVs, electric vehicle supply equipment (EVSE) in a charging system and further general requirements. For example, it specifies mechanisms such that, first, if the vehicle is not connected, the power is not supplied, and, second, the vehicle must be still for the whole connection time. IEC 62196 [24] comprises three main sections: (1) general requirements; dimensional compatibility and interchangeability requirements for (2) AC pin and contact-tube accessories, and (3) for DC and AC/DC pin and contact-tube vehicle couplers.

According to the standard every connector includes control signaling, allowing the control of local charging. By means of adapters, all connectors can be converted, although not with intact charging modes.

There are four connector types, namely:

- SAE J1772 (Type 1), mainly used in North America;
- VDE-AR-E 2623-2-2 (Type 2), known also as the Mennekes connector, it is used in Europe;
- EV Plug Alliance proposal (Type 3), known as the Scame connector, it is mostly used in Italy and France;

- JEVS G105-1993 (Type 4), traded as CHAdeMO, mostly used in Japan.

2.2.1 Charging modes

The standard applies to EV charging appliances with a rated operating voltage not exceeding 690 V (AC 50/60 Hz, rated current ≤250 A) or 1550 V (DC, rated current ≤400 A). In particular, this standard's reference is represented by the charging modes defined in the IEC 61851, presented in the next subsections.

<u>Mode 1</u>

Mode 1 (Fig. 2.3) is characterized by a direct and passive AC connection of the EV. It can be a 250 V 1-phase or a 480 V 3-phase, at a maximum current of 16 A. The connection is not equipped extra control pins. For safety reasons, the EVSE must provide ground to the EV and have ground fault protection. The fundamental problem is that not all household installations have the necessary grounding; in fact, charging in Mode 1 is illegal in certain nations, including the US.

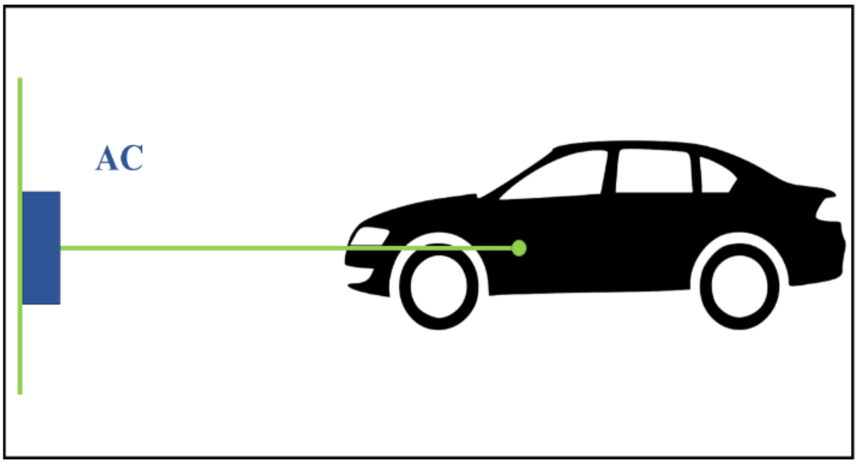

Fig. 2.3 Connection in "Mode 1" configuration.

<u>Mode 2</u>

Mode 2 (Fig. 2.4) connects the EV directly and semi-actively to the AC mains with a maximum current of 32 A at 250 V for a single phase or 400 V for a three-phase connection. In particular, the connection from the AC mains to the EVSE is a direct and passive while the connection between the EVSE and the EV is active, with the addition of the control pilot to the passive components.

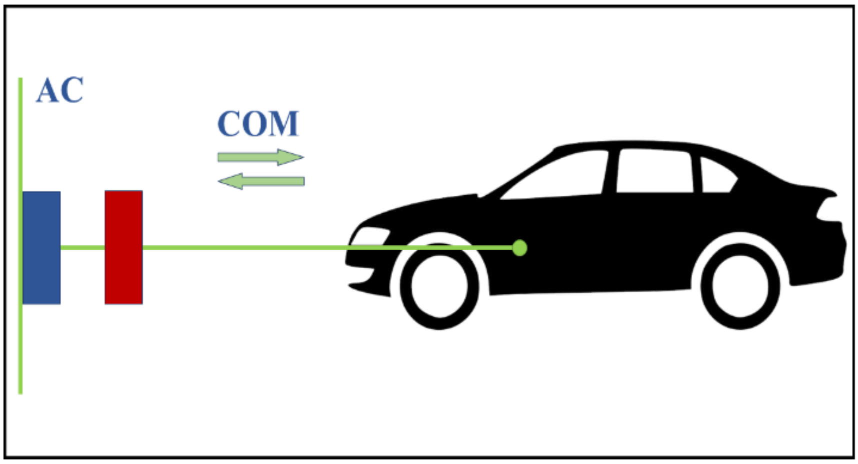

Fig. 2.4 Connection in "Mode 2" configuration.

Mode 3

Mode 3 (Fig. 2.5) is an active connection of the EV to a fixed EVSE. It can be 250 V (1-phase) or 480 V (3-phase) and includes grounding and control pilot. It may include a compulsorily captive cable with extra conductors. The charging supply is not active by default, and to enable it, a proper communication over the control pilot is necessary.

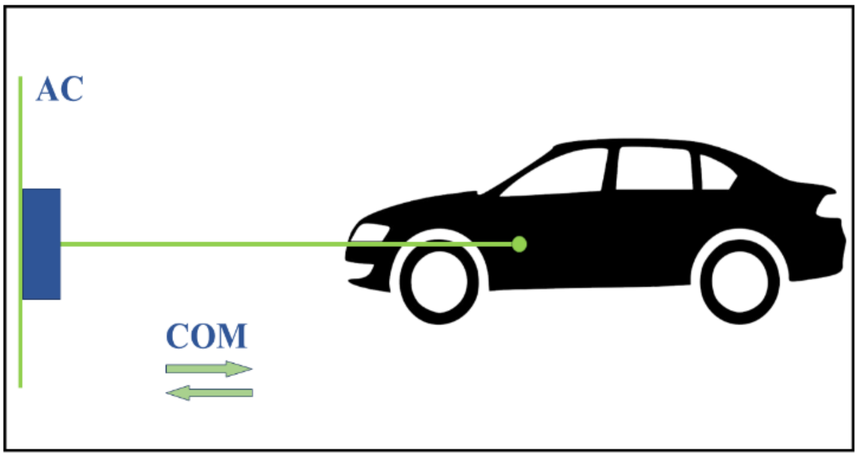

Fig. 2.5 Connection in "Mode 3" configuration.

Mode 4

Mode 4 (Fig. 2.6) is an active connection of the EV to a fixed EVSE. It is the only connection mode providing DC current (600 V), includes grounding and control pilot, and allows a maximum current of 400 A. The EVSE, which is more expensive than a Mode 3 EVSE, rectifies AC mains power into DC charging power.

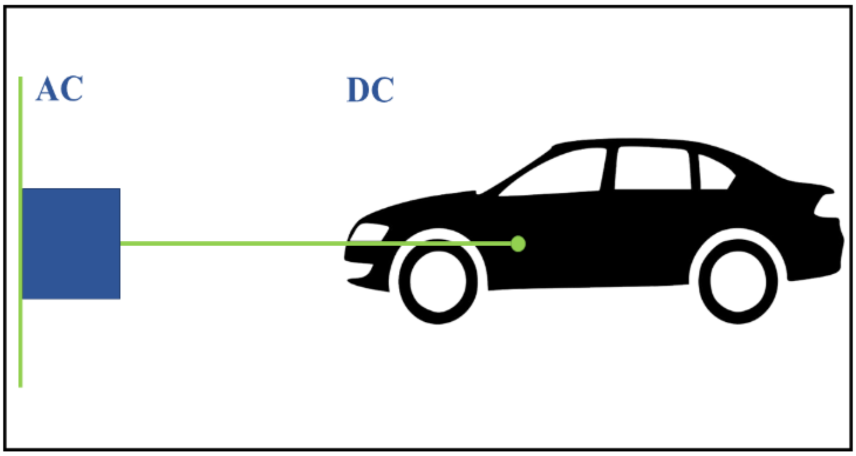

Fig. 2.6 Connection in "Mode 4" configuration.

2.2.2 Connectors

The connectors standardized in IEC 62196 are specialized for automotive use. The list of plug types includes four different connectors.

The Type 1 connector is a single-phase vehicle coupler, reflecting the SAE J1772/2009 automotive plug specifications. The Type 2 connector can be either single-phase or three-phase and reflects the VDE-AR-E 2623-2-2 plug specifications. As Type 2, Type 3 connector can be single or three-phase (includes also shutters), and reflects the EV Plug Alliance proposal. The last connector is Type 4, a direct current coupler, reflecting the Japan Electric Vehicle Standard (JEVS) G105-1993 specifications.

Type 1

As introduced, Type 1 (Fig. 2.7) connector comes from the standard SAE J1772/2009, which is a North American standard maintained by SAE International. The standard provides the fundamental physical, electrical, communication, and performance specifications for the conductive charge system and coupler of an electric vehicle.

The Type 1 has five pins, with three different pin sizes from the grater to the smaller, namely: AC (2 pins), Ground (1 pin) ; Proximity detection and control pin.

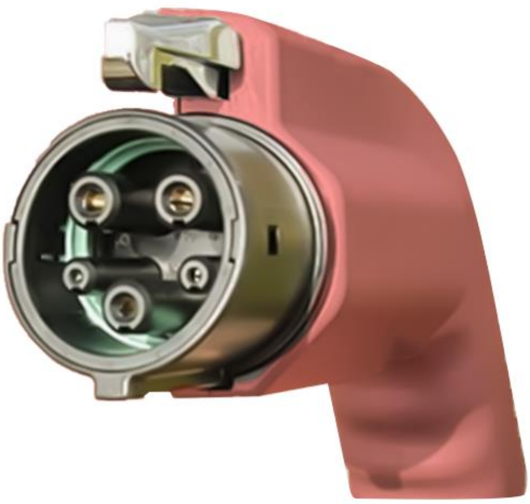

Fig. 2.7 Type 1 (SAE J1772) connector.

Type 2

The Type 2 connector (commonly referred to as Mennekes) is used for charging electric cars in Europe (Fig. 2.8). The connector is specified for charging battery EVs at 3–120 kilowatts. Electric power is provided as single-phase or three-phase alternating current (AC), or direct current (DC). The Type 2 connector has been selected by the European Commission as official charging plug within the European Union.

Fig. 2.8 Type 2 (Mennekes) connector.

Type 3

Type 3 is the EV Plug Alliance connector (Fig. 2.9). The IEC 62196 framework proposes an automotive plug, specified as Type 3, derived from the earlier Scame (italian company) plugs already in use for light EVs. Type 3 connector can provide 3-phase charging up to 32 A.

Fig. 2.9 Type 3 connector.

Type 4

Type 4, connector is reported in Fig. 2.10. Commonly know by its trade name (CHAdeMO), this connector represents a quick charging method for battery EVs delivering up to 62.5 kW by 500 V, and 125 A direct current. CHAdeMO is an abbreviation of "CHArge de MOve", equivalent to "move using charge" or "move by charge". It is proposed as a global industry standard by an association of the same name and included in IEC 62196 as Type 4.

Fig. 2.10 Type 4 (CHAdeMO) connector.

Moreover, it is necessary to introduce the Combined Charging System (CCS) adds DC charging to the Type 1 and Type 2 connectors. These are commonly known as Combo 1 or Combo 2 connectors (Fig. 2.11). Generally, Combo 2 is the most used except for the North America where Combo 1 is preferred.

Fig. 2.11 CCS Combo 2 connector.

Note that there are other available connectors. An example is given by the well known company, the american Tesla, which has developed its own connectors and its charging stations, but also provides adapter to Type 2, CHadeMO, and CCS Combo 2 connectors.

2.3 EVs in the power network

In this section a description of the main operations of the EVs in the power network is provided. First it is necessary to introduce the concept of Vehicle-to-Everything (V2X) [25], a communication between a vehicle and another entity. In particular, the most used terms used in the EVs' charging processes are Vehicle-to-Grid (V2G) and Vehicle-to-Building/Home (V2B/V2H). Both of them refers to a power exchange from the EV to the grid/building. It is also quite common to find the opposite nomenclature when referring to the charging of the vehicle, i.e. Grid-to-Vehicle (G2V) and Building/Home-to-Vehicle (B2V/H2V) [26]. Since about 95 % of cars are parked [27], the batteries in EVs could be used to let electricity flow from the car to the electric distribution network and back.

The idea behind the V2X is to provide a service to the grid by using the EV as an energy storage. Since the EVs' batteries usually have quite large capacities, and since their presence in the grid is expected to grow significantly, this approach can provide to the power network a lot of flexibility.

2.3.1 EVs as services providers

Generally, all the controlled load variations are collected in the so-called Demand Response (DR), which can be considered as a part of the Demand Side Management (DSM). According to the requested operation, it is possible to distinguish among the valley filling (increase the load demand is low), peak shaving (increasing the generation when demand is high), and load shifting (moving a load from an high demand period to a low demand one); note that these operations are often related to the duck curve [28]. As previously introduced, V2X vehicles can provide power to the grid, and this can have a key role in balancing the loads (Fig. 2.12).

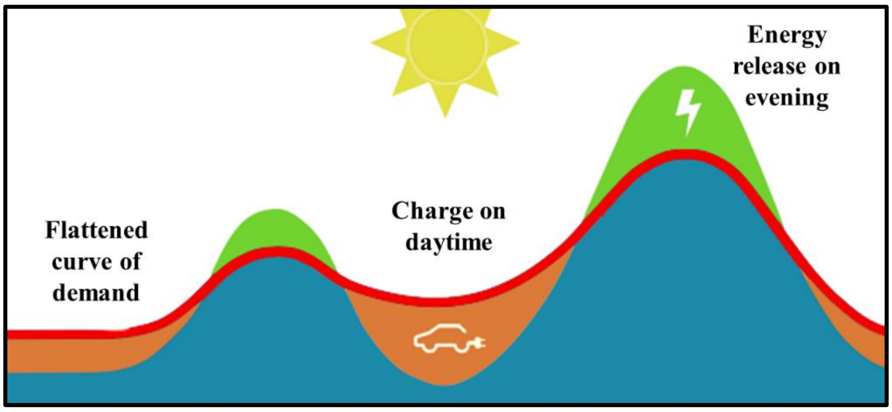

Fig. 2.12 Vehicle-to-Grid mechanism.

DR policies are also used to provide regulation services (keeping voltage and frequency stable [29], [30],[31]) and spinning reserves (meet sudden demands for power [32]). Through these applications, EVs could be one of the main actors in stabilizing the intermittency of renewable power and incentivating the penetration of renewables in the electric market [33].

One of the most recent applications is using EVs in the energy communities (ECs) paradigm. It is not directly a topic faced in this thesis, but ECs are nowadays a new approach for energy management. They consist of communities of users from the same portion of the grid (whose size depends on national regulations, which is still a matter of discussion). The participants in the EC receive an incentive for the shared energy, which is virtually exchanged among them (defined as the maximum between the produced power and the consumed one). In this particular framework, since simultaneous production and consumption are the basis for the incentive, using EVs as temporary storage has a crucial role. In fact, they could allow a better fitting of the consumption and the generation profiles leading to higher incentives.In general, when discussing about the use of charging policies to provide services, it is also common to talk about Smart Charging (SC).

2.3.2 Smart charging

SC is the intelligent charging of EVs that can be shifted based on grid loads and under the vehicle owner's needs. The utility can offer EV owners monetary and non-monetary benefits in exchange for enrolment in a program that permits controlled charging when curtailment capacity is needed for the grid.

The fundamental issue is the impact of EV charging on electricity supply and demand. Left unmanaged, EV owners may charge their cars when they return from work, producing spikes in electricity demand at the worst possible time (electricity use already peaks in the evening [34], [35]). This could, in turn, require companies to build costly new power plants that sit unused most of the day.

Nevertheless, utilities can match supply and demand by coordinating EV charging with periods of cheap and abundant power. In some areas, this may mean charging cars in the middle of the day, when solar panels are most productive; in others, optimal charging may occur in the middle of the night, powered by the wind.

These "smart charging" strategies can cut emissions, lower electricity rates, and provide a helpful new suite of grid services.

A "smart charging" infrastructure must have the following fundamental features:

- Load Balancing distributes the available capacity proportionally over all the active charging stations. In doing so, Load Balancing ensures that optimal charging is provided to all EVs at a specific location, within the limits of the charging stations' capacity.
- HUB/satellite connection, which can collect in one time the data coming from multiple charging facilities.
- Peak shaving, which automatically reduces the consumption of a charging session, or even pauses the sessions altogether until enough power becomes available, to not surpass the constraints given by the contract or by the EV charging component.
- Drivers' priority. Drivers should not find their vehicles uncharged when they need them. This concern is lessened as more EVs are deployed.
- Time-of-use pricing consciousness. Pricing electricity based on supply and demand can help avoid costly peak hour charging.

Then, smart charging is used to provide ancillary services, which can bring advantages to the grid and thus lead to an advantage for the customers who can now have an income from these services. Of course, since this particular framework is currently evolving, there is no unique solution. Authors in [36] provide an interesting review of the latest advances in this topic.

2.3.3 Integration of EVs and Smart Grids

Smart grids are one of the most exciting topics of the last decade. They are usually medium and small size power networks characterized by sensors that give information about the system and control power management better. Usually, a smart grid integrates different technologies such as renewables and traditional plants. EVs recently hold an essential role in smart grids design since one of their main characteristics is the large amount of power they involve. An example is given by [37], which proposes a novel load management solution for coordinating the charging of multiple EVs in a smart grid system. They consider cost minimization by incorporating time-varying market energy prices and preferred charging time zones for EV owners.

Regarding DR policies in the smart grids, an application is given by [38]. The authors present an EMS that manages the EVs charge-discharge plan and PV curtailment to reduce the operational cost while preserving the EVs' usage for driving. Another work focusing on DR policies is [39], where a mathematical formulation includes innovative distribution companies owners of renewable power plants and EVs parking lots.

A pretty novel approach is presented in [40], where the authors present a model for managing the charging process of slow-charge EVs and fast-charge EVs while providing dynamic regulation of the grid. They consider that some slow-charge EVs can provide enough power to reduce the peak caused by the fast-charge EV.

The authors in [41] investigate the optimal energy management problem of a microgrid with EVs. The objective is to minimize the cost by generating power with local generators and trading energy with the power market considering the market price. The EVs owners can be incentivized to take part in the DR programs as a flexible load since it brings profit for EVs and microgrid owners. However, the a linear model of the EV battery is considered.

2.3.4 Aggregators and their role in EVs management

In this section, attention is focused on the role of EVs in the newest regulation frameworks related to smart grids, which have introduced the presence of new actors such as Aggregators in the energy balancing market.

Specifically, an Aggregator is an entity in charge of interacting with the Transmission System Operator (TSO) to reduce a load of a portion of territory through the coordination of different prosumers and users.

Specifically referring to the management of EVs, Electric Vehicles Aggregators (EVAs) are defined. They have the responsibility to assemble the individual energy demands for overall management in smart buildings. An EVA can collect the specific EV information such as charging demand, arrival and departure times, maximal charging power, and driver preferences. In [42], EVs are pooled into forming virtual Local Electricity Markets, and it is investigated the impact of EVs' flexibility on its creation. The objective is to allow a set of EVs to trade electricity with other EVs or houses during their availability. In [43], it is assessed that Peer-to-Peer (P2P) is expected to be particularly suitable to complement embedded PV generation and EVs. In particular, the authors simulate P2P energy sharing for a local microgrid of 50 households with community energy storage, PV and EVs (uni-directional EV chargers, chargers that can discharge EV battery energy to the home or the grid). According to the results, P2P trading with V2G can lead to an increase in shared energy, modest improvements to microgrid self-sufficiency, and improvements to household bills. However, the combination of P2P with V2H brings substantially greater advantages.

As regards the balancing market driven by an Aggregator, the P2P mechanism is replaced by decision architectures. One arbiter/broker (i.e., the Aggregator) receives information from local users/prosumers and has the responsibility to coordinate the overall load reduction. These market structures are helpful both for providing economic advantages to the market participants and helping the distribution's grid manager alleviate the pressure over the grid of distributed and intermitted load and productions. EVs represent a huge and intermittent load over the territory. However, at the same time, they can provide flexibility (through load shifting, energy storage and V2G capabilities). Thus they can be used as a user/prosumer coordinated by an aggregator to participate in DR programs [44]. In this framework, the growing number of new EVs seems to be a real challenge.

There are two different ways, i.e., direct or indirect, to achieve and incentivize DR to consumers. Indirect DR programs try to change the behavior of the loads through different methods of rewards: the use of different periods in which the price of electricity changes and incentive payments designed to induce lower electricity use at times of high wholesale market prices or when system reliability is at risk. In the latter case, there are DR programs such as the Special Case Resource program or the Day-Ahead Demand Response Program promoted by New York Independent System Operator [45]. Special Case Resource provides an upfront payment for capacity, a payment for load reductions when dispatched, and it may include penalties for non-compliance with capacity obligations. Day-Ahead Demand Response Program allows participants to submit load reduction bids in the Day-Ahead Market, where they compete with generators.

Interestingly, attention to load management was promoted in the U.S. by the rise of air conditioning that caused short load peaks. Among the U.S., there was a real increase in the number of entities offering DR programs, from 126 in 2006 to 274 in 2008, an increase of 117% [46]. Direct DR programs happen when the aggregator or the distribution system operator adjusts the demand profile at its own decision, directly disconnecting the consumer's equipment, who are notified at short notice. Participants in the program are compensated for their participation with a bill credit or discount. In other cases, participating customers are rewarded with money based directly on the amount of load reduction during critical conditions.

Most of the works in the recent scientific literature on DR include V2G technology. They are focused on deciding when and how frequently to charge or discharge the battery by using optimization models. For example, Saber et al. in [47] propose a Particle Swarm Optimization, a kind of evolutionary algorithm, to solve V2G of car parks; this technique has been demonstrated to solve complex constrained optimization reliably and accurately. In particular, V2G and EVs are included in an overall Unit Commitment decision problem. A multi-objective function minimizes costs (including fuel cost, start-up cost, and shut-down cost of a thermal device) to efficiently schedule on/off states of the available system resources.

In [48], an aggregator using a combined portfolio with direct and indirect techniques of DR is proposed. The main problem here is to select a balanced combination of DR contracts to achieve the best results. For this purpose, it is proposed that the selection and the weight of each contract are defined by three different criteria: higher profit to the aggregator, higher utility for end-user, and higher reduction in electricity consumption. The work in [49] also applies the combination of two types of demand response for EVA, which avoids the limits of choosing a single type of DR. Incentive-based demand response is used to improve the total effect of demand response, while the price-based demand response forces unwilling users to participate in the program. EVA is the entity that provides charging facilities to a group of EVs and acts as an intermediary between the distribution system operator and EVs owners to solve techno-economic problems in the operation and control of the electrical grid [50]. Aggregators must sign an agreement with EVs user indicating remuneration, the method of charging or discharging, limits on power production and reduction, etc. Contreras-Ocana et al. in [51] develop a decentralized framework to jointly schedule loads in a commercial building and the charging behavior of an EVs fleet. Huang et al. [52] use a Building Integrated Energy System (BIES), a combination of on-site or DG technologies with thermally activated technologies to provide users with different energy sources, such as heating, cooling, and electricity.

2.4 Discrete Event Approach

Several systems in very different application areas deal with discrete quantities (typically involving counting integer numbers) and with processes that depend on instantaneous "events" such as the pushing of a button, a traffic light, the on/off status of a portion of the grid or of a charging station, etc.

A discrete event system is characterized by a set (0,1,2…) and state transitions (or events). An event can be identified by a specific action taken or a spontaneous occurrence dictated by nature or suddenly met conditions (a water level in a reservoir, a temperature in the production plant, etc.). In discrete-state systems, the state changes only at a certain point through instantaneous transitions. The timing mechanism based on which the event takes place can be:

- *Time driven systems*: state transitions are supposed to happen at times known in advance. If no event occurs, the state does not change, and the process repeats. State transitions are, in this case, synchronized.
- *Event-driven systems*: every event represents a process in which times of occurrence are determined. They are asynchronous and concurrent.

A discrete event system (DES) is a discrete-state, event-driven system in which the evolution of its state entirely depends on the occurrence of asynchronous discrete event over time. Thus, the state can only change at discrete points in time. As a consequence, time is not an independent variable.

The continuous-time state equations are no longer valid, and the state equations for DES should be determined.

Different systems can be represented like DES, such as queueing, computer, communication, traffic, and manufacturing. Often, a DES representation can help in reducing the number of variables in optimization problems and thus improve the computational time. In recent literature, Miao [53] focuses on prioritized DESs with real-time constraints, motivated by applications in power-limited systems where a trade-off exists between resource efficiency and system performance. For off-line control, structural properties of the optimal sample path have been found to reduce the search space of the optimal task execution sequence. In contrast, a receding horizon approach has been adopted for online control. In [54], a methodology is proposed to deal with planning problems in flexible manufacturing systems for the planning in large batches of production. The proposed methodology was tested in a plant of moderate size. The results show that planning for batches as large as desired can be achieved efficiently at a very reduced computational cost. In [55], a discrete event approach controls temperature through HVAC in buildings. An event-based control adjusts actions when certain events occur, which may be faster and more scalable than state-based or time-driven control methods. Since the choice of events is a tradeoff between the computational efficiency and the control performance, the authors study events for the HVAC control problem and define how to select events that capture sufficient state information with relatively small event space.

The operational management of a grid with production plants and storage systems to satisfy an electrical demand is a problem usually faced through discrete-time models, with an optimization horizon and a time interval. However, a discrete-time formalization could lead to a high computational effort if the target is to schedule EVs.

Later in Chapter 5, a discrete event approach is considered in the operational management of a microgrid. The system behavior is described as a discrete sequence of state transitions that coincides with discrete event. Thus, the system state immediately changes when an event occurs. The discrete event approach has been chosen because it reduces the number of variables in the optimization problem. Authors in [56] confirm that a discrete-time approach implies many decision variables when time intervals grow in number. Conversely, a discrete event approach can significantly reduce the number of variables and track the system behavior whenever an event takes place [57], [58].

However, in the case of problems like the microgrid management presented, the discrete event approach has some difficulties. The problem statement is strongly conditioned by forecasted powers (e.g., renewables and load) in discrete time. This makes mandatory the introduction of some hypotheses.

Certainly, the problem here considered and formalized falls among the scheduling problems [59]–[61]. This problem typology includes the assignment, sequencing, and timing of a given set of jobs to a given set of resources to provide a certain service for these jobs. In general, the solution of a scheduling problem requires the determination of optimal decisions as regards assignment, sequencing and timing. In the present case, only "Timing decisions" are to be determined, that specify when (in which time interval) the resources execute the various jobs.

In the recent literature, event-driven approaches for the integrated management of EVs, microgrids, charging stations, and parking areas are present in many works. In [62], the possibility of controlling the batteries' recharge processes (to smooth the peak energy demand during critical periods) has been investigated. In [63], the concept of a park and-charge system is introduced; this permits the customers to park their EVs at a parking lot, where the vehicles are charged during the parking time. Even model predictive control schemes are applied, like in [64], with the objective of finding a proper trade-off between minimizing the cost of energy withdrawal and the error in tracking a reference charging profile.

All event-driven approaches previously mentioned are essentially online scheduling algorithms whose objective is that of "correcting" a previously determined schedule when something happens making this correction necessary. The necessity may occur, for instance, in case of the arrival of a new customer (a vehicle to be charged), or the occurrence of some failure in one of the servers (i.e., the charging stations). Instead, here the optimization of the charging schedule of a given set of vehicles is dealt with.

Chapter 3
Modelling, simulation, and optimization for the optimal management of EVs

This chapter discusses the role of modeling and simulation for the optimal planning and management ofEVs). In particular, a crucial point for EVs is related to the modelling and simulation of batteries, which are very important to estimate the driving range of a vehicle but also for EVs' integration in smart grids, microgrids and buildings as storage systems (both for smart charging and vehicle-to-grid operations). For these reasons, in this chapter, attention is focused on batteries' models and management systems. Moreover, it is also discussed how these models are used in controllers for charging stations, and optimization models for smart grids and buildings. Indeed, when EVs are integrated in general power and energy systems, it is also necessary to model all the other elements that contribute to the overall power balance. These elements correspond to the electrical and thermal networks, the production plants, components like transformers, inverters, etc. at different spatial and temporal scales. This chapter is a general introduction to the topics of modelling and simulation. Then, in the next chapters, attention will be focused on the mathematical formalizations useful for the optimal scheduling of the EVs charging processes and the CSs' optimal planning. A specific attention will be focused on the different possible representations of battery models, on how to deal with non-linear behavior and bi-directional flows, both in the case of discrete-time and discrete event optimization problems.

3.1 Storage systems modeling and management

3.1.1 Modeling batteries

Electrical storage systems play a crucial role in managing smart grids and EVs. As regards smart grids, they can store energy and use it in periods in which the power from the external grid has a high price or when demand response programs are needed. For EVs, when the V2G mode is possible, the vehicle's battery works like a storage system in a smart grid, and thus it has cycles of charging and discharging. Moreover, in the case of EVs, it is also necessary to model the charge/discharge of the battery over a path that depends on many factors such as territorial characteristics, vehicle mass, velocity, acceleration, etc. Battery models aim to predict the operation of a battery based on discharge rate, charge rate, battery age, battery type, and temperature, and often, when accurate models are considered, result in complex non-linear functions [65]. There are many methods of modeling battery operation, and the major categories are mathematical models, electrochemical models, and electrical equivalent circuit networks [66]–[69].

Electrochemical models are based on the physics and are represented in general by non-linear equations, which may be simplified under many different approximations [66]. A popular model is the lumped parameter, which assumes a uniform spatial distribution of chemical products and it is described by a small set of differential equations. Indeed, this model is considered too simplified for modern Li-ion cells because it doesn't well represent the complex electrochemical processes. Instead, the porous electrode theory is considered more reliable for Li-ion cells because it is possible to include mass transport and diffusion, side reactions, temperature, ion distribution, and aging. Finally, there are those models that use electrical components to model the battery behavior. These circuital models (of which the most common are the Thévenin models) can represent time-dependent effects and generally include a series of resistors and capacitors (see Fig 3.1). During discharging, the chemical products near the cathode and anode are consumed, and voltage gradually decreases, while during charging products diffuse from the battery's body to the anode and cathode.

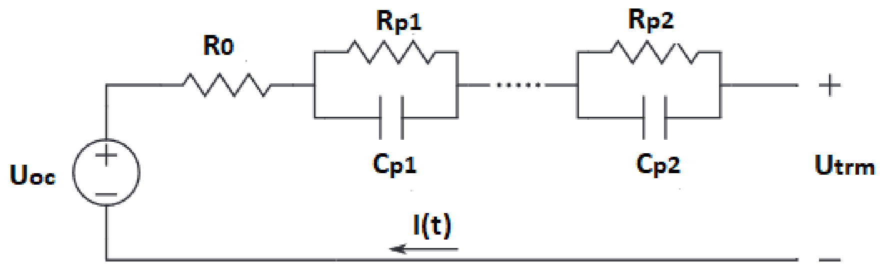

Fig 3.1 Dynamic RC battery model.

Fig 3.1 represents a circuital model in which U_{oc} is the open circuit battery voltage, R_0 represents the internal Ohmic resistance of circuits and electrodes, R_{p1} and C_{p1} describe the fast battery dynamics related to reaction kinetics and surfaces effects on the electrodes arising from double-layer formation, whereas R_{p2} and C_{p2} represent the slower dynamics typical of diffusion processes in the electrolyte and active materials.

Also in the case of circuit-equivalent models, there exist different degrees of complexity that mainly depend on the numbers of elements (resistors, capacitors) that are included. Moreover, it is possible to improve these models by including different internal battery's states and the effects of temperature.

In the field of EVs, battery modeling is essential to estimate the recharging time at a charging station, the prediction of the range of an electric vehicle, and the optimal operation when inserted in microgrids, smart grids, and charging parks. In [67], a survey is presented to model batteries with specific reference to EVs. Also in this case, the major categories are mathematical models, electrochemical models, and electrical equivalent circuit networks. The literature also contains examples of combined model types (analytical–electrochemical models) and battery thermal models. In the specific case of battery modeling for EV application, the following issues are critical:

- Battery State of Charge estimation (in this case, it is assessed that it is more important a rough estimation than a detailed model of the battery).
- There is the need for real-time computations in a battery management system (BMS), and fast models are preferred rather than complex and accurate models.
- High discharge rates might not be well represented by model simplification methods that, instead, work well at low discharge rates.

3.1.2 Battery Management Systems

A Battery Management Systems (BMS) is a tool for the monitoring and control of charging and discharging in a battery in order to optimally manage it, to prevent damages, and to guarantee a long life of the component [70]. In particular, it is important to reduce overcharging, to avoid that the battery is empty, to analyze and store the State-Of-Charge (SOC), to maintain low the supply voltage, and to receive and export data from/to external platforms. Fig 3.2 reports the architecture of a classical BMS.

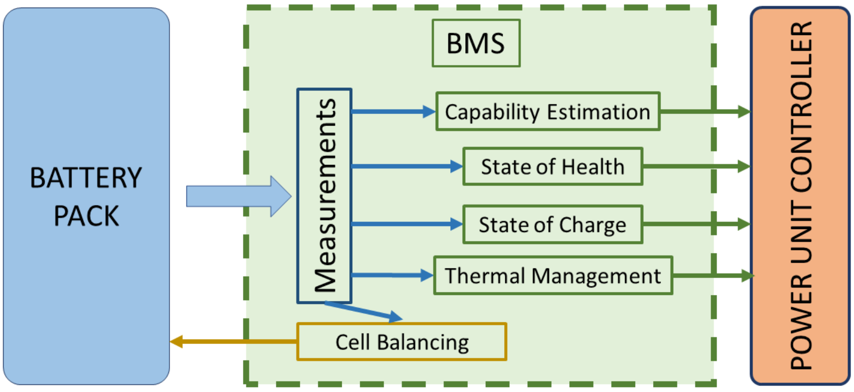

Fig 3.2 BMS architecture.

A significant function of the BMS is the estimation of SOC [67], and, in this case, generally, simple models are used in order to guarantee a fast operation and control of the battery. In fact, the used techniques are for example: fuzzy-logic, least squares regression models, Extended Kalman Filter. Another important parameter (more difficult to estimate and measure) is the State-OfHealth (SOH), i.e. the battery's gradual loss of maximum capacity. In [71], a comprehensive review is presented on battery modeling and state estimation approaches for advanced BMSs: the physically-based electrochemical models, the integral and fractional order equivalent circuit models, and data-driven models. The survey in [72] regards methods for the SOC estimation for EVs. It assesses that algorithms based on control theory and intelligent algorithms are the focus of research in this field. A review on the SOH estimation is instead reported in [73], with specific reference to Li-Ion batteries.

Regarding thermal issues, always concerning Li-ion batteries, a survey is presented in [74]. A battery thermal management system, which can keep the battery pack working in an acceptable temperature range, significantly affects the system performance and is also vital for safety and stability. The multi-physical battery thermal management systems are divided into three categories based on different methods such as air-cooled system, liquid-cooled system, and heat-pipe-cooled system. For the specific case of electrical buses for public transportation, a survey is presented in [75]; in this case, BMSs are particularly important because vehicles have a shorter driving range compared with conventional internal combustion engines, require large battery packs, face practical challenges such as long charging time and high cost of battery with large size. In particular, the following issues are treated as a priority for the research in this field: the development of technologies such as energy storage systems, powertrains, interleaving elements, and electric motors; the development of tools and ICT based automation systems for energy storage systems sizing, power/energy management, range remedy methods, charging /design/scheduling, etc.; the modeling of charging demands and impact on power systems.

BMSs can be also seen as ICT platforms that communicate with hardware in field and in relation with a local component, which may include simulation and optimization models and that can receive inputs from external platforms. The typical case is the one of a storage system/vehicle that is connected to a microgrid and/or to a building. In this case, the microgrid's management system has to coordinate several components and provides to local controllers (i.e., BMS, building automation systems, controllers for production plants, etc.) reference working points. The BMS tries to follow such reference values but preserving at the same time the good health and operation of the component; this may result in a discrepancy between what the microgrid's controller asks and what the battery really implements. For this reason, the modelling of storage systems is very important also for its inclusion in energy management systems for microgrids and building automation systems.

3.1.3 Modeling energy consumption over a path

EVs' batteries have charging and discharging cycles during a trip. It is essential to model the state of charge over a path for several reasons: to quantify energy consumption to be used in optimal charging strategies, to develop optimization models for the optimal routing and charging of EVs, to design the size and the location of charging stations over a territory, and to control velocity and acceleration of an EV dynamically. The energy consumption over a path depends on the energy required to proceed on different slopes and the energy obtained by the Kinetic Energy Recovery System (KERS) in the downward stroke and the braking phases. In literature, there are many papers related to the motion of vehicles. In [76], a survey of the existing mathematical models of EVs is presented. Simple models and complex multi-body dynamic models are discussed in detail, focusing on their application in controllers' design. In addition to vehicles' dynamics, the paper consolidates dynamic models of the different components of an EV, including the transmission, brake, battery, wheel, and tire dynamics. In [77], a torque demand control approach is proposed to optimize the driving energy consumption of battery EVs, which consists of a demand control approach and model predictive controller. It is important to note that there are some simplifications of vehicle dynamics for EVs routing and charging, planning, and scheduling accepted in literature [78]–[80].

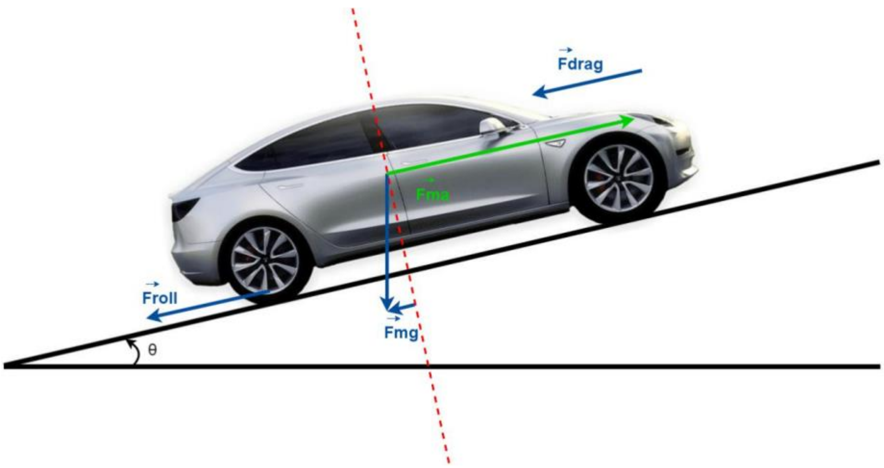

Fig 3.3 The forces of a vehicle in motion.

The force required for the propulsion is the summation of the acceleration force, the force necessary for the elevation of the EV F_{mg}, the force required to overcome the friction between the tires and the road F_{roll} and the drag force F_{drag} (see Fig 3.3) [78], [79]. The rolling resistance force F_{roll} is given by $F_{roll} = C_r mg\cos(\theta)$, with θ the road gradient in radians or degrees, C_r is the rolling resistance coefficient (function of tire material, structure, temperature and inflation pressure, road roughness and material), m is vehicle mass, and g is the gravity acceleration. The aerodynamic drag force F_{drag} expressed as $F_{drag} = \frac{\rho A C_d v^2}{2}$, with C_d is the aerodynamic drag coefficient, A is the electric vehicle's frontal area, ρ is the air density, and v is velocity. The grading resistance F_{mg} is given by $F_{mg} = mg\sin(\theta)$.

The electric power consumption can be generally written as [80]:

$$P_{el} = \frac{v(t)}{\eta_{te}\eta_e\eta_{in}}\left(\psi m\,\frac{dv(t)}{dt} + C_r m\,g\cos(\theta) + m\,g\sin(\theta) + C_d\,\frac{\rho A v(t)^2}{2}\right) + P_{HVAC} \tag{3.1}$$

where ψ is the mass factor for converting the rotational inertia of rotating components into translational mass, $v(t)$ the speed of the vehicle, η_e the electrical motor efficiency, η_{in} the power converter efficiency, η_{te} the electric vehicle's transmission efficiency and P_{HVAC} the internal power consumption of the vehicle (e.g., for air-conditioning).

The regenerative braking power P_{rb}, which can be partially (according to factor $K \in [0,1]$) recovered and restored into the battery, can be modeled as

$$P_{rb} = Kv(t)\eta_{te}\eta_e\eta_{in}\left(\psi m_{tot}\,\frac{dv(t)}{dt} + C_r m_{tot} g\cos(\phi) + m_{tot} g\sin(\phi) + C_d\,\frac{\rho A v(t)^2}{2}\right) \tag{3.2}$$

It is important to note that there are other aspects that strongly influence the EVs' consumption. The first one is related to the number of start-and-stops over a path. Let Θ be the number of start-and-stops over a path that can be estimated on the basis of traffic, length, road characteristics. Fig 3.4 shows the start and stop for a path with Θ =3 and constant velocity between start and stops. In this case, it is necessary to evaluate the additional contribution in consumption and recovery by the use of equations similar to (3.1) and (3.2) and multiplied by the number of start and stops Θ over a path.

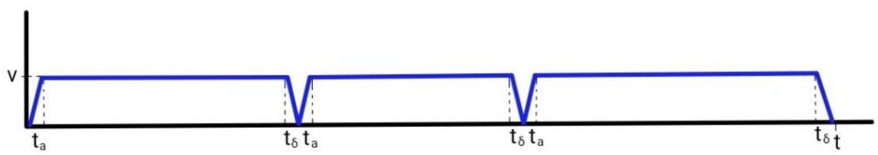

Fig 3.4 Start and stops over a path with Θ =3.

3.2 Optimization models for EVs' planning and scheduling in smart grids

Optimization models are widely used for the planning and management of EVs. In particular, the main decision problems that should be faced are:

- *Optimal sizing and siting of charging stations*. Decisions are taken in a long-term time horizon regarding installing plants and components. In particular, it is necessary to define the charging station, the size, the geographical location, and which bus of the electrical grid the charging station should be connected to.

- *Optimal schedule of the EVs' charging in buildings and microgrids*. This case refers to decisions in the short term (day-ahead, intra-day). It is necessary to define how much power to provide, when and at which vehicle, based on release time, due date, and deadline associated with each vehicle. Moreover, since the charging station is within an electrical network in which there are production plants, storage systems, and loads, it is necessary to jointly schedule the charging, the production and storage systems, and flexible loads.
- *Power management in charging stations*. This is the case there are multiple vehicles already connected to a socket in a charging park. It is necessary to set all vehicles as soon as possible but respect the constraint of the maximum power taken from the external grid. Here the reference is to short-term and real-time decisions.
- *Optimal routing and charging of EVs*. This is the case in which EVs transport goods or persons but also have to recharge in their path (and decide in which charging station to recharge, how much, and which route to follow). This case is referred to short-term decisions.

In this thesis, the focus is on the first two classes of decision problems, which are detailed in the following.

From the existing literature, it is clear that the siting and sizing of charging stations (CSs) are crucial issues for the wide spreading of EVs. Several points should be taken into account:

- *Territorial constraints*. The characteristics of an area may influence the choice of the siting of CSs: a) in some places, it is not possible to install CSs due to lack of space or limits given by regulation or risk assessment (natural areas, hydrogeological risk, etc.); b) private citizens, commercial centers, public administration, and companies may have the willingness to install some CSs in priority areas.
- *Electrical grid management*. CSs are connected to the distribution grid, and EVs represent intermittent and significant loads. Moreover, when V2G capabilities are enabled, EVs can be treated as a particular type of storage system and may help manage the electrical grid. From a purely electrical grid point of view, EVs charging and discharging are part of the overall power balance and optimal power flow. Typically, they are treated together with other loads and production systems.

- *Energy demand assessment*. The energy demand for charging is a crucial point that, for private transportation, depends on user choices, traffic models, and the characteristics of the transportation network. For public transportation (electrical buses) energy demands for all possible paths can be estimated through a model of consumptions over the territory and the forecasting of the number of passengers and traffic modeling.

In the literature of planning problems, Pagany et al., 2018 [81], present a survey of spatial localization methodologies for the electric vehicle charging infrastructure to minimize costs while guaranteeing a high coverage of a charging station and trip length. User choices' modeling is present in various contributions in literature. For example, in [82], a User Equilibrium (UE) traffic assignment approach assesses traffic and energy demands in a transportation network. In contrast, in [83], [84], UE conditions are used as part of multilevel architectures in which they are considered as constraints of an optimization problem or part of an iterative procedure. Other articles extend these approaches to the case in which the electrical grid is modeled in detail [85]–[87] or stochastic equilibrium is considered [88].

Different from the sizing and sizing of charging stations, which refer to long-term decision problems for installing technologies, in the short term (when all CSs are all defined over the territory) there is another significant decision problem: the optimal scheduling of EVs' charging. This should be integrated with the optimal management of the system in which CSs are located (i.e., smart grids, microgrids, buildings), as represented in Fig 3.5. EVs can fit this system since they represent not only a load that can be modulated but also a resource. In a not-so-futuristic vision, they can act as distributed energy resources since they can favor active short-response participation on storage resources by providing regulation services and power supply.

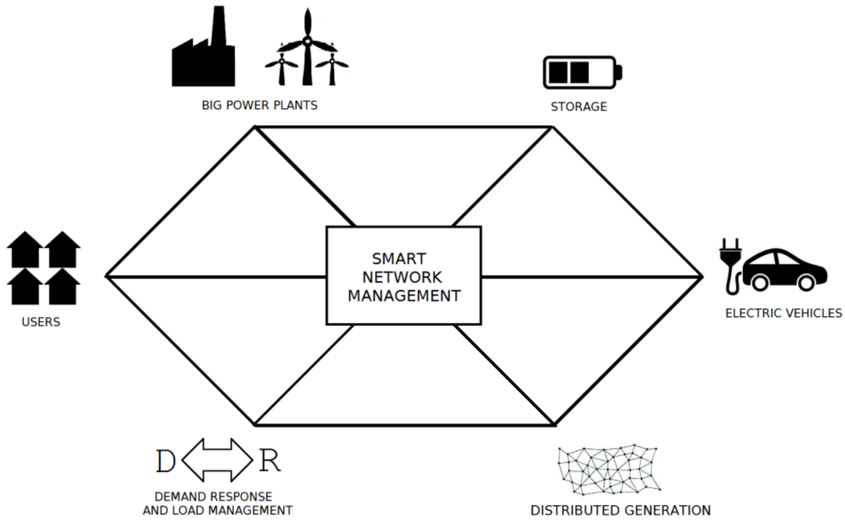

Fig 3.5 A smart grid that includes EVs.

In fact, with the arrival of the smart grid era and the advent of advanced communication and information infrastructures, bidirectional communication, and advanced metering infrastructure Energy Management Systems (EMSs) for microgrids and districts and home energy management systems are becoming crucial for the optimal scheduling of production systems, storage systems and loads [89]. An EMS is a system of ICT tools used by operators of electric utility grids microgrids and responsible for local areas to monitor, control, and optimize the performance of the generation and distribution systems. Optimization models are the “intelligence” of such EMSs, and in [90], a comprehensive survey of different control issues in microgrids is presented. All possible approaches are classified in centralized, decentralized, distributed, and hierarchical frameworks. In [91], the specific case of buildings is reviewed considering the management of loads under a demand response framework, including EVs, renewable resources, storage systems, and automation in the field for monitoring and control. In [92], the authors present a problem for the optimal control of a storage system in a microgrid. Authors in [93] propose a robust optimal energy management for a microgrid while considering uncertainties and find the optimal schedule solving a mixed integer quadratic programming problem. In [94], a multi-objective scenario-based day-ahead energy management system decreases the operation cost and increases a microgrid's reliability considering electrical and thermal loads. In [95], a comprehensive EMS at the Savona Campus pilot site includes different electrical models, EVs, storage systems, CHPs (combined heat and power production plants), and multiple objective functions. Wencong et al. [96] formulate a stochastic problem for microgrid energy scheduling, taking into account intermittent energy resources such as wind and solar and more controllable loads (e.g., plug-in EVs), distributed generators (e.g., micro gas turbines and diesel generators), and distributed energy storage devices (e.g., battery banks). In [97] the authors propose a decentralized strategy for the optimal charging of EVs with congestion management. Another decentralized approach which also take into account the uncertainties on inelastic demand is presented in [98]. You et al. [99] propose a charging strategy for EVs stations in the dynamic electricity pricing environment. The scheduling problem is formulated as a constrained mixed-integer linear program to capture the discrete nature of the battery states, i.e., charging, idle, and discharging. In the work proposed in [100] the authors solve the scheduling problem while taking into account the battery degradation. Authors in [101] also consider battery degradation as well as uncertainties on the energy prices in the optimal schedule of some EVs. Authors in [56] present a model for the optimal scheduling of some EVs in a microgrid characterized by the presence of renewables, storage systems, and traditional plants. It is thus clear that the primary modeling needs regarding:

- Production systems (both renewables and fossil fuel plants);
- Thermal and electrical storage systems;
- Batteries of EVs in charging and discharging modes;
- Charging stations;
- Thermal and electrical distribution networks;
- Performance indicators: costs, emissions, primary energy savings, etc.

As described in the following chapters, optimization problems can be found in the literature for discrete-time and discrete event optimization problems.

In the former case, required information and models are reported in Fig 3.6. Firstly, it is necessary to obtain the following data required in each time interval of the optimization horizon:

- The prediction of power from renewable resources, which is calculated based on forecasted environmental parameters (temperature, solar radiation, wind velocity, etc.), and that can be derived by physically-based models, data-driven models, and the model of the plants;
- Energy contracts can be used to derive the prediction of unit costs and benefits;
- Forecasts over loads, which are generally derived by black-box models and the use of machine learning techniques;
- Information about vehicles arrival, energy request, and due date.
- Initial state of charge of the batteries (measured in the field).

After all inputs have been calculated, it is necessary to run the optimization model with the desired performance criteria (costs, emissions, primary energy savings, etc.) and the system model's constraints.

By running the optimization problem, one obtains the optimal schedule in each time interval for all production plants and components.

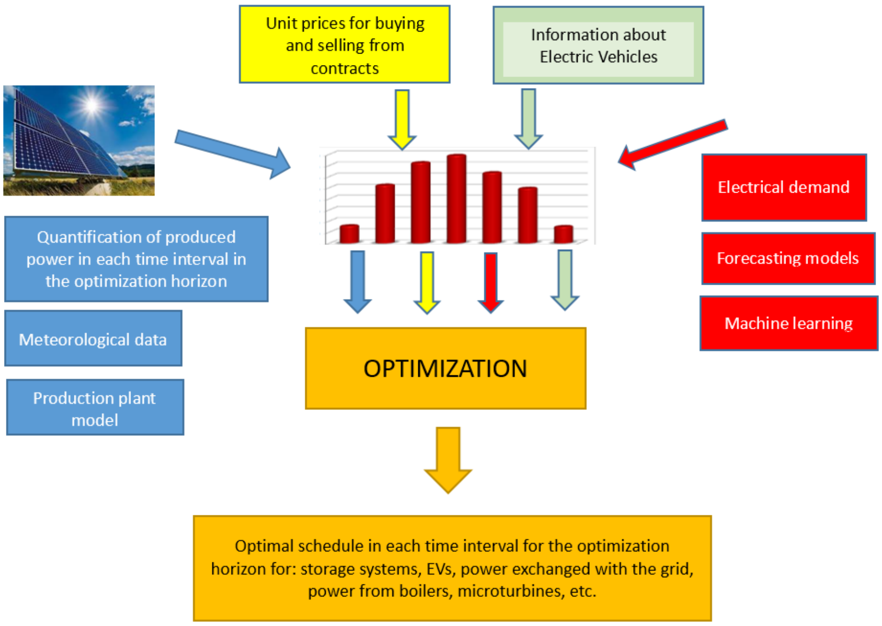

Fig 3.6 Inputs and outputs for an optimization model with time discretization.

A similar approach can be done in the case of discrete event optimization, in which time intervals are not present and there is a system change whenever an "event" occurs at a certain time. The main difference, in terms of information in input and output to/from the optimization problem, is that the EMS collects data in discrete time, but then it is required to fit them with an analytical function (as described in the following chapters). Moreover, all control and state variables are not discretized in time. Fig 3.7 reports the inputs and outputs for an optimization problem in a discrete event approach.

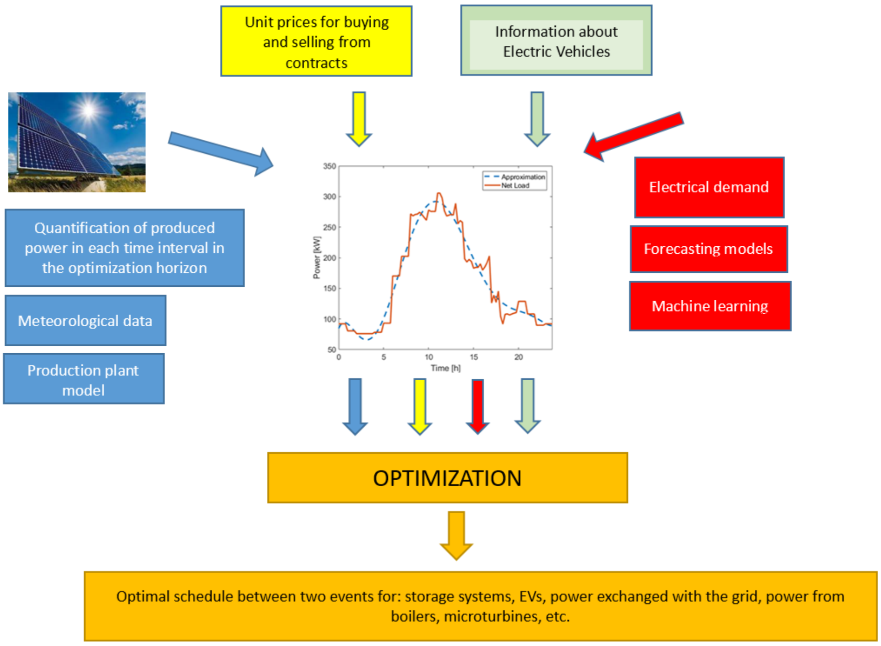

Fig 3.7 Inputs and outputs for an optimization model in a discrete event approach.

Some examples of a discrete event approach are presented in [57], [58], where the authors use this approach in the optimal scheduling of some EVs charging processes.

Chapter 4
Optimal charging of EVs in smart grids discrete time optimization

4.1 Introduction

In this chapter, attention is focused on formalizing a discrete-time optimization problem for the scheduling of EVs. Specifically, all variables and parameters are discretized in time (therefore on a fixed time interval of length *T*).

The choice of the time interval length and the time horizon is particularly important because it influences the number of decision variables and constraints and thus has implications on the run time of the optimization problem solution. Optimization problems for the scheduling of EVs are generally inserted in EMSs and modeled in discrete time [102]–[106]. EVs are typically considered as forecasted static loads in the decision models without considering the decisions related to their scheduling based on arrival, desired energy, and due dates. The reason is that EVs are few over the territory. Often a reservation service is not available, and EMSs do not exploit the similarities that the charging process has with the scheduling of manufacturing systems. In a future in which EVs will increase considerably, there will be a need for designing and managing the process in a more structured way to limit queues and negative impacts on the electrical grid. Such an approach is particularly interesting in the case of demand response programs, i.e. when there is the necessity of shifting power demands to help the distribution grid manager and/or receive remuneration from a market aggregator.

In the literature,EMSs based on optimization models are used for the operational management of production and storage systems and also to manage demand response programs (see, for example, the works proposed in [95], [107]). EVs are generally considered as additional loads, and their schedule is not detailed. Usually, optimization-based EMSs are used to define the optimal operational management including cost and environmental performance indexes for a set of different technologies (renewables, EVs, traditional sources and storages). Zhao et al. [108] in this purpose, reviews different charging methodologies and strategies. Instead, the work of Delaimi et al. [109] investigates the contribution of plug in EVs in smart grids. While Allard et al. [110] compare the impact of smart charging strategy compared to traditional EVs charging in power grids with large penetration of renewables. Authors in [111] develop a strategy to regulate the vehicle's charging process, introducing different priorities for the various objectives, like achieving maximum flexibility, the effective management of the power flows to smooth the demand curve, increasing the system's power quality.

In this chapter, the integration of EVs in smart grids is addressed. In particular, the decision problem is here characterized by the definition of the optimal charging strategies to feed EVs and the scheduling of production plants and storage systems. Specifically, the charging station is considered like a machine that has to schedule different jobs (i.e., EVs) whose sequence is fixed (according to the arrival order). Still, the charging pattern and time have to be defined. The approach is inspired by approaches usually adopted in smart manufacturing systems. The decision variables are represented by optimal scheduling of power plants and the recharging process of EVs while different classes of constraints have been introduced.

The resulting optimization problem is deterministic, non-linear, and has continuous and binary variables, and it is based on forecasting for demands and renewable power availability.

A microgrid's system model with a detailed dissertation about the electrical storage is presented in the following Section (4.2). Then, Section 4.3 reports the modeling of EVs. Finally, in Section 4.4, the optimization problem is formalized and then applied to a case study in Section 4.5.

4.2 The system model

For the entire thesis, these general rules about nomenclature hold:

- upper case letters will be parameters.
- lower case letters will be variables.
- subscript letters will be indices.
- superscript letters will be descriptive.
- minimum (maximum) values are represented with a line below (above) the letter.

The proposedsystem consists of a local area composed of the following elements (see Fig. 4.1) production from renewable resources (wind turbines and photovoltaics), internal combustion engines, electrical storage systems; a connection with the main grid, a CS for EVs, electrical loads.

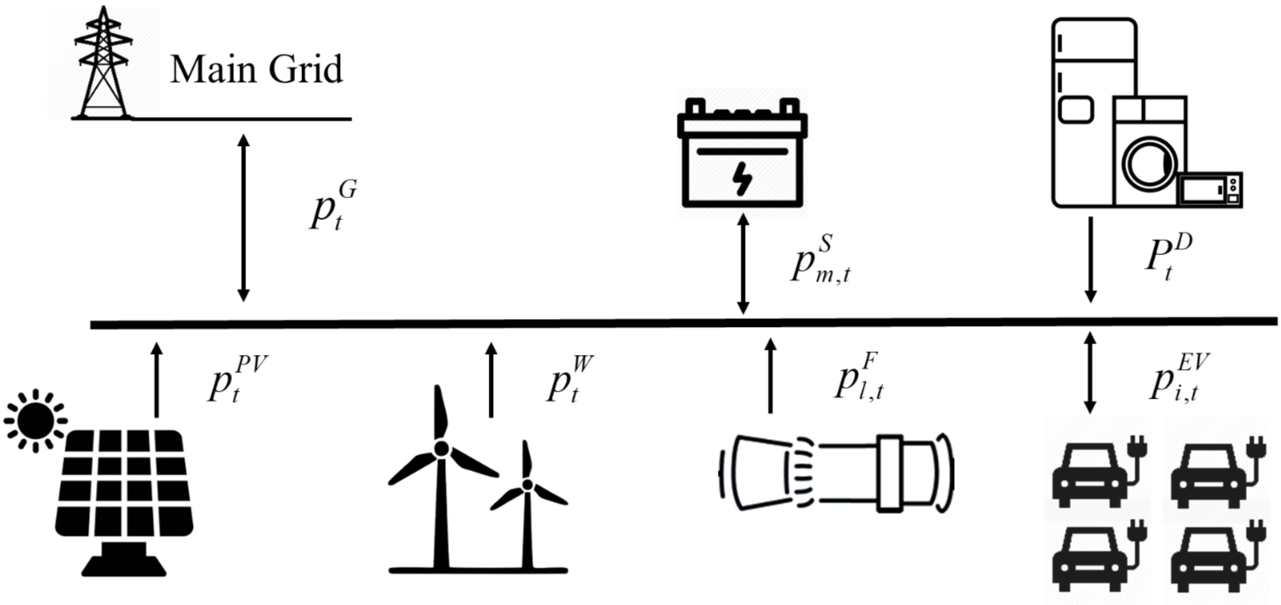

Fig. 4.1 The considered system

The forecasts in each time interval (for all the duration of the optimization horizon) of power produced by renewable resources have been calculated based on meteorological forecasting and/or black-box models and machine learning techniques. To define the mathematical model, the following sets are introduced

- $T = \{1,...,N^T\}$ set of time intervals.
- $L = \{1,...,N^F\}$ set of fossil fuel generators.
- $M = \{1,...,N^S\}$ set of storage systems.
- $EV = \{1,...,N^{EV}\}$ set of EVs.

The power flows in the system are:

- $p_{i,t}^{EV}$, that is the power flow to the *i-th* EV;
- p_t^G, that is the power flow from the main grid to the microgrid; the active sign convention is adopted; namely, the power flow is assumed positive when power is drawn (bought) from the main grid (and negative when power is given (sold) to the main grid;
- P_t^{PV} (P_t^W), that is the (monodirectional) power coming from photovoltaic power plants (wind turbines)
- $p_{l,t}^F$, that is the (monodirectional) power flow from the *l-th* energy source fed by fossil fuel to the microgrid;
- P_t^D, that is the (monodirectional) power flow representing the non-deferrable power demand;
- $p_{m,t}^S$, that is the (bi-directional) power flow from the *m-th* energy storage element; this flow is assumed positive when power is drawn from this element.

Photovoltaic and wind power forecasts must be provided as data, as well as the power demand.

The net load is defined as the summation of all the contribution given by the renewables and the power demand. It is possible to write

$$P_t^D - P_t^W - P_t^{PV} = P_t^{NL} \qquad t \in T \tag{4.1}$$

The power balance constraint that should be satisfied is given by

$$p_t^G + \sum_{l \in L} p_{l,t}^F + \sum_{m \in M} p_{m,t}^S = P_t^{NL} + \sum_{i \in EV} p_{i,t}^{EV} \qquad t \in T \tag{4.2}$$

where p_t^G is power exchanged with the main grid, $p_{l,t}^F$ is the power from the *l-th* fossil fuel production plant, $p_{m,t}^S$ is the power exchange with the *m-th* storage system, $p_{i,t}^{EV}$ is the power exchange with the *i-th* electric vehicle connected to the charging station, and P_t^{NL} is the power demand. Note that the EVs and the storage have opposite sign in the equation. This is because in the thesis the EVs are considered as a load while th storage is considered as a generator.

Each storage system can be represented by the following state equation (active sign convention is considered):

$$x_{m,t+1}^{S}=x_{m,t}^{S}+\frac{\Delta}{CAP_{m}^{S}}\left(\Gamma_{m}^{S,in}p_{m,t}^{S,in}-\Gamma_{m}^{S,out}p_{m,t}^{S,out}\right)\qquad t\in T,m\in M \tag{4.3}$$

where Δ is time interval length, $x_{m,t}^{S}$ is the state of charge of the *m-th* battery with a capacity CAP_{m}^{S} [kWh], $\Gamma^{S,out}$ is efficiency in discharging mode, and $\Gamma^{S,in}$ is efficiency in charging mode.

Note that $p_{m,t}^{S,out}$ is power exchange during discharging and $p_{m,t}^{S,in}$ is power exchange during charging, being

$$p_{m,t}^{S,out}-p_{m,t}^{S,in}=p_{m,t}^{S}\qquad t\in T,m\in M \tag{4.4}$$

Note that the mutual exclusiveness of $p_{m,t}^{S,out}$ and $p_{m,t}^{S,out}$ is ensured by the presence of the charging and discharging efficiencies in (4.3). This may be not evident at a first sight, but since the energy selling price is always lower than the energy buying price, the waste of energy that could be determined by a simultaneous charge/discharge of the battery cannot provide a benefit in the objective function and thus it is avoided.

4.2.1 Piecewise linear storage modelling

In real storage systems, the maximum power level depends on the state of charge [107]. Specifically, considering a storage system characterized by its battery management system and that receives commands from a central controller like an EMS for a microgrid, the maximum power that can be requested is lower when approaching the higher values of the state of charge.

This phenomenon can be expressed through a piecewise linear formulation as follows

$$\underline{P}^{S}(x_{m,t}^{S})=\begin{cases}P_{m}^{S,rated} & if \quad x_{m,t}^{S}\le A_{m}^{S}\\ C_{m}^{S}x_{m,t}^{S}+D_{m}^{S} & if \quad x_{m,t}^{S}\ge A_{m}^{S}\end{cases}\qquad t\in T,m\in M \tag{4.5}$$

where $P_{m}^{S,rated}$ is the rated power [kW], and $A_{m}^{S},C_{m}^{S},D_{m}^{S}$ are parameters typical of the specific storage system. The model (4.5) allows defining a polytope (see Fig. 4.2) in which the values of the power and the state of charge (SOC) are acceptable (the light grey area in the figure).

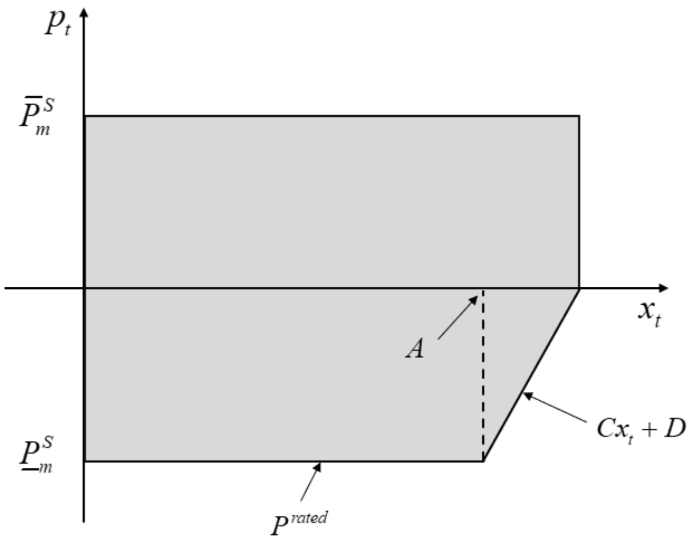

Fig. 4.2 Piecewise storage constraints

The feasible area represented in Fig. 4.2 is defined by the constraints

$$\underline{X}_m^S \le x_{m,t}^S \le \overline{X}_m^S \qquad t \in T, m \in M \qquad (4.6)$$

$$0 \le p_{m,t}^{S,out} \le \overline{P}_m^S \qquad t \in T, m \in M \qquad (4.7)$$

$$0 \le p_{m,t}^{S,in} \le -\underline{P}^S(x_{m,t}^S) \qquad t \in T, m \in M \qquad (4.8)$$

where $\underline{X}_m^S$ and $\overline{X}_m^S$ are the minimum and maximum working limits for the state of charge, $\overline{P}_m^S$ is the maximum power the storage system can deliver when discharging (assumed constant) and $\underline{P}^S(x_{m,t}^S)$ is the (negative) lower limit of the power the storage can absorb when recharging, expressed as a function of the state of charge.

4.3 Modelling EVs scheduling

The EVs are identified by index i, which is assigned according to the arrival order. Since it is a discrete time approach, all variables are considered in discrete time instants t with unit length of Δ. Finally, the overall optimization horizon is $t \in T$ and consists of N^T time intervals. The charging process is defined by two different time intervals:

- $(t_i^{st}, t_i^{st}+1)$ i.e., the starting interval in which EV i begins the charging procedure;
- $(t_i^{fi}, t_i^{fi}+1)$ i.e., the final interval in which EV i concludes the charging procedure.

The following data characterize each EV:

- T_i^{rel} the release time in which the vehicle is available to charge.

- T_i^{dd} the due-date time at which the charging process of the vehicle *should* be concluded.
- T_i^{dl} the deadline time at which the charging process of the vehicle *must* be concluded.
- Λ_i the tardiness penalty cost [€/h].

The state of charge of each vehicle is governed by first order integrator system

$$x_{i,t+1}^{EV} = x_{i,t}^{EV} - \frac{\Delta}{CAP_i^{EV}}\left(\Gamma_i^{EV,in} p_{i,t}^{EV,in} - \Gamma_i^{EV,out} p_{i,t}^{EV,out}\right) \qquad t \in T, i \in EV \tag{4.9}$$

$$\underline{X}_i^{EV} \leq x_{i,t}^{EV} \leq \overline{X}_i^{EV} \qquad t \in T, i \in EV \tag{4.10}$$

$$\underline{P}^{EV}(x_{i,t}^{EV}) = \begin{cases} P_i^{EV,rated} & if \quad x_{i,t}^{EV} \leq A_i^{EV} \\ C_i^{EV} x_{i,t}^{EV} + D_i^{EV} & if \quad x_{i,t}^{EV} \geq A_i^{EV} \end{cases} \qquad t \in T, i \in EV \tag{4.11}$$

$$0 \leq p_{i,t}^{EV,in} \leq -\underline{P}^{EV}(x_{i,t}^{EV}) \qquad t \in T, i \in EV \tag{4.12}$$

$$0 \leq p_{i,t}^{EV,out} \leq \overline{P}_i^{EV} \qquad t \in T, i \in EV \tag{4.13}$$

where $p_{i,t}^{EV,out}$ is power exchange during discharging and $p_{i,t}^{EV,in}$ is power exchange during charging, being

$$-p_{i,t}^{EV,out} + p_{i,t}^{EV,in} = p_{i,t}^{EV} \qquad t \in T, i \in EV \tag{4.14}$$

Note that the battery model il the same described in equations (4.5)-(4.8), substituting the variables with the one relevant to the EVs. Moreover, note that the mutual exclusiveness of $p_{i,t}^{EV,in}$ and $p_{i,t}^{EV,out}$ is ensured by the presence of the charging and discharging efficiencies in (4.9). In fact, a simultaneous charge and discharge would lead to a waste of energy.

4.4 The overall optimization problem

The objective function includes four different terms of cost:

- c^F : non renewable sources operating cost;
- c^{buy} : main grid energy purchase cost;
- c^{sell} : main grid energy selling benefit;
- c^{tard} : cost associated with the tardiness of the charging processes.

The control variables for the optimization problem are.

- p_t^G (unrestricted in sign): the power exchanged with the main grid [kW];
- $p_{l,t}^F$: the power from the *l-th* fossil fuel production plant;
- $p_{m,t}^S$ (unrestricted in sign): the power exchange with the *m-th* storage system;

- $p_{i,t}^{EV}$ (unrestricted in sign): the power exchange with the *i-th* electric vehicle connected to the charging station;
- $t_i^{st}\left(t_i^{fi}\right)$ time in which vehicle *i* starts (finishes) the charging process;
- $\theta_{i,t}^{EV}$: binary variable equal to 1 if vehicle *i* is connected to the charging station in a time interval $\left(t,t+1\right)$ and 0 otherwise;

The state variables for the optimization problem are.

- $x_{i,t}^{EV}$: state of charge of *i*-th vehicle at time *t*.
- $x_{m,t}^{S}$: state of charge of *m*-th storage at time *t*.

Before introducing the cost function some further constraints must be introduced. In fact, it is necessary to avoid that more than N^{sock} are charged simultaneously

$$\sum_{i\in EV}\theta_{i,t}^{EV}\le N^{sock} \qquad t\in T \qquad (4.15)$$

The binary variable $\theta_{i,t}^{EV}$ is linked with the power exchanged with the i-th EV by

$$K^{EV}\theta_{i,t}^{EV}-p_{i,t}^{EV}\ge 0 \qquad t\in T \qquad (4.16)$$

where K^{EV} is a large number [112].

Note that, this avoids the charging of the *i-th* EV if it is disconnected ($\theta_{i,t}^{EV}=0$).

There is also the need of introducing a constraint that imposes the consistency of the beginning of the charging process with the release time

$$t_i^{st}\ge T_i^{rel} \qquad i\in EV \qquad (4.17)$$

Similarly, the charging procedure must end before the deadline

$$t_i^{fi}\le T_i^{dl}+1 \qquad i\in EV \qquad (4.18)$$

A further constraint has the function of relating the state of the charging station with the time interval during which the charging of a vehicle *i* takes place

$$\begin{array}{llll}
if \ \left(T_i^{rel}-t\right)\ge 0 & & \rightarrow \ \theta_{i,t}^{EV}=0 & \\
if \ \left(T_i^{rel}-t\right)\ge 0 \ \ or & \left(t-\left(t_i^{f}+1\right)\right)\ge 0 & \rightarrow \ \theta_{i,t}^{EV}=0 & t\in T, i\in EV \qquad (4.19)\\
if \ \left(T_i^{rel}-t\right)\le 0 \ \ and & \left(t-\left(t_i^{f}+1\right)\right)\ge 0 & \rightarrow \ \theta_{i,t}^{EV}\in\left[0,1\right] &
\end{array}$$

Constraints (4.19) can be substituted by the following linear constraints

$$\left(1-\theta_{i,t}^{EV}\right)K^{avail} \geq \left(T_i^{rel}-t\right) \qquad t \in T, i \in EV \qquad (4.20)$$

$$\left(1-\theta_{i,t}^{EV}\right)K^{avail} \geq \left(t-(t_i^{fi}+1)\right) \qquad t \in T, i \in EV \qquad (4.21)$$

Afterwards, it is imposed that the EV leaves the charging station only when reaching the desired state of charge.

$$x_{i,t}^{EV} = X_i^{EV,fi} \qquad t = t_i^{fi},\ i \in EV \qquad (4.22)$$

Then, it is necessary to consider the constraints relevant to the dynamics of the charging process.

At the beginning of the charging process the state of charge must be equal to the initial one

$$x_{i,t}^{EV} = X_i^{EV,st} \qquad t = t_i^{st},\ i \in EV \qquad (4.23)$$

Moreover, the power exchange with the external should be limited within the minimum and maximum values

$$-\bar{P}^G \leq p_t^G \leq \bar{P}^G \qquad t \in T \qquad (4.24)$$

Similarly, the rated power should be considered for production plants from fossil fuels. That is,

$$0 \leq p_{l,t}^F \leq \bar{P}_l^F \qquad t \in T, l \in L \qquad (4.25)$$

Finally, the overall objective function is given by

$$\min\,(c^F + c^{buy} - c^{sell} + c^{tard}) \qquad (4.26)$$

with

$$c^F = \Delta C^F \sum_{t \in T}\sum_{l \in L} p_{l,t}^F \qquad (4.27)$$

$$c^{buy} = C_t^{buy}\Delta\sum_{t \in T}\max\left(p_t^G, 0\right) \qquad (4.28)$$

$$c^{sell} = C_t^{sell}\Delta\sum_{t \in T}\max\left(-p_t^G, 0\right) \qquad (4.29)$$

$$c^{tard} = \sum_{i \in EV}\Lambda_i \max\left(t_i^{fi}+1-T_i^{dd}, 0\right) \qquad (4.30)$$

where (4.27) represents the overall energy production cost for all non-renewables, where C^F [€/kWh] is the unit cost; (4.28) is the cost paid to buy energy from the main grid, with C_t^{buy} [€/kWh] the time-varying unit price; (4.29) is the income due to the sale of energy to the main grid, with C_t^{sell} [€/kWh] the time-varying unit benefit; (4.30) is the total tardiness cost with respect to the due date.

The optimization problem in (4.26) (MINLP) is solved with constraints (4.2)-(4.25).

4.5 Case study Application

In this Section, the developed optimization problem is applied to a case study. There are two traditional plants, one storage system, one photovoltaic plant, one wind turbine, one charging station equipped with only one socket ($N^{sock} = 1$), and electrical demand.

Data are reported in Table 4.1 (parameters of the microgrid) and Fig. 4.3 (forecasted power demand and production from photovoltaics) for a whole day.

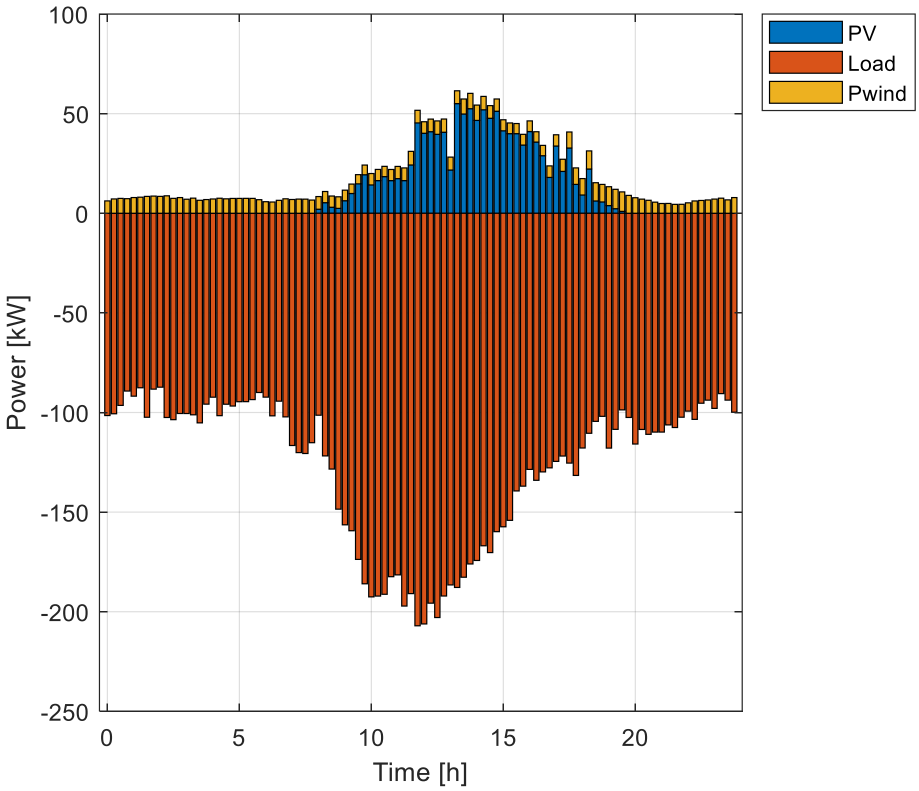

Fig. 4.3 Load and renewable generation

The piecewise constant pattern of unit cost C_t^{buy} [€/kWh] for the energy purchased by the external grid is shown in Fig. 4.4, while the energy selling price C_t^{sell} is kept constant to 0.08 [€/kWh].

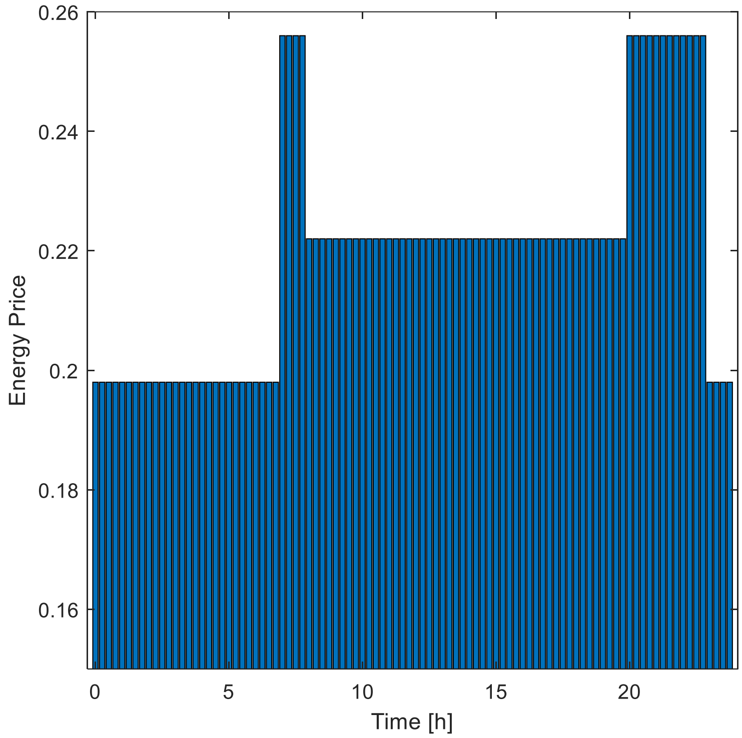

Fig. 4.4 Buying price pattern

In Table 4.1 the overall parameters of the microgrid's plants are reported

Table 4.1 Microgrid data

Parameter	Value	Parameter	Value
$\bar{P}_1^F$,	30[kW],	D^S	80
$\bar{P}_2^F$	65[kW]	$\underline{X}_m^S$	0.2
CAP^S	100[kWh]	$\bar{X}_m^S$	0.8
$\Gamma^{S,out}$	1.1	$\bar{P}_m^S$,	35[kW]
$\Gamma^{EV,out}$	1.1	C^F	0.2 [€/kWh]
$\Gamma^{S,in}$	0.9	$\bar{P}^G$	300 [kW]
$\Gamma^{EV,in}$	0.9	$P_m^{S,rated}$	-35 [kW]
A_m^S ,	0.8	K^{EV}	1000
A_i^{EV}	0.8	$K^{arrival}$	1000

The optimization problem has been implemented , by using Lingo optimization tool [113] on a PC Intel i7-6500U - 3.5GHz, 16 GB RAM. The overall optimization horizon consists of 24 hours and a time interval of 15 minutes (Δ =0.25 [h]). In the proposed simulation, four vehicles are considered, whose data are reported in Table 4.2.

Table 4.2 EVs' data

Parameter	Vehicle 1	Vehicle 2	Vehicle 3	Vehicle 4
$X_i^{EV,init}$	0	0	0	0
$X_i^{EV,fi}$	0.6	0.75	0.95	0.53
CAP_i^{EV}	22 [kWh]	25 [kWh]	31 [kWh]	22 [kWh]
$\overline{P}_i^{EV}$	13[kW]	13[kW]	13[kW]	13[kW]
T_i^{rel}	1.25[h]	2.5[h]	4.5[h]	8.75[h]
T_i^{dd}	5.5 [h]	9 [h]	12.5 [h]	15 [h]
T_i^{dl}	7.5 [h]	12 [h]	15.75 [h]	17.5 [h]
Λ_i	0.1 [€/h]	0.1 [€/h]	0.1 [€/h]	0.1 [€/h]

This instance of the scheduling problem has been solved in 33[s] with a cost of 340.12 [€]. The detailed scheduling of the microgrid is reported in Fig. 4.5.

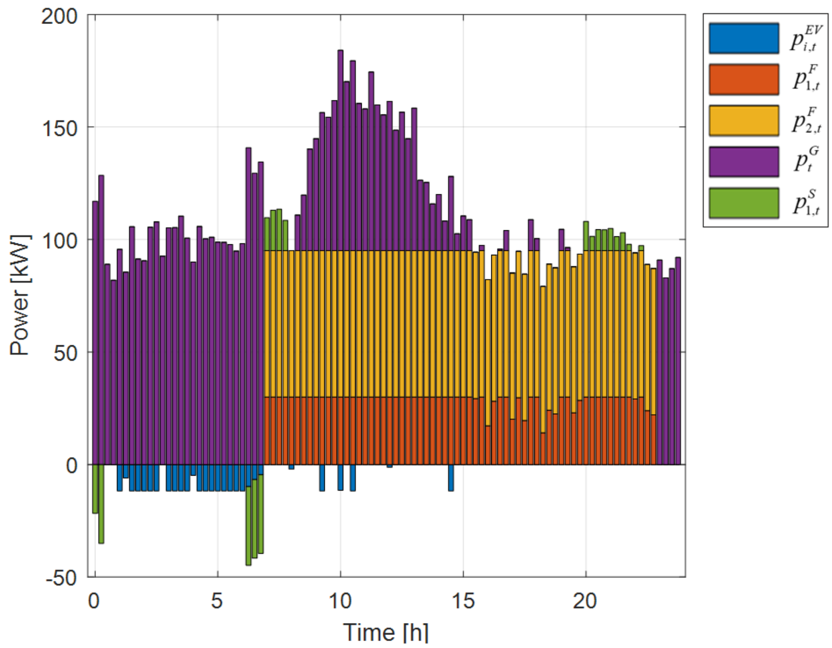

Fig. 4.5 Optimal microgrid scheduling

It is important to note that the power into the storage system and into the vehicles is negative when they are charged. Fig. 4.5 shows a consistent behavior of the traditional generators concerning the buying price pattern, as a matter of fact, are used only when the fuel price C^F is less than C_t^{buy}.

Fig. 4.6 depicts the Gantt diagram of the charging station (corresponding to the evolution of $\theta_{i,t}^{EV}$ variable). As can be seen from this figure the process of vehicle 3 is preempted with respect to vehicle 4.

Finally, as regards the charging vehicles, scheduling is reported in Fig. 4.7. Each vehicle is recharged with respect to the timing constraints. Particularly is the power pattern of vehicle 3, where is clear the activation of the constraints related to the battery charge (4.11) when the state of charge is close to 90%, the power absorbed is far from the maximum (i.e., 13 [kW]).

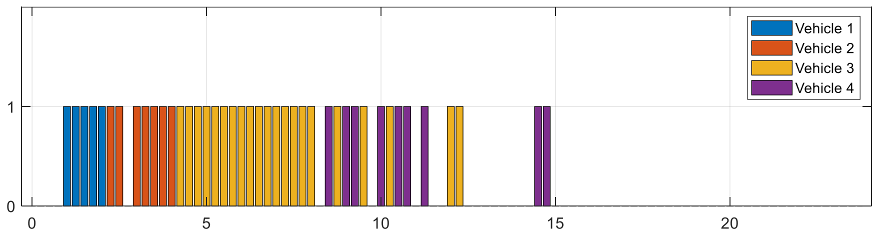

Fig. 4.6 Charging station Gantt diagram

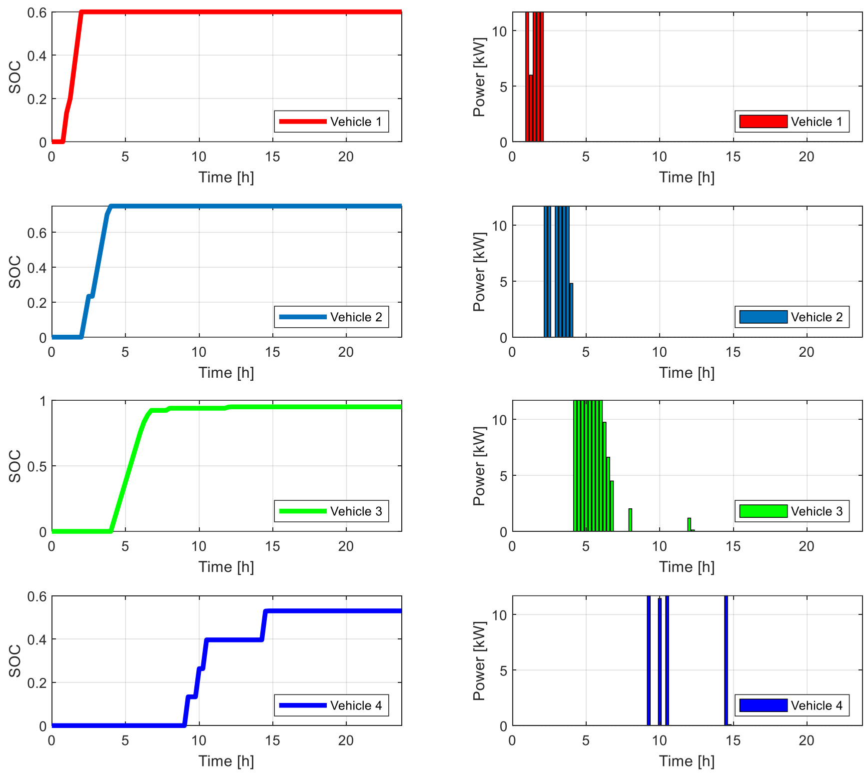

Fig. 4.7 Optimal EV scheduling

Chapter 5
Optimal charging of EVs in smart grids: discrete event optimization for a-periodic scheduling

In the next subsections, a discrete event approach is proposed for the optimal scheduling of EVs in which vehicles are the customers and charging stations are the machines. It has a central importance to highlight that in this formulation of the problem it is considered a system with one charging station, equipped with a single socket. The optimization model is applied to a real case study in the Savona Campus of the University of Genoa, which includes the connection to the main grid, different renewable source plants, an electrical storage system, a conventional plant for power generation, and a vehicle charging station.

Specifically, the rest of the chapter is organized as follows. In Section 5.1 the system model will be introduced. Section 5.2 is dedicated to the piecewise linear model of the battery. In Section 5.3 the developed approach for determining the optimal schedule and the actual power flow is presented. The application of the proposed model to a case study is described in Section 5.4.

Moreover, in Section 5.5 an extension to the multi-socket formalization is provided. Finally, in Section 5.6 a discussion about the periodic scheduling is presented.

5.1 The considered model

As seen in the previous chapter, these general rules about nomenclature hold:

- upper case letters will be parameters.
- lower case letters will be variables.
- subscript letters will be indices.
- superscript letters will be descriptive.
- minimum (maximum) values are represented with a line below (above) the letter.

Fig. 5.1 represents the system considered in this model formulation.

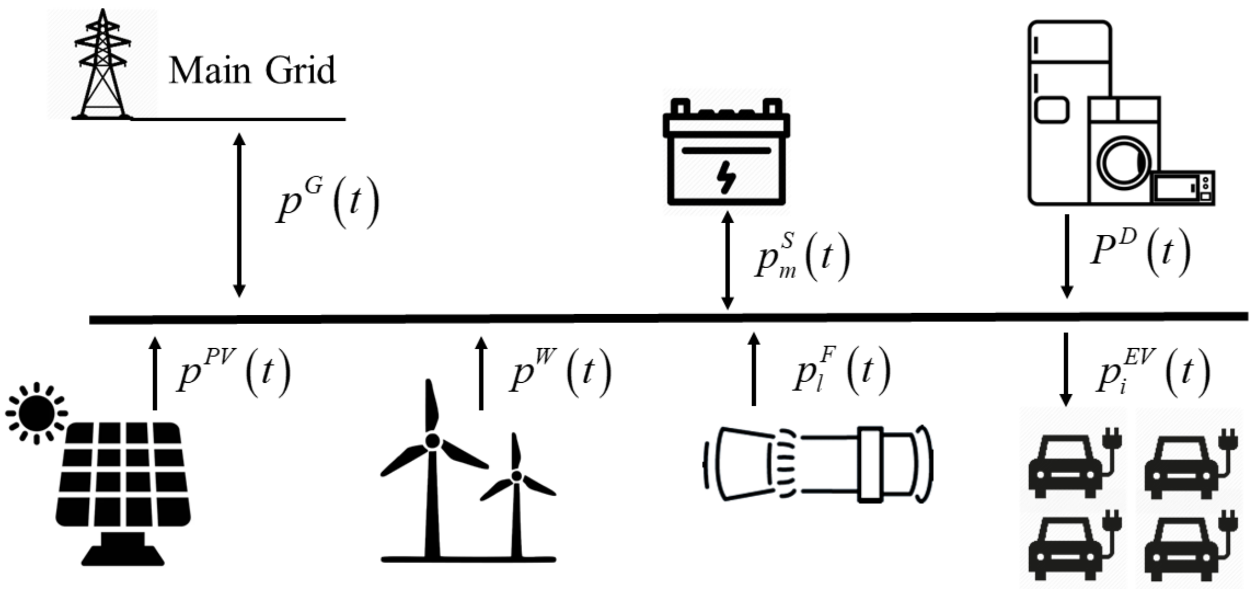

Fig. 5.1The considered system.

In order to define the mathematical model, the following sets are introduced

- $T = \{1,...,N^T\}$ set of time intervals.
- $L = \{1,...,N^F\}$ set of fossil fuel generators.
- $M = \{1,...,N^S\}$ set of storage systems.
- $EV = \{1,...,N^{EV}\}$ set of EVs.

The power flows in the system are:

- $p_i^{EV}(t)$, that is the (monodirectional) power flow to the *i-th* EV; obviously, $p_i^{EV}(t) = 0$ if at time instant *t* there is no vehicle under charge;
- $p^G(t)$, that is the (bi-directional) power flow from the main grid to the microgrid; the active sign convention is adopted; namely, the power flow is assumed positive when power is drawn (bought) from the main grid (and negative when power is given (sold) to the main grid;
- $P^{PV}(t)$ ($P^W(t)$), that is the (monodirectional) power coming from photovoltaic power plants (wind turbines)
- $p_l^F(t)$, that is the (monodirectional) power flow from the *l-th* energy source fed by fossil fuel to the microgrid;
- $P^D(t)$, that is the (monodirectional) power flow representing the non-deferrable power demand;
- $p_m^S(t)$, that is the (bi-directional) power flow from the *m-th* energy storage element; here again, this flow is assumed positive when power is drawn from this element.

The value of the state of charge at time instant t in the *m-th* storage element will be denoted by $x_m^S(t)$

In the considered model, it is assumed that *the service sequence is given*, that is, the vehicles are charged following the order of their arrivals. Thus, the only decisions to be taken in the considered scheduling model *are those concerning the timing of services* (in this case, the *starting time* and the *duration* of the charging time intervals).

For each vehicle V_i requiring the charging service, it is assumed that all information regarding arrival times, charging requests, and departure due times is known *a priori*. Such information is reported in Table 5.1 in detail.

Table 5.1 Known parameters for EVs.

Symbol	**Name**	**Description**
T_i^{rel}	Release time	the time instant at which the vehicle becomes available for service (this may correspond to the forecasted arrival time at the service station)
T_i^{dd}	Due date	the time instant at which the service for the vehicle should be completed (according to the customer's preference)
T_i^{dl}	Deadline	the time instant at which the service must be completed (mandatory)
E_i	Energy request	the amount of energy requested for the charging service
Λ_i	Penalty coefficient	the cost paid for a unit delay (with respect to the due date for the service completion, dd_i), per unit of energy requested. It is expressed in [€/(h)].

In the considered model, the energy request E_i by the *i-th* vehicle must be completely satisfied. Thus, customer dissatisfaction may only refer to tardiness concerning the due date and not to the lack of complete demand satisfaction. In addition, no preemption in the charging services is allowed. It is assumed that the service station manager cannot refuse service to any customer. Finally, the presence of deadline constraints (regarding service completion times) is taken into account.

The service sequence can thus be represented as in Fig. 5.2, where the lengths of the rectangles corresponding to the various services represent the charging service durations.

Fig. 5.2 The service sequence for the charging of vehicles.

The completion time instant of the charging of the *i-th* vehicle is denoted as t_i^C. Then, the time interval between the charging completion time instants of two subsequent vehicles can be divided into (see Fig. 5.3):

- t_i^{CH} that is the charging time (interval) for the *i*-th vehicle;

- t_i^{IDLE} that is the idle time interval *before* the charging of the *i*-th vehicle.

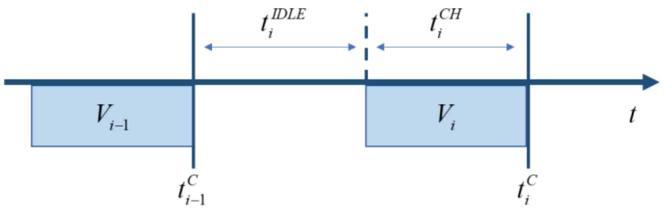

Fig. 5.3 The time intervals between two successive completion time instants.

Having chosen to adopt a discrete event representation of the dynamics of the system, the only values of the state variables of the system (i.e., $x_m^S(t)$) that must be evaluated are those corresponding to the completion of the services, that is $x_m^S(t_i^C)$, assuming that the initial state $x_m^S(0)$ is given.

Note that, for brevity all the variables referred to the interval corresponding to the *i-th* EV, will assume the index i .

Then, the following *restrictive assumption* is introduced, with the objective of defining a parametric (instead of a functional) optimization problem. The values of the power purchased/sold from/to the main grid $p^G(t)$, and the (costly) power generated by the *l-th* fossil source $p_l^F(t) \quad l \in L$ are kept at a constant value (resp. p_i^{G1} and p_l^{F1}) within each idle time interval $\left(t_{i-1}^C, t_{i-1}^C + t_i^{IDLE}\right)$ and at another constant value (resp. p_i^{G2} and p_l^{F2})), within each charging time interval $\left(t_{i-1}^C + t_i^{IDLE}, t_i^C\right)$, for $i \in EV, l \in L$.

Although the value of the power flow to the charging station $p^{EV}(t)$ cannot be kept constant within each charging time interval $\left(t_{i-1}^C + t_i^{IDLE}, t_i^C\right)$, owing to the necessity of modelling the non-linear behavior of the vehicles' battery, in a first formulation of the problem the average values $p_i^{EV} \quad i \in EV$ will be considered as decision variables. Note that due to the nature of the model, the index relevant to the vehicle (i) is automatically referring to the specific time interval in which the charging process will take place. In fact, the power p_i^{EV} is the power flow to the *i-th* EV in the time interval $\left(t_{i-1}^C + t_i^{IDLE}, t_i^C\right)$.

It is assumed that the forecasts of the renewable powers $P^W(t)$ and $P^{PV}(t)$, as well as the power demand $P^D(t)$, and the selling/buying prices ($c^{sell}(t)$ and $c^{buy}(t)$) to/from the main grid, are available and completely reliable for $t \geq 0$. That is to say, no uncertainty modeling is introduced. Thus, the function $P^{NL}(t)$ which represents the net load and is defined as

$$P^{NL}(t) = P^D(t) - P^W(t) - P^{PV}(t) \tag{5.1}$$

5.2 Piecewise linear battery modelling

In real storage systems, the maximum injectable power depends on the state of charge, as described in the results of [92]. Specifically, considering a storage system, equipped with its battery management system, which receives commands from a central controller like an EMS, it happens that, beyond a certain value of the state of charge, the maximum power that can be injected is lower than the rated value. This phenomenon can be (approximately) represented through a piecewise linear model as depicted in Fig. 5.4, where the feasible pairs (state of charge, injectable power) are those inside or on the contour of the grey polygon. For simplicity's sake, the following model for the EV's battery is presented in this section. However, it can be easily converted to the one relevant to the storage by specifying the proper variables' names in the superscripts.

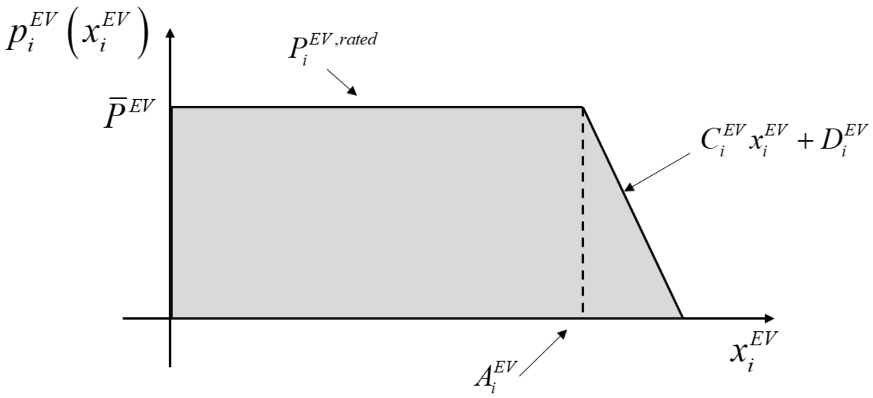

Fig. 5.4 Piecewise linear battery constraints (charging of EVs).

The function represented in Fig. 5.4, providing the maximum injectable power for any value of the state of charge, can be expressed as

$$\overline{P}^{EV}(x_i^{EV})=\begin{cases}P_i^{EV,rated} & if \quad x_i^{EV}\le A_i^{EV}\\ C_i^{EV}x_i^{EV}+D_i^{EV} & if \quad x_i^{EV}\ge A_i^{EV}\end{cases} \qquad i\in EV \tag{5.2}$$

where of course parameters A_i^{EV} , C_i^{EV} and D_i^{EV} must satisfy the condition $C_i^{EV}A_i^{EV}+D_i^{EV}=P_i^{EV,rated}$. Besides, $\overline{P}^{EV}\left(1\right)=0$ and thus it turns out $D_i^{EV}=-C_i^{EV}$.

Hence parameter D_i^{EV} is simply given by

$$D_i^{EV}=\frac{P_i^{EV,rated}}{1-A_i^{EV}} \qquad i\in EV \tag{5.3}$$

In this chapter, it is assumed that the charging process of a vehicle battery takes place according to the profile represented in Fig. 5.5 by the blue line, indicated in the following as the function

$$\overline{P}^{EV}(x_i^{EV}) = \begin{cases} p_i^{EV,init} & if \quad x_i^{EV} \le B_i^{EV} \\ D_i^{EV}\left(1 - x_i^{EV}\right) & if \quad x_i^{EV} \ge B_i^{EV} \end{cases} \qquad i \in EV \tag{5.4}$$

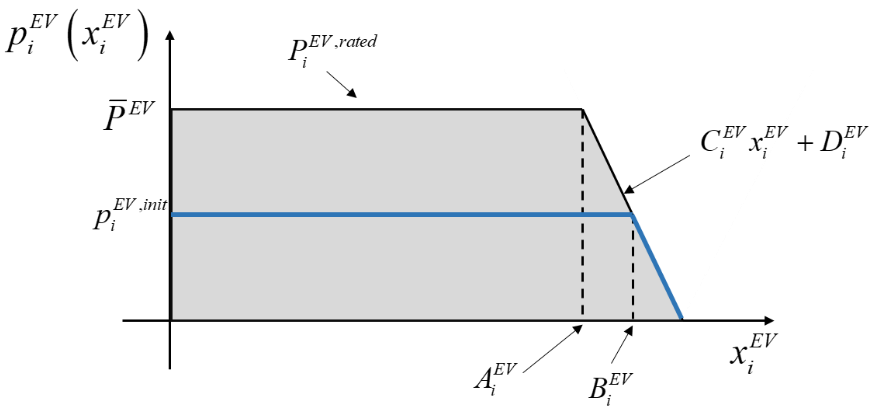

Fig. 5.5 The charging profile of the battery.

where $p_i^{EV,init}$ is the “nominal” power at which the charging process takes place, and parameter B_i^{EV} satisfies the condition $D_i^{EV}\left(1 - B_i^{EV}\right) = p_i^{EV,init}$, that is

$$B_i^{EV} = 1 - \frac{p_i^{EV,init}}{D_i^{EV}} \qquad i \in EV \tag{5.5}$$

Of course, the choice of imposing that the charging process takes place according to a profile like the one represented in Fig. 5.6 is arbitrary. In fact, any profile lying below the piecewise function in (5.2) is acceptable. Nevertheless, as the aim is to defining a parameter optimization problem (and not a functional one), it is imposed that the charging profile is characterized by only a parameter, like $p_i^{EV,init}$ in Fig. 5.5.

The following conditions are assumed to be valid

$$X_i^{EV,init} \le A_i^{EV} \qquad i \in EV \tag{5.6}$$

$$B_i^{EV} \le X_i^{EV,fin} \qquad i \in EV \tag{5.7}$$

so that the actual charging profile is that represented in Fig. 5.6. The above assumption that (5.6) and (5.7) hold is equivalent to assuming that the requested charging service for any vehicle starts from relatively low values and finishes at relatively high values of the state of charge of its battery.

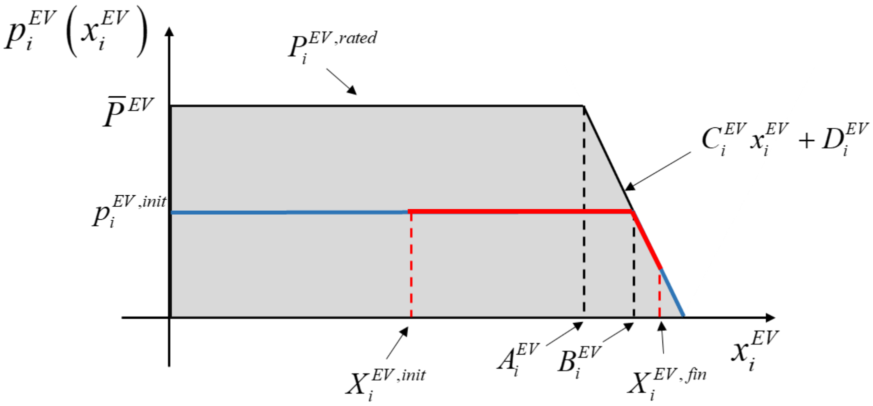

Fig. 5.6 The actual power profile of the battery (red line).

In the following, the value of $p_i^{EV,init}$, that of course has to satisfy the condition $p_i^{EV,init} \le P_i^{EV,rated}$, will be considered as a decision variable of the problem.

On this basis, if the (known) initial state of charge of the battery at the beginning of the charging process is assumed to be $X_i^{EV,init}$ and that the (known) required state of charge, at the end of the charging process is $X_i^{EV,fin}$, the time needed for the charging process can be evaluated as

$$t_i^{CH} = CAP_i^{EV} \int_{X_i^{EV,init}}^{X_i^{EV,fin}} \frac{dx}{P^{EV}\left(x_i^{EV}\right)} \qquad i \in EV \qquad (5.8)$$

Given the above expression of B_i^{EV}, condition (5.7) becomes

$$X_i^{EV,fin} \ge 1 - \frac{p_i^{EV,init}}{D_i^{EV}} \qquad i \in EV \qquad (5.9)$$

that is,

$$p_i^{EV,init} \ge D_i^{EV}\left(1 - X_i^{EV,fin}\right) \qquad i \in EV \qquad (5.10)$$

The above inequality represents a constraint over the choice of the parameter $p_i^{EV,init}$ that is induced by the value of the desired $X_i^{EV,fin}$.

Thus, the time interval required for charging can be evaluated as

$$t_i^{CH}\left(p_i^{EV,init}\right)=CAP_i^{EV}\left(\int_{X_i^{EV,init}}^{B_i^{EV}}\frac{dx}{\Gamma^{EV,in}P^{EV}\left(x_i^{EV}\right)}+\int_{B_i^{EV}}^{X_i^{EV,fin}}\frac{dx}{\Gamma^{EV,in}D_i^{EV}\left(1-x_i^{EV}\right)}\right)=$$

$$=CAP_i^{EV}\left(\frac{B_i^{EV}-X_i^{EV,init}}{\Gamma^{EV,in}p_i^{EV,init}}-\frac{\ln\left(D_i^{EV}-D_i^{EV}x\right)\Big|_{B_i^{EV}}^{X_i^{EV,fin}}}{\Gamma^{EV,in}D_i^{EV}}\right)=$$

$$=CAP_i^{EV}\left(\frac{1-\frac{p_i^{EV,init}}{D_i^{EV}}-X_i^{EV,init}}{\Gamma^{EV,in}p_i^{EV,init}}-\frac{\ln\left(D_i^{EV}-D_i^{EV}X_i^{EV,fin}\right)-\ln\left(p_i^{EV,init}\right)}{\Gamma^{EV,in}D_i^{EV}}\right)= \qquad i\in EV \tag{5.11}$$

$$=CAP_i^{EV}\left(\frac{1-\frac{p_i^{EV,init}}{D_i^{EV}}-X_i^{EV,init}}{\Gamma^{EV,in}p_i^{EV,init}}-\frac{\ln\frac{d_{EV,i}\left(1-X_i^{EV,fin}\right)}{p_i^{EV,init}}}{\Gamma^{EV,in}D_i^{EV}}\right)$$

Note that in (5.11) it has been put into evidence the dependence of the duration of the charging service time on the initial input power $p_i^{EV,init}$.

Moreover, it must be recalled that the following constraints

$$0\le p_i^{EV,init}\le P_i^{EV,rated} \qquad i\in EV \tag{5.12}$$

5.3 The proposed optimization approach

To formalize the considered discrete event scheduling problem, the following approach is proposed.

5.3.1 Expressing the length of the charging interval as a function of the initial power

In fact, assuming the charging profile in Fig. 5.6 has been selected, $p_i^{EV}(t)$ can be represented as a function of the state of charge $x_i^{EV}(t)$ as given by (5.4).

In the following, the simplified notation

$p_i^{EV}(t) \to p(t)$
$x_i^{EV}(t) \to x(t)$
$CAP_i^{EV} \to CAP$
$D_i^{EV} \to D$
$B_i^{EV} \to B$
$p_i^{EV,init} \to p^{init}$
$X_i^{EV,init} \to X^{init}$
$X_i^{EV,fin} \to X^{fin}$
$\Gamma^{EV,in} \to \Gamma$
$P_i^{EV,rated} \to P^{rated}$

will be used.

The problem is that of integrating the differential equation

$$\dot{x} = \frac{\Gamma p(t)}{CAP} \tag{5.13}$$

over the considered time interval. Note that Γ is the charging efficiency and it is assumed to be constant during the charging process.

Integrating to the interval $X^{init} \leq x \leq B$

In this interval

$$p(t) = p^{init} \tag{5.14}$$

then

$$\dot{x} = \frac{\Gamma p^{init}}{CAP} \tag{5.15}$$

and thus, the solution is simply

$$x(t) = X^{init} + \frac{\Gamma p^{init}}{CAP} t \tag{5.16}$$

The time instant t' at which $x(t)$ reaches the value B must be determined. That is

$$B = X^{init} + \frac{\Gamma p^{init}}{CAP} t' \Rightarrow t' = \frac{B - X^{init}}{\Gamma p^{init}} CAP \tag{5.17}$$

Since from (5.5) $B = 1 - \frac{p^{init}}{D}$, it is possible to obtain

$$t' = \frac{1 - \frac{p^{init}}{D} - X^{init}}{\Gamma p^{init}} CAP \tag{5.18}$$

Of course, it must be $t_{i-1}^{C} + t_i^{IDLE} + t' \leq t_i^{C}$.

Thus, it is

$$p(t) = p^{init} \qquad for \quad t_{i-1}^{C} + t_i^{IDLE} \leq t \leq t_{i-1}^{C} + t_i^{IDLE} + t' \tag{5.19}$$

Integrating to the interval $B \leq x \leq X^{fin}$

In this interval

$$p(t) = D\left(1 - x\right) \tag{5.20}$$

Thus, the differential equation that has to be integrated is

$$\dot{x} = \frac{\Gamma D(1-x)}{CAP} \tag{5.21}$$

that is

$$\dot{x} + \frac{\Gamma D}{CAP} x = \frac{\Gamma D}{CAP} \tag{5.22}$$

with the initial condition $x(t') = B$.

Solving the above differential equation (substituting $\frac{\Gamma D}{CAP}$), it is obtained

$$x(t) = 1\left(t - t'\right) + \left(B - 1\right) e^{-\frac{\Gamma D}{CAP}\left(t - t'\right)} 1\left(t - t'\right) \tag{5.23}$$

Question. When does the charging process end?

The conclusion of the charging process takes place when

$$x(t) = X^{fin} \tag{5.24}$$

then the charging process ends at time instant t'', where t'' satisfies

$$
\begin{aligned}
&X^{fin} = 1 + (B-1)e^{-\frac{\Gamma D}{CAP}(t''-t')} \\
&\frac{X^{fin}-1}{B-1} = e^{-\frac{\Gamma D}{CAP}(t''-t')} \\
&(t''-t') = -\frac{CAP}{\Gamma D}\ln\left(\frac{1-X^{fin}}{1-B}\right)
\end{aligned}
\tag{5.25}
$$

But, of course, it must be $t'' = t_i^{CH}$. And thus,

$$
t_i^{CH} = t' - \frac{CAP}{\Gamma D}\ln\left(\frac{1-X^{fin}}{1-B}\right) \tag{5.26}
$$

and thus the expression of t_i^{CH} as a function of p^{init} is

$$
t_i^{CH} = \frac{CAP}{\Gamma}\left[\frac{1-\frac{p^{init}}{D}-X^{init}}{p^{init}} - \frac{1}{D}\ln\left(\frac{D\left(1-X^{fin}\right)}{p^{init}}\right)\right] \tag{5.27}
$$

Of course, the power profile is given by

$$
p(t) = \begin{cases} p^{init} & if \quad t_{i-1}^{C} + t_i^{IDLE} \le t \le t_{i-1}^{C} + t_i^{IDLE} + t' \\ p^{init} e^{-\frac{\Gamma D}{CAP}(t-t')} & if \quad t_{i-1}^{C} + t_i^{IDLE} + t' \le t \le t_i^{C} \end{cases} \tag{5.28}
$$

5.3.2 Determining the minimum length of the charging interval

As the physical meaning of t_i^{CH} , this function is a monotonic nonincreasing function (see Fig. 5.7) and its minimum coincides with the maximum value of p^{init} , i.e. P^{rated} . Note that the function in (5.27) is in fact a function of p^{init} .

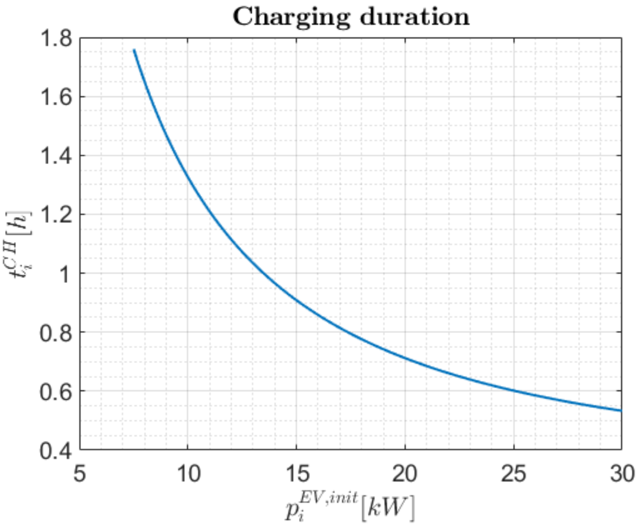

Fig. 5.7 Length of the charging interval according to the initial power.

Then, by substituting P^{rated} into (5.27), the minimum admissible duration for the charging interval t_i^{CH} is found, namely $\underline{T}_i^{CH}$, given by

$$\underline{T}_i^{CH} = \frac{CAP}{\Gamma}\left[\frac{1-\frac{P^{rated}}{D}-X^{init}}{P^{rated}}-\frac{1}{D}\ln\left(\frac{d\left(1-X^{fin}\right)}{P^{rated}}\right)\right] \tag{5.29}$$

From this equation it is clear how this minimum length of the time interval depends only on the data and can be calculated during the pre-processing.

5.3.3 Solving the optimization problem

An optimization problem is considered, which provides the scheduling of the charging processes determined considering average power flows. Specifically, the objective function which is composed by the following terms:

- The costs/benefits of energy taken/sold from/to the main grid during idle (c_i^{G1}) and charging (c_i^{G2}) time intervals;
- The cost of production by power plants from fossil fuel plants during idle (c_i^{F1}) and charging (c_i^{F2}) time intervals;
- The tardiness costs of the various vehicles (c_i^{tard}).

where terms referring to the idle intervals are characterized by a "1" in the apex, the ones referring to the charging intervals by a "2".

Namely, the optimization objective is

$$\min \quad \sum_{i=1}^{N} \left\{ c_i^{G1} + c_i^{G2} + c_i^{F1} + c_i^{F2} + c_i^{tard} \right\} \tag{5.30}$$

To express the first two terms inside the summation, it is convenient to define

$$p_i^{G1,in} = \max\left\{ p_i^{G1}, 0 \right\} \qquad i \in EV \tag{5.31}$$

$$p_i^{G1,out} = \max\left\{ -p_i^{G1}, 0 \right\} \qquad i \in EV \tag{5.32}$$

and similarly

$$p_i^{G2,in} = \max\left\{ p_i^{G2}, 0 \right\} \qquad i \in EV \tag{5.33}$$

$$p_i^{G2,out} = \max\left\{ -p_i^{G2}, 0 \right\} \qquad i \in EV \tag{5.34}$$

so that

$$p_i^{G1} = p_i^{G1,in} - p_i^{G1,out} \qquad i \in EV \tag{5.35}$$

$$p_i^{G2} = p_i^{G2,in} - p_i^{G2,out} \qquad i \in EV \tag{5.36}$$

Thus,

$$c_i^{G1} = \left\{ \left[\int_{t_{i-1}^C}^{t_{i-1}^C + t_i^{IDLE}} C^{buy}(t)\,dt \right] p_i^{G1,in} - \left[\int_{t_{i-1}^C}^{t_{i-1}^C + t_i^{IDLE}} C^{sell}(t)\,dt \right] p_i^{G1,out} \right\} \quad i \in EV \tag{5.37}$$

$$c_i^{G2} = \left\{ \left[\int_{t_{i-1}^C + t_i^{IDLE}}^{t_i^C} C^{buy}(t)\,dt \right] p_i^{G2,in} - \left[\int_{t_{i-1}^C + t_i^{IDLE}}^{t_i^C} C^{sell}(t)\,dt \right] p_i^{G2,out} \right\} \quad i \in EV \tag{5.38}$$

It is important to note that the integral terms appearing in (5.37) and (5.38), are indeed known functions of t_i^C, t_{i-1}^C, and t_i^{IDLE}, since it has been assumed the availability and the reliability of a forecast of the patterns $C^{buy}(t)$ and $C^{sell}(t)$.

The production costs for each non-renewable plant *l*, is given by of the unit cost of production C^F [€/kWh] (assumed equal for each fossil power plant) multiplied by the power produced by that plant and the duration of the time interval (for idle and charging, respectively). The value of the overall production cost, during each time interval, is given by

$$c_i^{F1} = C^F \sum_{l \in L} p_{l,i}^{F1} t_i^{IDLE} \qquad i \in EV \tag{5.39}$$

$$c_i^{F2} = C^F \sum_{l \in L} p_{l,i}^{F2} t_i^{CH} \qquad i \in EV \qquad (5.40)$$

The tardiness cost is given by the tardiness in charging d_i^{tard} ($d_i^{tard} = \max\left\{t_i^C - T_i^{dd}, 0\right\}$) multiplied by a penalty coefficient Λ_i [€/h] for unitary tardiness of the completion of charging service i. That is,

$$c_i^{tard} = \Lambda_i d_i^{tard} \qquad i \in EV \qquad (5.41)$$

It is possible to define two power balance constraints, one for each type of time intervals in which the time horizon is divided (i.e. idle and charging time intervals).

$$p_i^{G1} + \sum_{l \in L} p_{l,i}^{F1} + \sum_{m \in M} p_{m,i}^{S1} = p_i^{NL1} \qquad i \in EV \qquad (5.42)$$

$$p_i^{G2} + \sum_{l \in L} p_{l,i}^{F2} + \sum_{m \in M} p_{m,i}^{S2} = p_i^{NL2} + p_i^{EV} \qquad i \in EV \qquad (5.43)$$

when all the terms are defined as average values over the time intervals $\left(t_{i-1}^C, t_{i-1}^C + t_i^{IDLE}\right)$ and $\left(t_{i-1}^C + t_i^{IDLE}, t_i^C\right)$ respectively, apart from

$$p_i^{NL1} = \int_{t_{i-1}^C}^{t_{i-1}^C + t_i^{IDLE}} P^{NL}(t)\, dt \qquad i \in EV \qquad (5.44)$$

$$p_i^{NL2} = \int_{t_{i-1}^C + t_i^{IDLE}}^{t_i^C} P^{NL}(t)\, dt \qquad i \in EV \qquad (5.45)$$

which are indeed a known function of t_i^C, t_{i-1}^C, and t_i^{IDLE}, since the availability and the reliability of a forecast of the pattern $P^{NL}(t)$ has been assumed. Note that the variable p_i^{EV} is not specified for the idle interval according to its definition.

Then, some basic constraints on the electrical storage must be introduced

$$x_{m,i}^{S1,fin} = x_{m,i}^{S1,init} + \Gamma^{S,in} p_{m,i}^{S1,in} t_i^{IDLE} - \Gamma^{S,out} p_{m,i}^{S1,out} t_i^{IDLE} \qquad m \in M, i \in EV \qquad (5.46)$$

$$x_{m,i}^{S2,fin} = x_{m,i}^{S2,in} + \Gamma^{S,in} p_{m,i}^{S2,in} t_i^{CH} - \Gamma^{S,out} p_{m,i}^{S2,out} t_i^{CH} \qquad m \in M, i \in EV \qquad (5.47)$$

$$x_{m,i}^{S1,fin} = x_{m,i}^{S2,init} \qquad m \in M, i \in EV \qquad (5.48)$$

$$x_{m,i}^{S2,fin} = x_{m,i+1}^{S1,init} \qquad m \in M, i \in EV \qquad (5.49)$$

where the power flows are distinguished among charging and discharging contributions. Owing to the choice of the optimization objective, for any time interval $p_{m,i}^{S1,in}\left(p_{m,i}^{S2,in}\right)$ and $p_{m,i}^{S1,out}\left(p_{m,i}^{S2,out}\right)$ cannot be jointly positive. The constraints are

$$p_{m,i}^{S1} = p_{m,i}^{S1,in} - p_{m,i}^{S1,out} \qquad m \in M, i \in EV \tag{5.50}$$

$$p_{m,i}^{S2} = p_{m,i}^{S2,in} - p_{m,i}^{S2,out} \qquad m \in M, i \in EV \tag{5.51}$$

The total energy request of the EVs

$$p_i^{EV} t_i^{CH} = E_i \qquad i \in EV \tag{5.52}$$

where the energy request is given by

$$E_i = \left(X_i^{EV,fin} - X_i^{EV,init} \right) CAP_i^{EV} \qquad i \in EV \tag{5.53}$$

Then, the deadlines must not be overcome

$$t_i^C \le T_i^{dl} \qquad i \in EV \tag{5.54}$$

Then, service cannot begin before the release time, and thus the difference between completion time and the time necessary for charging should be greater or equal to the release time:

$$t_i^C - t_i^{CH} \ge T_i^{rel} \qquad i \in EV \tag{5.55}$$

The idle time interval for the *i-th* vehicle should be greater or equal to a minimum duration and it is related to the completion time (of the *i-th* vehicle and of the preceding one *i-1*) and to the charging time:

$$t_i^{IDLE} \ge \Omega \qquad i \in EV \tag{5.56}$$

Some fundamental constraints that must be introduced are those relevant to the minimum length of the charging interval (determined in Section 4.5.2) and the proper definition of that interval. That is,

$$t_i^{CH} \ge \underline{T}_i^{CH} \qquad i \in EV \tag{5.57}$$

$$t_i^{CH} = t_i^C - t_{i-1}^C - t_i^{IDLE} \qquad i \in EV \tag{5.58}$$

Besides, the constraints related to the definition of tardiness must be imposed

$$d_i^{tard} = \max\left\{ t_i^C - T_i^{dd}, 0 \right\} \qquad i \in EV \tag{5.59}$$

Then, the bounds to limit some power flows (exchange with the external grid, power exchange with the storage systems, power production from traditional plants) are, respectively

$$-\overline{P}^G \le p_i^{G1} \le \overline{P}^G \qquad i \in EV \tag{5.60}$$

$$-\overline{P}^G \le p_i^{G2} \le \overline{P}^G \qquad i \in EV \tag{5.61}$$

$$-\overline{P}_m^S \le p_{m,i}^{S1} \le \overline{P}_m^S \qquad m \in M, i \in EV \tag{5.62}$$

$$-\overline{P}_m^S \le p_{m,i}^{S2} \le \overline{P}_m^S \qquad m \in M, i \in EV \tag{5.63}$$

$$\underline{P}_l^F \le p_{l,i}^{F1} \le \overline{P}_l^F \qquad l \in L, i \in EV \tag{5.64}$$

$$\underline{P}_l^F \le p_{l,i}^{F2} \le \overline{P}_l^F \qquad l \in L, i \in EV \tag{5.65}$$

Moreover, some constraints relevant to the maximum and minimum state of charge

$$\underline{X}_m^S \le x_{m,i}^{S1,init} \le \overline{X}_m^S \qquad m \in M, i \in EV \tag{5.66}$$

$$\underline{X}_m^S \le x_{m,i}^{S2,init} \le \overline{X}_m^S \qquad m \in M, i \in EV \tag{5.67}$$

$$\underline{X}_m^S \le x_{m,i}^{S1,fin} \le \overline{X}_m^S \qquad m \in M, i \in EV \tag{5.68}$$

$$\underline{X}_m^S \le x_{m,i}^{S2,fin} \le \overline{X}_m^S \qquad m \in M, i \in EV \tag{5.69}$$

It is also necessary to impose

$$D_i^{EV}\left(1 - X_i^{EV,fin}\right) \le p_i^{EV} \le P_i^{EV,rated} \qquad i \in EV \tag{5.70}$$

Finally, all variables are understood to be non-negative, but $p_i^{G1}, p_i^{G2}, p_{m,i}^{S1}$, and $p_{m,i}^{S2}$.

Having introduced all the constraints it is possible then to solve the MINLP problem in (5.30) subject to constraints (5.35), (5.42)-(5.70)

It is important to note that the formalization of the optimization problem has been carried out assuming the availability of the forecasts of net non-deferrable load and the buying-selling prices for the whole optimization horizon. In the problem statement, these forecasts are considered as completely reliable, and no uncertainty modelling is introduced. This fact gives rise to a predictive control scheme. Then, one can imagine to repeatedly apply the proposed approach, each time conditioned by the most recent information about the system state and by the availability of the freshest predictions. For instance, one can state and solve a new problem at any service completion time (taking into account possible new service requests). In this way, a predictive (rolling horizon) discrete event control scheme is applied.

5.3.4 Determining the initial charging power

Once the problem has been solved it is possible to find the initial power by determining the relation between p_i^{EV} and the decision variable $p_i^{EV,init}$, integrating the function $p_i^{EV}(t)$ in (5.28) and the following constraints are obtained:

$$p_i^{EV} t_i^{CH} = \int_{t_{i-1}^{C}+t_i^{IDLE}}^{t_{i-1}^{C}+t_i^{IDLE}+t'} p_i^{EV,init} dt + \int_{t_{i-1}^{C}+t_i^{IDLE}+t'}^{t_i^{C}} \left[p_i^{EV,init} e^{-\frac{\Gamma^{EV} D_i^{EV}}{CAP}(t-t')} \right] dt$$

$$= p_i^{EV,init}[t'] + p_i^{EV,init} \left(-\frac{CAP_i^{EV}}{\Gamma^{EV} D_i^{EV}} \right) \left[e^{-\frac{\Gamma^{EV} D_i^{EV}}{CAP_i^{EV}}(t_i^{CH}-t')} - 1 \right] \qquad i \in EV \qquad (5.71)$$

$$= p_i^{EV,init} \left[t' - \frac{CAP_i^{EV}}{\Gamma^{EV} D_i^{EV}} \left(e^{-\frac{\Gamma^{EV} D_i^{EV}}{CAP_i^{EV}}(t_i^{CH}-t')} - 1 \right) \right]$$

Then, the average power is determined by

$$p_i^{EV} = \frac{p_i^{EV,init} \left[t' - \frac{CAP_i^{EV}}{\Gamma^{EV} D_i^{EV}} \left(e^{-\frac{\Gamma^{EV} D_i^{EV}}{CAP_i^{EV}}(t_i^{CH}-t')} - 1 \right) \right]}{t_i^{CH}} \qquad i \in EV \qquad (5.72)$$

Then, substituting t' with $\frac{B_i^{EV} - X_i^{EV,init}}{\Gamma^{EV} p_i^{EV,init}} CAP_i^{EV}$,and rearranging the equation

$$p_i^{EV} = \frac{p_i^{EV,init} CAP_i^{EV}}{t_i^{CH} \Gamma^{EV}} \left[\frac{1 - \frac{p_i^{EV,init}}{D_i^{EV}} - X_i^{EV,init}}{p_i^{EV,init}} - \frac{1}{D_i^{EV}} \left(e^{-\Gamma^{EV} D_i^{EV} \left(\frac{t_i^{CH}}{CAP_i^{EV}} - \frac{1 - \frac{p_i^{EV,init}}{D_i^{EV}} - X_i^{EV,init}}{\Gamma^{EV} p_i^{EV,init}} \right)} - 1 \right) \right] \quad i \in EV \qquad (5.73)$$

Then the equation is solved and the optimal value of $p_i^{EV,init}$ (for each vehicle i) is numerically determined.

5.3.5 Determining the optimal power flow profiles to the vehicles

Once calculated the value of $p_i^{EV,init}$, it is possible to find the profile of the charging power as described by (5.28). Fig. 5.8 shows an example of how the result can appear.

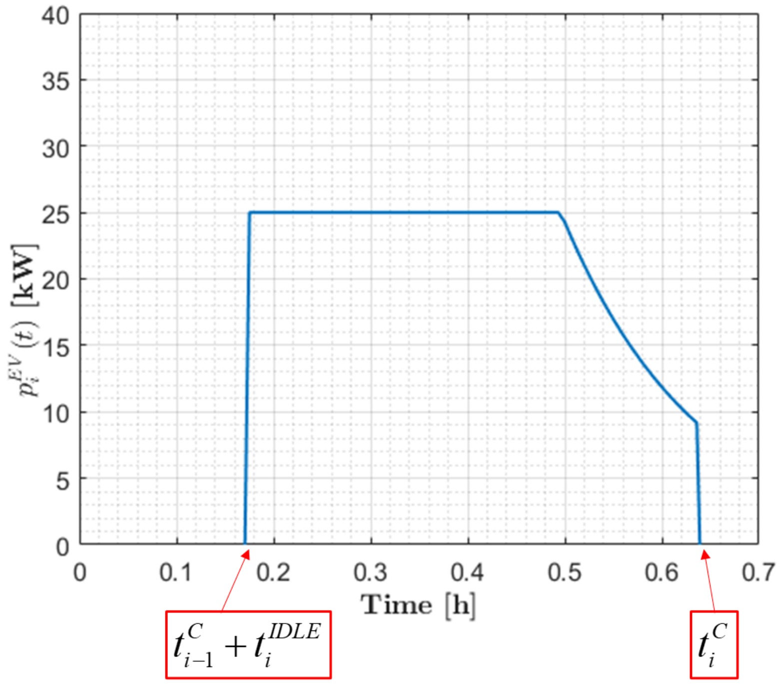

Fig. 5.8 Example of the time pattern of $p_i^{EV}(t)$.

5.3.6 Determining the power flows from/to the storage element

The same approach presented for the charging process of the EVs, can be extended to the electrical storage. In fact, the difference between the two elements is given by the energy request of the EVs which is mandatory while the storage is not constrained in that sense. Moreover, it is important to note that the storage is considered with the generator convention rather than the load one, thus the power is positive when the storage is discharged. The power profile must be within the region in Fig. 5.9.

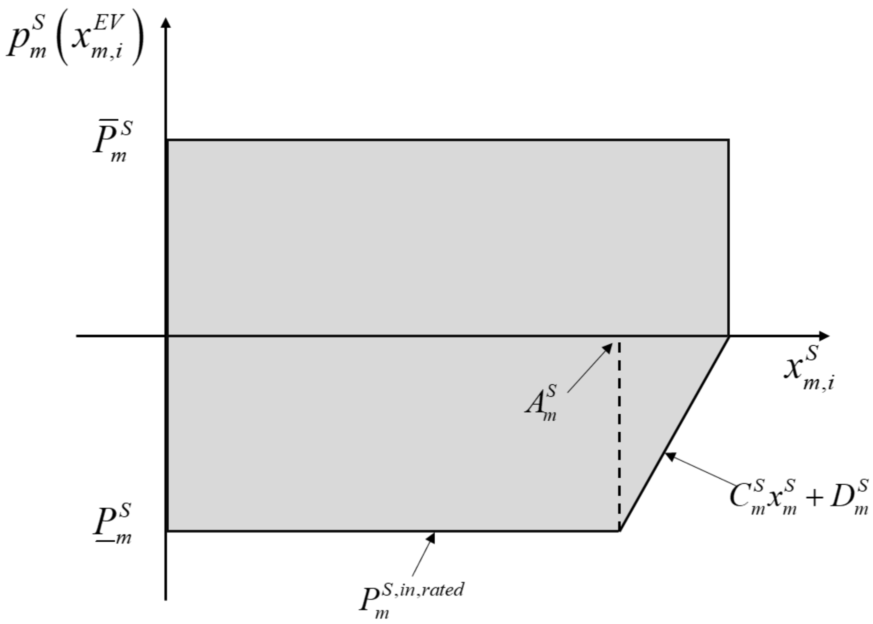

Fig. 5.9 Boundaries on the power exchange with the storage.

Using an approach similar to the one presented before, and assuming that during a generic time interval the storage is charged or discharged, it is possible to obtain the power profile of the storage.

If the storage is discharged, the solution is very simple

$$p_m^S(t) = p_m^{S,out} \qquad m \in M \qquad (5.74)$$

Instead, if the storage is charged, there are three possible outcomes for the state of charge of the storage at the edges of each time interval:

- Both $x_{m,i}^{S1,init}$ and $x_{m,i}^{S1,fin}$ fall within the constant part (i.e. they are less or equal A_m^S);
- Both $x_{m,i}^{S1,init}$ and $x_{m,i}^{S1,fin}$ fall within the descendent part (i.e. they are greater than A_m^S);
- $x_{m,i}^{S1,init} \leq A_m^S \leq x_{m,i}^{S1,fin}$ as in the case considered for the EVs.

In the first case the power profile is equal to the average value

$$p_m^S(t) = p_m^{S,in,init} \qquad m \in M \qquad (5.75)$$

In the second case the power is given by

$$p_m^S(t) = D_m^S(1 - x_{m,i}^{S1,init}) e^{\frac{\Gamma^S D_m^S}{CAP_m^S} t} \qquad m \in M \qquad (5.76)$$

while, in the third case, it is

$$p_m^S(t) = \begin{cases} p_m^{S,in,init} & t_{i-1}^C + t_i^{IDLE} \leq t \leq t_{i-1}^C + t_i^{IDLE} + t_S^{'} \\ p_m^{S,in,init} e^{\frac{\Gamma^S D_m^S}{CAP_m^S}\left(t - t_S^{'}\right)} & t_{i-1}^C + t_i^{IDLE} + t_S^{'} \leq t \leq t_i^C \end{cases} \qquad m \in M \qquad (5.77)$$

where the initial power $p_m^{S,in,init}$ is determined by solving the following equation

$$p_m^{S,in} = \frac{p_m^{S,in,init} CAP_m^S}{t_i^{IDLE} \Gamma^S} \left[\frac{1 - \frac{p_m^{S,in,init}}{D_m^S} - x_m^{S1,init}}{p_m^{S,in,init}} - \frac{1}{D_m^S} \left(e^{-\Gamma^S D_m^S \left(\frac{t_i^{CH}}{CAP_i^{EV}} - \frac{1 - \frac{p_m^{S,in,init}}{D_m^S} - x_m^{S1,init}}{\Gamma^S p_m^{S,in,init}} \right)} - 1 \right) \right] \qquad m \in M \qquad (5.78)$$

Note that here the initial (and final) state of charge of the storage is a solution of the optimization problem in Section 4.5.3, and also that in this case $p_m^{S,in,init}$ and D_m^S assume negative values. An example of what can be obtained is presented by Fig. 5.10.

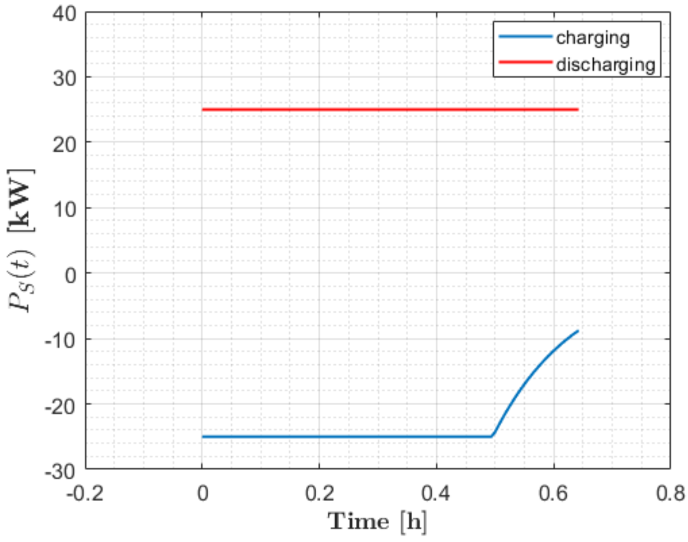

Fig. 5.10 Example of the charging (blue)/discharging (red) process of the storage.

5.3.7 Establish the power exchanged with the grid

It has simply established that

$$p_l^F(t) = \begin{cases} p_{l,i}^{F1} & if \quad t_{i-1}^C \le t < t_{i-1}^C + t_i^{IDLE} \\ p_{l,i}^{F2} & if \quad t_{i-1}^C + t_i^{IDLE} \le t < t_i^C \end{cases} \qquad l \in L \tag{5.79}$$

Once the patterns $p_l^F(t), p_m^S(t)$, and $p_i^{EV}(t)$ have been determined, the pattern $p^G(t)$ can be determined as

$$p^G(t) = -\sum_{l \in L} p_l^F(t) - \sum_{m \in M} p_m^S(t) + P^{NL}(t) + \sum_{i \in EV} p_i^{EV}(t) \tag{5.80}$$

Of course, it will surely result that

$$\int_{t_{i-1}^C}^{t_{i-1}^C + t_i^{IDLE}} p^G(t)\,dt = p_i^{G1} t_i^{IDLE} \qquad i \in EV \tag{5.81}$$

$$\int_{t_{i-1}^C + t_i^{IDLE}}^{t_i^C} p^G(t)\,dt = p_i^{G2} t_i^{CH} \qquad i \in EV \tag{5.82}$$

where p_i^{G1} and p_i^{G2} are exactly the values determined by solving the scheduling problem.

5.4 Application to a case study

In this section, the optimization model is solved for two different scenarios. The first one is similar to the one presented in Chapter 3 with the discrete time model, the number (N^{EV}) of the considered EVs is 4. In the second scenario the number of vehicles to be charged is larger ($N^{EV} = 10$) and a higher value of the maximum charging power is considered. Note that only one electrical storage ($N^S = 1$) and two fossil fuel generators ($N^F = 2$) are considered.

The optimal schedule of production plants, storage systems and EV charging is obtained by solving the optimization problem above introduced, by using Lingo optimization tool [113] on a PC Intel i7, 16 GB RAM.

5.4.1 Scenario I

Table 5.2, provides the values of the parameters relevant to the elements of the microgrid in the first considered scenario.

Table 5.2 Scenario I: System Parameters.

Parameter	**Value**	**Parameter**	**Value**
$\bar{P}_1^F$,	30[kW],	$\underline{X}_m^S$	0.2
$\bar{P}_2^F$	65[kW]	$\bar{X}_m^S$	0.8
CAP_m^S	100[kWh]	Ω	0.08 [h]
$\Gamma^{S,out}$	1.1	$\bar{P}^G$	300 [kW]
C^F	0.2 [€/kWh]	$P_i^{EV,rated}$	10 [kW]
$\Gamma^{S,in}$	0.9	A_m^S	0.8
$P_m^{S,rated}$	-30 [kW]	A_i^{EV}	0.8
$\bar{P}_m^S$,	30[kW]		

In Table 5.3 the data relevant to each EV are reported.

Table 5.3 Scenario I: EVs' data.

EV	**1**	**2**	**3**	**4**
CAP_i^{EV} [kWh]	22	25	31	22
$X_i^{EV,init}$	0.35	0.20	0	0.42
$X_i^{EV,fin}$	0.95	0.95	0.95	0.95
Λ_i [€/h]	0.1	0.1	0.1	0.1
T_i^{rel} [h]	1.25	2.5	4.5	8.75
T_i^{dd} [h]	5.5	9	12.5	15
T_i^{dl} [h]	7.5	12	15.75	17.5

In the statement of the optimization problem, one of the most critical issues is how to express function $P^{NL}(t)$. It is assumed that the forecast of the net load $P^{NL}(t)$ is available over a whole day with a time discretization step equal to 15 minutes. Then, to compute the above function, it is possible to interpolate the available forecasts via a polynomial function of suitable order. In this case an eighth order polynomial has been considered

$$P^{NL}(t) = a_8 t^8 + a_7 t^7 + a_6 t^6 + a_5 t^5 + a_4 t^4 + a_3 t^3 + a_2 t^2 + a_1 t + a_0$$

Using the MATLAB tool, the parameters of the above function are determined as provided in Table 5.4.

Table 5.4 Net Load Polynomial Approximation Parameters.

Parameter	**Value**	**Parameter**	**Value**
a_8	1.07E-05	a_3	-3.05E+01
a_7	-1.06E-03	a_2	4.77E+01
a_6	4.09E-02	a_1	7.41E+01
a_5	-7.68E-01	a_0	1.07E-05
a_4	7.20E+00		

In Fig. 5.11 the original pattern of the net load $P^{NL}(t)$ is represented, as well as the interpolating curve.

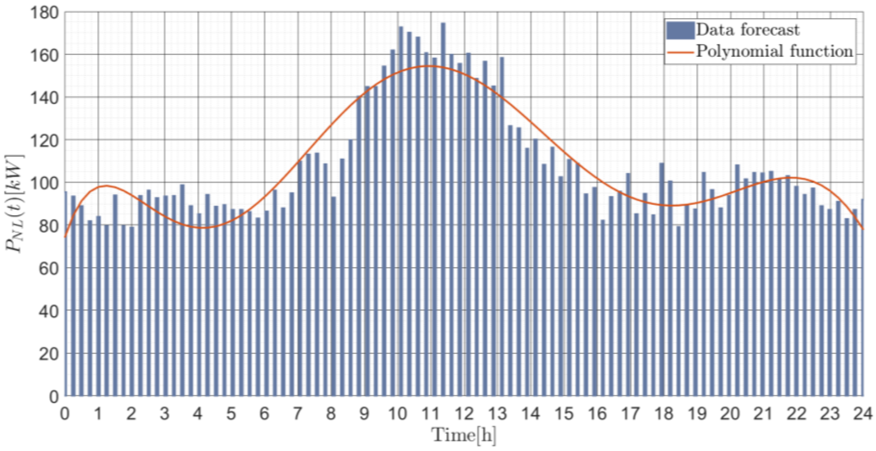

Fig. 5.11 Net load function and its polynomial approximation.

As for the net load, also in the case of the buying price a polynomial function has been determined. In this case the polynomial interpolation (see Fig. 5.12) is an eighth order one and the coefficient calculated by means of the previously introduced MATLAB tool are reported in Table 5.5.

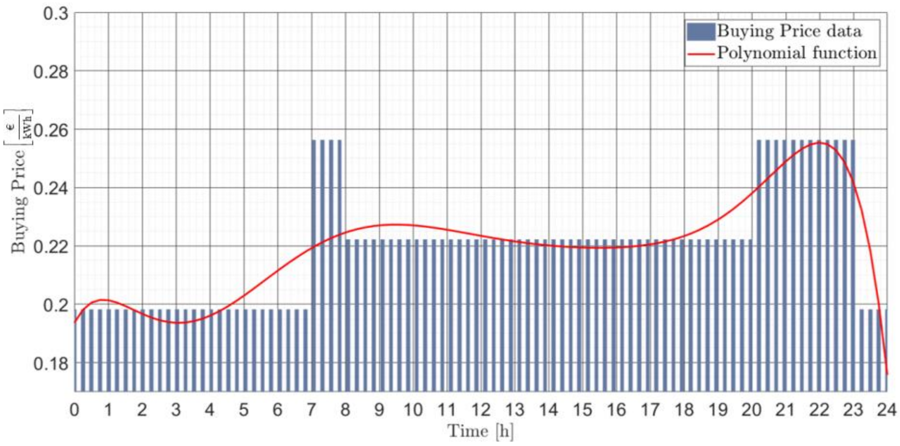

Fig. 5.12 Buying price function approximation.

Table 5.5 Buying price polynomial approximation coefficients

Parameter	Value	Parameter	Value
b_8	1.35 E-09	b_3	7.06 E-03
b_7	1.26 E-07	b_2	-2.08 E-02
b_6	-4.85 E-06	b_1	2.25 E-02
b_5	9.90 E-05	b_0	1.94 E-01
b_4	-1.13 E-03		

The results of this scenario are presented in Fig. 5.13 and Fig. 5.14.

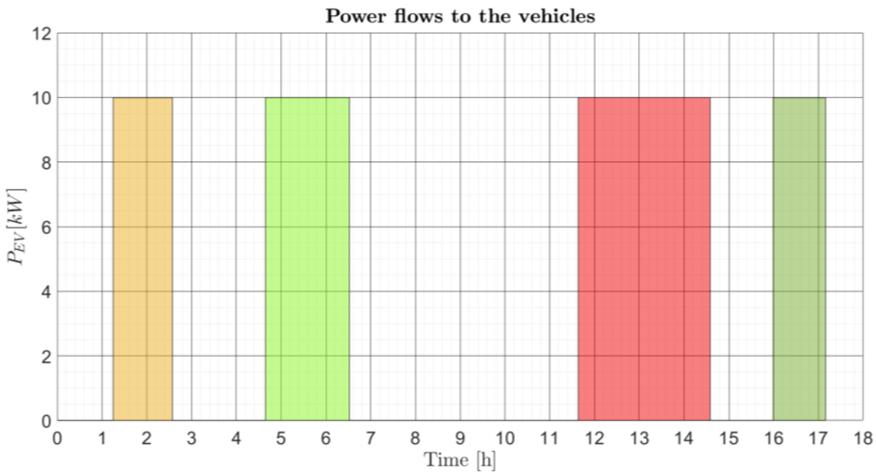

Fig. 5.13 Scenario I: Power to the vehicles.

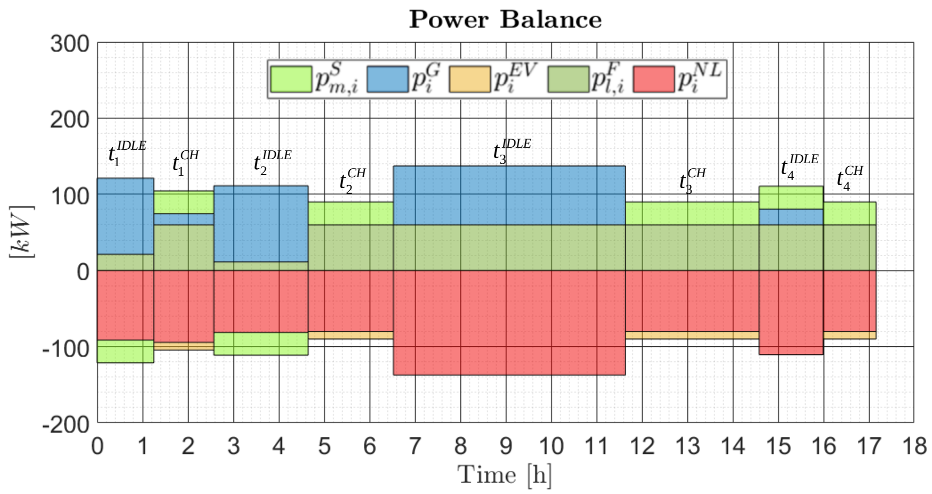

Fig. 5.14 Scenario I: Power balance.

From the results it is possible to denote that the EVs are charged at the maximum available power and the largest portion of the power demand is satisfied by the fossil plants. Since the energy cost function is higher in the last part of the day, the system finishes the charging process around 17 o'clock.

The computational time in this case is about 1 second and the overall cost is 355.05€.

5.4.2 Scenario II

The second scenario considered in this case study has the same values of the parameters in Table 5.2 but for the maximum power available for charging the EVs which is now doubled (i.e. $P_i^{EV,rated} = 20\,[kW]$). The data relevant to the vehicles are presented in Table 5.6.

Table 5.6 Scenario II: EVs' data

EV	1	2	3	4	5	6	7	8	9	10
CAP_i^{EV} [kWh]	22.00	22.00	30.00	30.00	22.00	25.00	25.00	30.00	22.00	25.00
$X_i^{EV,init}$	0.35	0.20	0.00	0.42	0.55	0.60	0.30	0.15	0.42	0.50
$X_i^{EV,fin}$	0.95	0.95	0.95	0.95	0.95	0.95	0.95	0.95	0.95	0.95
Λ_i [€/h]	0.10	0.10	0.10	0.10	0.10	0.10	0.10	0.10	0.10	0.10
T_i^{rel} [h]	1.25	2.50	4.50	5.00	6.50	8.00	8.00	9.00	9.50	11.00
T_i^{dd} [h]	5.50	9.00	12.00	12.50	13.00	16.00	16.00	19.00	20.00	22.00
T_i^{dl} [h]	8.00	10.00	14.00	14.00	16.00	19.00	19.00	22.00	23.00	23.00

The polynomial approximations for the net load function and the buying price are the same considered in the previous scenario.

The results obtained from the optimization problem using these data are presented below in Fig. 5.15 and Fig. 5.16.

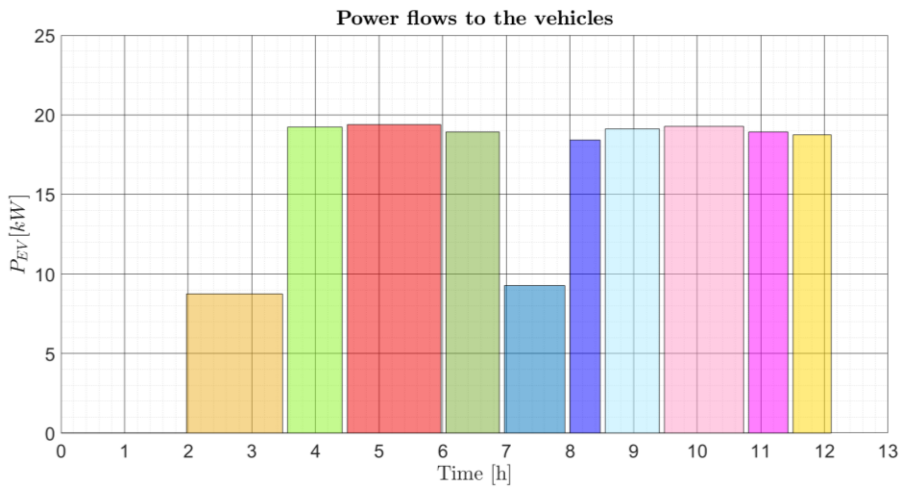

Fig. 5.15 Scenario II: Power to the vehicles.

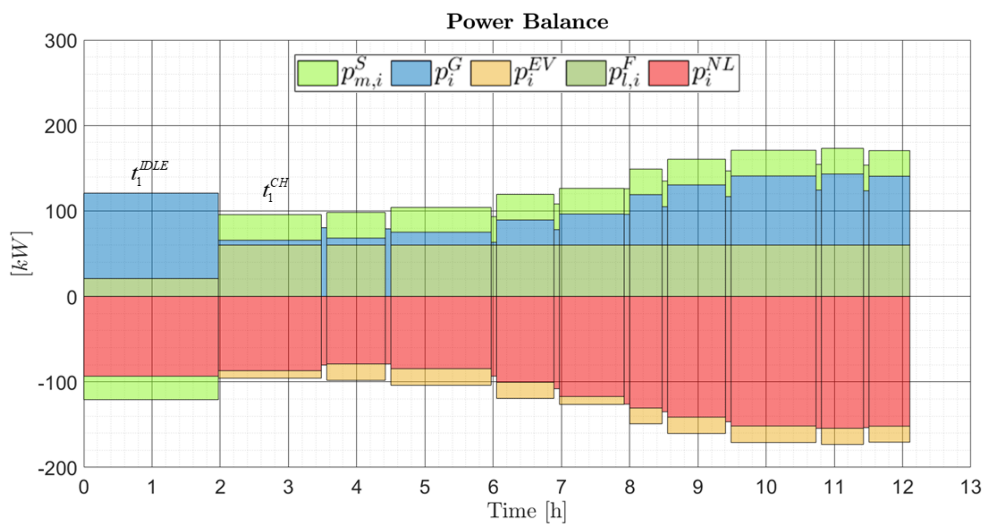

Fig. 5.16 Scenario II: Power balance.

As it happens in the first scenario, the charging process takes place in the first part of the day but in this case the IDLE intervals are reduced as much as possible. The power flow which charges the EVs is close to the maximum value in each interval except for vehicles 1 and 5. The fossil plants still provide a large portion of the power demand. The problem is solved in few seconds (~3 s), the overall cost is 750.15€.

5.5 Discrete event approach: multi-sockets extension

This extension is due to introduce the possibility of considering a multi-socket system configuration. In the work published in [57], a multi-socket system has been considered but the battery of the EVs is described by means of a linear model. Introducing the piece-wise linear model becomes very complicated in this case since it is now necessary to take into account the intermediate states of the EVs' batteries. In fact, it would be necessary to consider the three options in Fig. 5.17.

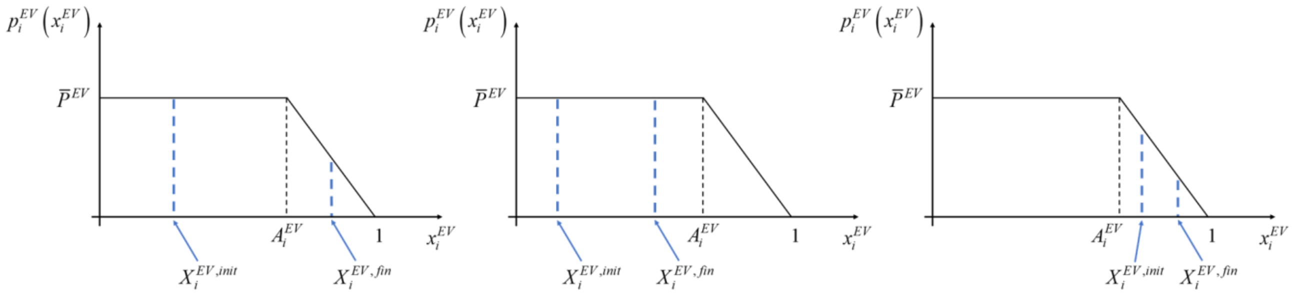

Fig. 5.17 Multi-socket extension: possible scenarios for each interval's state of charge behaviour.

This problem cannot be easily solved and several different approaches are now under investigation. A solution is the one presented below.

The system architecture is exactly the one presented in Fig. 5.1. In order to allow multiple charging during the same interval a new variable is introduced, namely p_i^{CS}, representing the overall contribution of the power flows coming from the EVs during time intervals $\left(t_{i-1}^C, t_{i-1}^C + t_i^{IDLE}\right)$ or $\left(t_{i-1}^C + t_i^{IDLE}, t_i^C\right)$. Note that the IDLE intervals $\left(t_{i-1}^C, t_{i-1}^C + t_i^{IDLE}\right)$ are now characterized by the possibility of charging vehicle *j*, when *j*>*i*. Note that, this variation implies that both p_i^{CS} and $p_{i,j}^{EV}$ are now defined for $i \in EV^{MS} = \left\{1,\ldots,2\cdot N^{EV}\right\}$, $j \in EV = \left\{1,\ldots,N^{EV}\right\}$. The average total power flow provided to the vehicles is then

$$p_i^{CS} = \sum_{j\in EV} p_{i,j}^{EV} \qquad i \in EV^{MS} \tag{5.83}$$

$$0 \le p_i^{CS} \le \bar{P}^{CS} \qquad i \in EV^{MS} \tag{5.84}$$

Constraint (5.52), relevant to the total energy request, becomes

$$\sum_{i=1}^{j} p_{2i-1,j}^{EV} t_i^{IDLE} + p_{2i,j}^{EV} t_i^{CH} = E_j \qquad j \in EV \tag{5.85}$$

It is now necessary to introduce a binary variable $\theta_{i,j}^{EV}$ which is defined as

$$\theta_{i,j}^{EV} = \begin{cases} 1 & \text{if vehicle } V_j \text{ is under charging} \\ 0 & \text{otherwise} \end{cases} \qquad i \in EV^{MS}, j \in EV \tag{5.86}$$

This variable is then considered in the following constraints

$$\theta_{i,j}^{EV} \cdot K^{EV} - p_{i,j}^{EV} \ge 0 \qquad i \in EV^{MS}, j \in EV \tag{5.87}$$

$$\left(1-\theta_{i,j}^{EV}\right)K^{EV} - \left(T_j^{rel} - \left(t_i^C - t_i^{CH}\right)\right) \ge 0 \qquad i \in EV^{MS}, j \in EV \tag{5.88}$$

$$\sum_{j\in EV} \theta_{i,j}^{EV} \le N^{sock} \qquad i \in EV^{MS} \tag{5.89}$$

Constraint (5.87) is equivalent to imposing that when the power flow $p_{i,j}^{EV}$ is greater than zero, the binary variable $\theta_{i,j}^{EV}$ is equal to 1. Note that K^{EV} is the so-called “big M” constant whose value is arbitrarily chosen provided that it is considerably higher than the possible values of the variables and parameters. In (5.88) it is imposed that the charging process of a vehicle cannot start before the release time of the vehicle itself.

In this way, when $t_i^C - t_i^{CH} < T_j^{rel}$, that is, when vehicle V_j is not yet ready for service at the end of time interval $\left(t_{i-1}^C, t_{i-1}^C + t_i^{IDLE}\right)$, $\left(1-\theta_{i,j}^{EV}\right)$ is forced to be equal to 1. This implies that $\theta_{i,j}^{EV}$ is equal to 0, and for this reason vehicle V_j cannot be under charging in time interval $\left(t_{i-1}^C + t_i^{IDLE}, t_i^C\right)$. The binary variable $\theta_{i,j}^{EV}$ is also used to limit the number of vehicles that can be charged at the same time by using the constraint in (5.89).

Now there is an important assumption of this formalization. In fact, the average power considered in the charging process of a vehicle V_j is supposed to be the same for any time interval in which the charging process takes place. Thus, it is possible to write

$$p_{i,j}^{EV} = \theta_{i,j}^{EV} p_j^{CP} \qquad i \in EV^{MS}, j \in EV \qquad (5.90)$$

where p_j^{CP} is the constant average rate of charge.

It is also necessary to define the overall length of the charging process for each vehicle, which is

$$d_j^{CP} = \sum_{i \in EV} \left(\theta_{2i-1,j}^{EV} t_i^{IDLE} + \theta_{2i,j}^{EV} t_i^{CH}\right) \qquad j \in EV \qquad (5.91)$$

and to impose the minimum length of these intervals calculated in the same way presented in the single socket formalization (now $\underline{T}_j^{CP}$ rather than $\underline{T}_j^{CH}$)

$$d_j^{CP} \geq \underline{T}_j^{CP} \qquad j \in EV \qquad (5.92)$$

Besides, according to (5.70) in the model of the battery in Section 5.4,

$$p_i^{CP} \geq D_i^{EV}\left(1 - X_i^{EV,fin}\right) \qquad j \in EV \qquad (5.93)$$

The cost function to be considered in this case is

$$\min \quad \sum_{i \in EV} \left\{c_i^{G1} + c_i^{G2} + c_i^{F1} + c_i^{G1} + c^{tard} + c_i^{occ}\right\}$$

where the first five terms are exactly the same defined in (5.37)-(5.41) while the last one is related to the socket occupancy and is defined as

$$c_i^{occ} = \sum_{j \in EV} \theta_{2i-1,j}^{EV} + \theta_{2i,j}^{EV} \qquad j \in EV \qquad (5.94)$$

Constraints (5.42) and (5.43), according to the definition of p_i^{CS}, must be substituted by

$$p_i^{G1} + \sum_{l \in L} p_{l,i}^{F1} + \sum_{m \in M} p_{m,i}^{S1} = p_i^{NL1} + p_{2i-1}^{CS} \qquad i \in EV \qquad (5.95)$$

$$p_i^{G2} + \sum_{l \in L} p_{l,i}^{F2} + \sum_{m \in M} p_{m,i}^{S2} = p_i^{NL2} + p_{2i}^{CS} \qquad i \in EV \qquad (5.96)$$

As already shown in the case of the single-socket formalization, once the problem is solved it is possible to find the actual charging power profile that, in this case, can look like the one in Fig. 5.18.

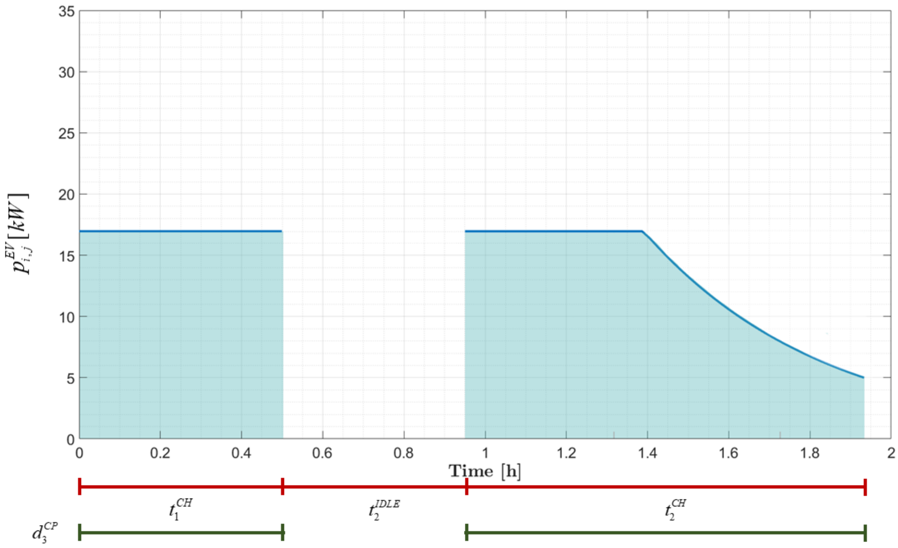

Fig. 5.18 Multi-socket extension: actual power profile example

As expected, thanks to the multi-sockets configuration, it is possible to have preemption of some EVs.

5.5.1 Application to a case study

In the following instance, the considered data are the same presented for Scenario I in Section 4.6 (Table 5.2 and Table 5.3). Only the release time T_j^{rel} have been changed by fixing them to zero (the EVs are immediately available).

The new data needed for the new formalization are reported in Table 5.7.

Table 5.7 Multi-socket extension: system data

Parameter	**Value**
N^{sock}	3
$\overline{P}^{CS}$	25 [kW]

In the following (Fig. 5.19) the resulting Gantt diagram is presented

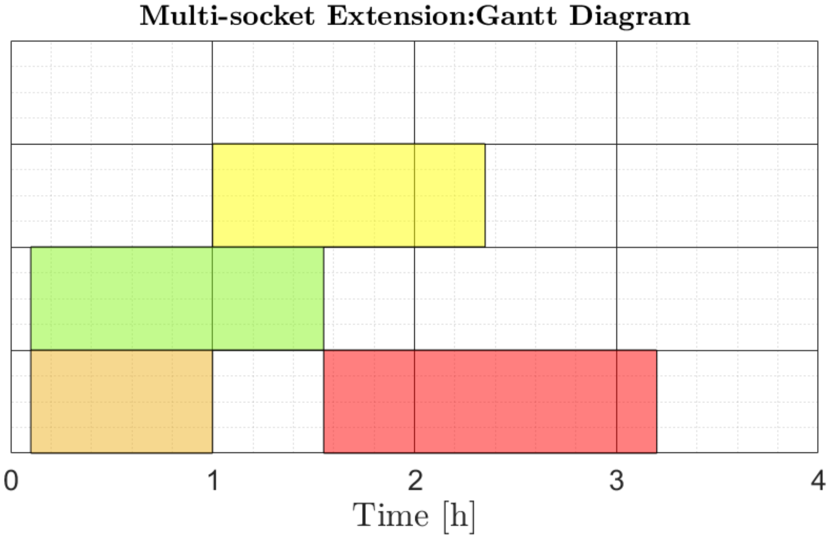

Fig. 5.19 Multi-socket extension: Gantt Diagram

5.6 Discrete event approach: EBs periodic scheduling

In the EVs framework, a very interesting application is the one relevant to the EBs. They represent a particular type of EVs since they usually have large batteries, already defined time schedules, and know paths (then, energy consumption can be estimated more precisely). All these aspects can represent a huge advantage in the solution of a scheduling problem. In this section a variation to the model presented in this chapter is provided. In particular, a periodic scheduling of the charging process is presented.

The considered system consists of a depot including the following elements (see Fig. 5.20): a connection to the main grid, an electrical storage element, a unique charging station, N^{EB} electric buses to be charged.

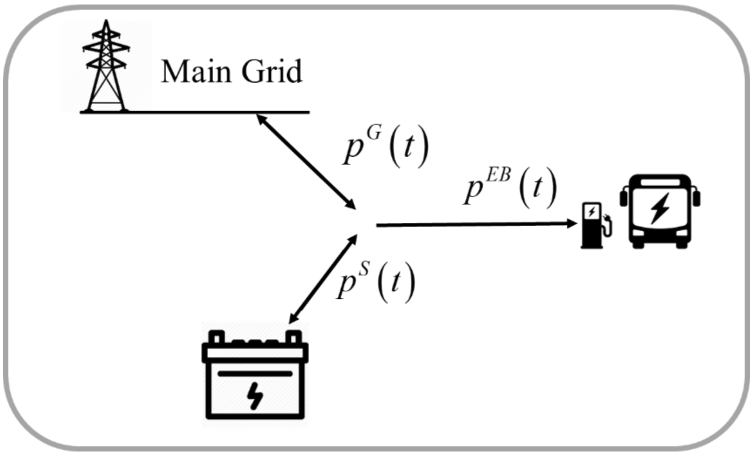

Fig. 5.20 Periodic EBs charging scheduling: the considered system

The system model includes the following power flows, that are functions of time t:

- $p^G(t)$: the power flow from the main grid.
- $p^{EB}(t)$: the power flow to the bus in charge.
- $p^S(t)$: the power flow from the main gr the power flow from/to the storage unit (active sign convention is used, as in other cases).

Each bus has an integer index $i \in EB = \{1,...,N^{EB}\}$ assigned according to the arrival order. The following information is known a priori for each bus:

- *Arrival time* (T_i^{arr}): the instant when the charging of the *i-th* bus can start.
- *Energy consumption* (E_i): the energy requested to charge the *i-th* bus (the request must be completely satisfied).
- *Available charging window* ($D_i^{ch,avail}$): time interval in which for charging service for the *i-th* bus can take place.

The service times are controllable and are include within the set of the decision variables of the problem. Fig. 5.21 represents the time windows concerning the *i*-th bus.

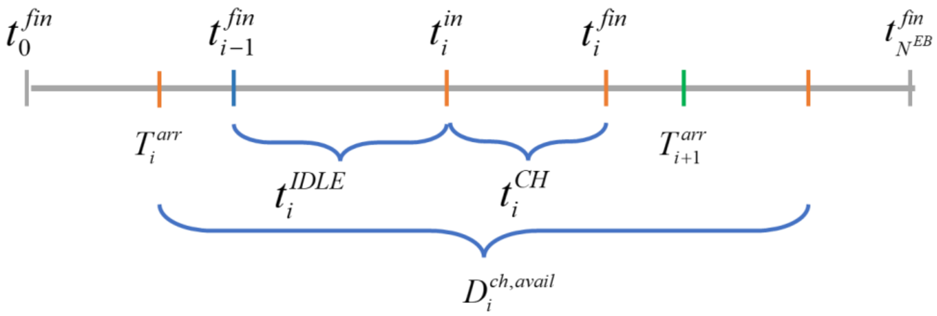

Fig. 5.21 The considered time windows for the i-th vehicle

The following decision variables must be introduced for each EB:

- t_i^{in}: starting instant of recharge for the *i-th* bus.
- t_i^{fin}: time instant at which the recharge for the *i-th* bus ends.

Two additional decision variables, namely t_i^{CH} and t_i^{IDLE}, are necessary, which are the time needed for charging the *i-th* bus and the time between the end of a charging process and the beginning of another one, respectively. They correspond to

$$t_i^{CH} = t_i^{fin} - t_i^{in} \qquad i \in EB \qquad (5.97)$$

$$t_i^{IDLE} = t_i^{in} - t_{i-1}^{fin} \qquad i \in EB \qquad (5.98)$$

The objective function includes the cost related to the power taken from the grid (that is comprehensive of operational costs, costs for emissions, calculated as a function of an emission factor, and the unit cost for 1 ton of CO_2). That is

$$\min\ J = \sum_{i=1}^{N} c_i^G \tag{5.99}$$

with

$$c_{G,i} = \left\{ \left[\int_{t_{i-1}^{fin}}^{t_i^{in}} C^G(t)dt \right] p_i^{G1} + \left[\int_{t_i^{in}}^{t_i^{fin}} C^G(t)dt \right] p_i^{G2} \right\} \qquad i \in EB \tag{5.100}$$

where the power exchange with the grid is defined as p_i^{G1} and p_i^{G2} in the idle and charging intervals, respectively. It is important to note that control variables in the following are considered for idle (identified by subscript 1) and charging (identified by subscript 2) intervals. They are assumed to be constant during each event and this is valid for all control variables described in the following.

Finally, the unit cost $C^G(t)$ considers the energy price as well as the CO_2 emission cost.

Then, the basic state equation of the system, describing the dynamics of the state of charge of the storage element $x^S(t)$ can be represented, within a discrete event setting, as

$$x_i^S = x_{i-1}^S + \left(\Gamma^{S,in} p_i^{S1,in} - \Gamma^{S,out} p_i^{S1,out} \right) t_i^{IDLE} + \left(\Gamma^{S,in} p_i^{S2,in} - \Gamma^{S,out} p_i^{S2,out} \right) t_i^{CH} \qquad i \in EB \tag{5.101}$$

$$p_i^{S1} = p_i^{S1,out} - p_i^{S1,in} \qquad i \in EB \tag{5.102}$$

$$p_i^{S2} = p_i^{S2,out} - p_i^{S2,in} \qquad i \in EB \tag{5.103}$$

$$p_i^{S1,out}, p_i^{S1,in}, p_i^{S2,out}, p_i^{S2,in} \geq 0 \qquad i \in EB \tag{5.104}$$

where the variables $p_i^{S1,out}, p_i^{S1,in}, p_i^{S2,out}, p_i^{S2,in}$ are the “positive” and “negative” components of p_i^{S1} and p_i^{S2} respectively, and $\Gamma^{S,in}$ and $\Gamma^{S,out}$ are charging and discharging efficiencies.

In equation(5.105), the initial state of charge x_0^S is not known, since the overall system has a periodical behavior. This will be modelled in the following through constraints.

Then some constraints on the time variables are presented in (5.106)-(5.107).

$$t_i^{fin} \leq T_i^{arr} + D_i^{ch,avail} \qquad i \in EB \tag{5.108}$$

$$t_{i+1}^{in} \geq t_i^{fin} + \Omega^{idle} \qquad i \in EB \tag{5.109}$$

$$t_i^{in} \geq T_i^{arr} + \Omega^{arr} \qquad i \in EB \tag{5.110}$$

$$T_i^{arr} + t_i^{CH} < T_{i+1}^{arr} + t_{i+1}^{CH} \qquad i \in EB \tag{5.111}$$

In particular, inequality (5.108) imposes that the charging process for the *i-th* bus must end within the available charging window $D_i^{ch,avail}$. Constraint (5.109) gives the minimum length of an idle interval, i.e. Ω^{idle}. The minimum time difference Ω^{arr} between the arrival time T_i^{arr} and the beginning of the charging process t_i^{in} is given by (5.110). Constraints (5.111) are necessary to order the charging processes according to the arrival order.

The periodicity of the problem is ensured by introducing constraints (5.112) and (5.113) where x_0^S and $x_{N^{EB}}^S$ are the states of charge (decision variables) of the storage at the time instants t_0^{fin} and $t_{N^{EB}}^{fin}$, respectively.

$$t_{N^{EB}}^{fin} = t_0^{fin} + T \qquad (5.112)$$

$$x_0^S = x_{N^{EB}}^{fin} \qquad (5.113)$$

Constraints from (5.114) to (5.119) are physical limits on the power flows and the state of charge.

$$0 \le p_i^{G1} \le \overline{P}^G \qquad i \in EB \qquad (5.114)$$

$$0 \le p_i^{G2} \le \overline{P}^G \qquad i \in EB \qquad (5.115)$$

$$0 \le p_i^{EB} \le \overline{P}^{EB} \qquad i \in EB \qquad (5.116)$$

$$\underline{P}^S \le p_i^{S1} \le \overline{P}^S \qquad i \in EB \qquad (5.117)$$

$$\underline{P}^S \le p_i^{S2} \le \overline{P}^S \qquad i \in EB \qquad (5.118)$$

$$\underline{X}^S \le x_i^S \le \overline{X}^S \qquad i \in EB \qquad (5.119)$$

Then, there are constraints related to power balance during idle and charging time intervals. That is,

$$p_i^{G1} + p_i^{S1} = 0 \qquad i \in EB \qquad (5.120)$$

$$p_i^{G2} + p_i^{S2} = p_i^{EB} \qquad i \in EB \qquad (5.121)$$

Finally, it is necessary to introduce a constraint related to the satisfaction of the energy demand for each vehicle. That is,

$$E_i = \Gamma^{EB} p_i^{EB} t_i^{CH} \qquad i \in EB \qquad (5.122)$$

where Γ^{EB} is efficiency of the EBs' battery and represents energy consumption.

It is important to note that, in the case of EBs, E_i corresponds to the bus energy consumption during the daily trips.

5.6.1 Application to a case study

This section applies the proposed approach to a specific case study. A scenario with five EBs is considered (i.e. $N^{EB} = 5$).

The solve the nonlinear optimization problem previously defined, the software tool Lingo [113] has been used.

The buses considered in the study are vehicles that work on lines 516 and 517 of the bus company operating in Genoa (AMT). In particular, on the software QGIS, a project for each route has been realized in order to calculate the mileage, the duration of the runs has been calculated based on the information reported by some data collected on the buses and, finally, Google Earth Pro has allowed calculating the overall height difference of each route. The height difference is calculated since it affects fuel consumption and the possibility of regenerative braking.

Line 516 takes approximately 22 minutes to complete a full ride. The outward and return routes (Fig. 5.22) are equal, and the overall length is 6 km with 24 stops and a total height difference of about 280 m.

Note that the bus must go to the Nervi terminus to start the assigned run at the beginning of the service and therefore travels about 8.9 km from the depot.

Fig. 5.22 Line 516 path

In line 517, a complete round trip takes about 22 minutes. Unlike line 516, the two round-trip routes (Fig. 5.23 and Fig. 5.24) are very different: on the outward journey, the bus reaches the Nervi cemetery and makes 22 stops, covering a distance of about 4.5 km, while on the return journey, it covers a distance of about 1.8 km divided into six stops. The outward journey covers a total height difference of about 127 m, while the return journey covers about 65 m. Also, in this case, at the beginning of the service, the bus must go to the Nervi terminus to start the assigned run.

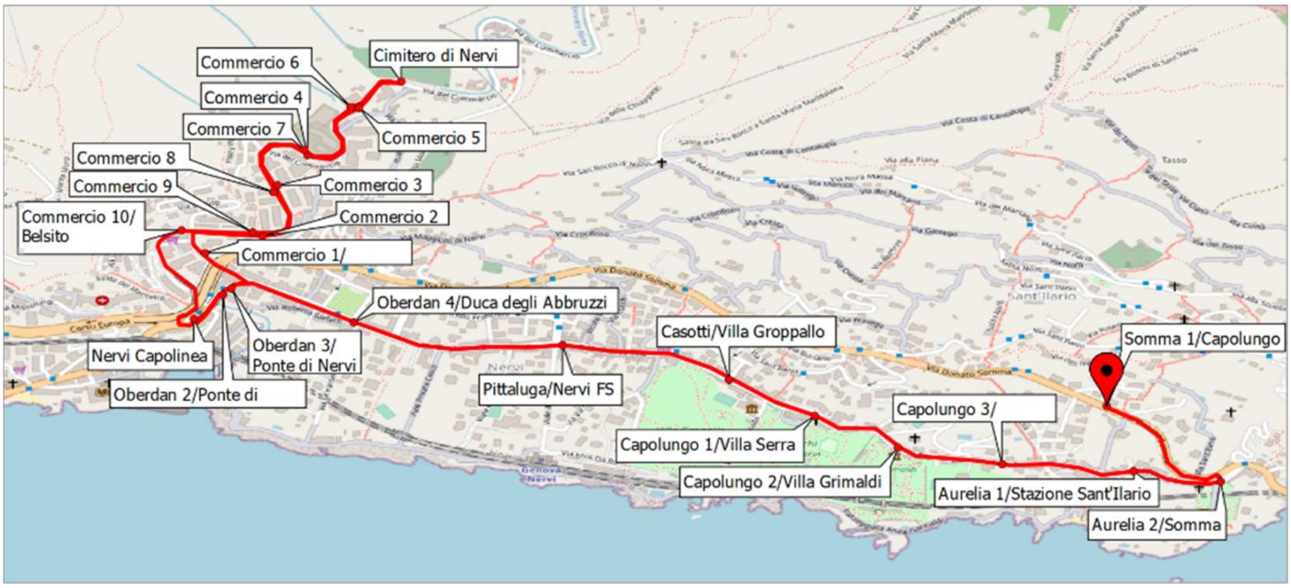

Fig. 5.23 Outward path of line 517

Fig. 5.24 Backward path of line 517

The data considered for the case study are presented in Table 5.8 and Table 5.9. The values relevant to the calculation of the energy consumption E_i, for each of the considered paths, have been determined using the software tool QGIS. In particular, note that the first two buses are assigned to line 516 and the other three buses are assigned to line 517.

Table 5.8 Data relevant to buses

i	$t_{arr,i}$ **[hh:mm:ss]**	$ch_{w,i}$ **[hh:mm:ss]**	EC_i **[kWh]**
1	12:00:00	3:12:00	65,55
2	12:43:00	6:22:00	76,24

3	16:58:00	13:22:00	75,86
4	17:12:00	14:00:00	52,29
5	18:49:00	17:58:00	59,42

Table 5.9 System Parameters

Parameter	**Value**
CAP	180 [kWh]
$\varepsilon 1$	0.1 [h]
$\varepsilon 2$	0.1 [h]
x_{min}	0.1 [-]
x_{max}	0.9 [-]
$P_{g,max}$	20 [kW]
$P_{ch,max}$	30 [kW]
$P_{s,min}$	-30 [kW]
$P_{s,max}$	30 [kW]

To calculate the integral functions in (5.100), the cost function has been created via a sixth-order polynomial approximation of a stairs function, in the form

$$p(x) = a_6 x^6 + a_5 x^5 + a_4 x^4 + a_3 x^3 + a_2 x^2 + a_1 x^1 + a_0$$

The coefficients are reported in Table 5.10.

Table 5.10 Polynomial Function Coefficient

Parameter	**Value**	**Parameter**	**Value**
a_6	-1.18E-09	a_2	-2.37E-03
a_5	1.70E-07	a_1	8.35E-03
a_4	-9.10E-06	a_0	2.04E-01
a_3	2.22E-04		

Note that this curve presents a lower cost around midday and a higher cost around midnight.

In this scenario, the optimization problem results show that five buses can be recharged with one charging station. According to the results obtained, the total charging cost is equal to 70.87€, and the system starts the process cycle with a storage state of charge of about 0.5.

Table 5.11 shows the results obtained using the Lingo software [113].

Table 5.11 Results

BUS i	$t_{fin,i-1}$ [h]	$t_{in,i}$ [h]	$P_{g1,i}$ [kW]	$P_{s1,i}$ [kW]	$P_{g2,i}$ [kW]	$P_{s2,i}$ [kW]	$P_{ch,i}$ [kW]
BUS 1	11.51	12.10	20.00	-20.00	20.00	2.24	22.24
BUS 2	15.20	15.30	20.00	-20.00	20.00	1.28	21.28
BUS 3	19.07	19.17	0.00	0.00	20.00	0.00	20.00

BUS 4	23.16	27.45	0.00	0.00	14.68	0.00	14.68
BUS 5	31.20	32.39	0.00	0.00	20.00	0.00	20.00

The following figures show the power profiles.

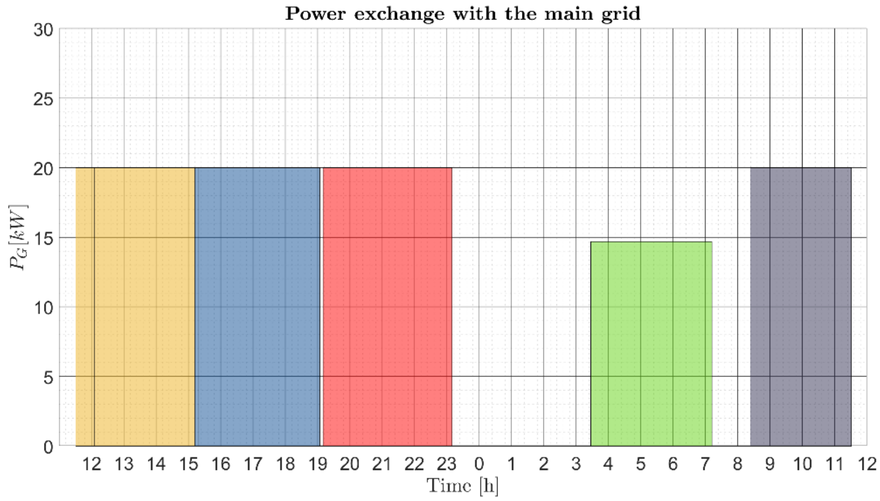

Fig. 5.25 Power purchased from the grid

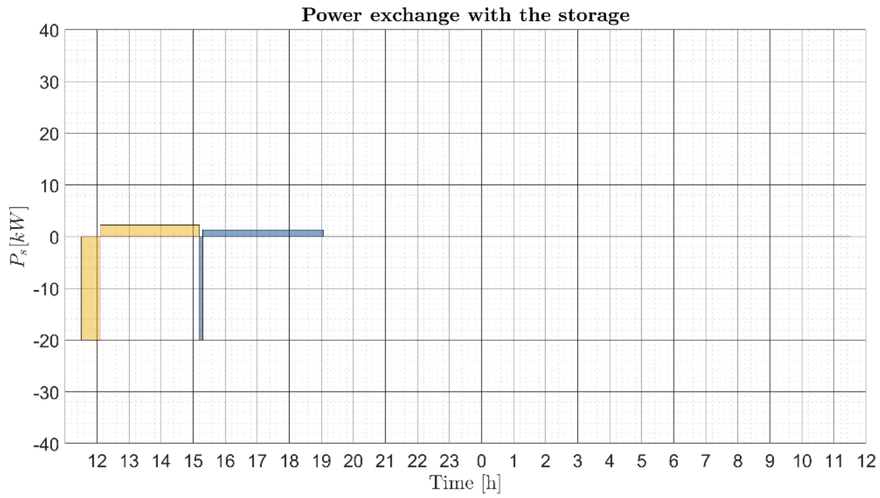

Fig. 5.26 Power exchanged with the storage

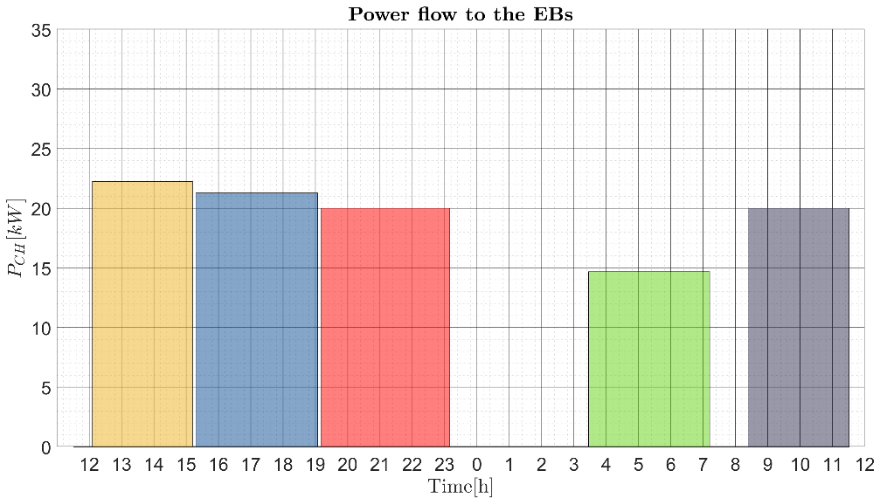

Fig. 5.27 Power exchanged with the EBs

As it is possible to see from the figures, the maximum power available from the grid is purchased for four buses out of five. The storage element remains almost unused but for the first time intervals in which the power is used to charge the buses. There is a long idle time between the third and the fourth vehicle because of the time constraints and the cost functions, which decreases in the night.

Chapter 6
Optimal location and line assignment for electric bus charging stations

As anticipated in Chapter 3, in this thesis the focus is on scheduling and planning problems. After the presentation of the two models relevant to the optimal scheduling in both discrete time and discrete events, in this chapter, the work published in [114] is proposed. It consists of a new approach for the optimal location and line assignment for EBs' charging station. In fact, public electric transportation represents a crucial topic in the transition from traditional fuels and the new CSs must be optimally located in order to ensure an optimal service.

In particular, it is assumed that a given number of eligible sites for charging stations has been preliminarily identified. These sites could be, for example, already existing depots or areas in which the buses stop along the path that may be equipped with charging stations. Let this set of sites be $\{S_i, i=1,2,...,N\}$. In the following, the symbol S_i will be used to indicate either the site or the (potential) charging station located at that site. These stations must ensure the charging service for the buses operating on a given set of lines $\{L_j, j=1,2,...,M\}$.

The routes corresponding to these lines are assumed to have been already established. Moreover, for any line L_j, there is a set of sites that are allowed to be selected (according to the site localization and to the specific route for line L_j) to provide the charging service to the buses operating on that line. This set will be denoted by $R_j \subseteq \{S_i, i=1,2,...,N\}$.

A representation of an instance corresponding to this description is provided by Fig. 6.1.

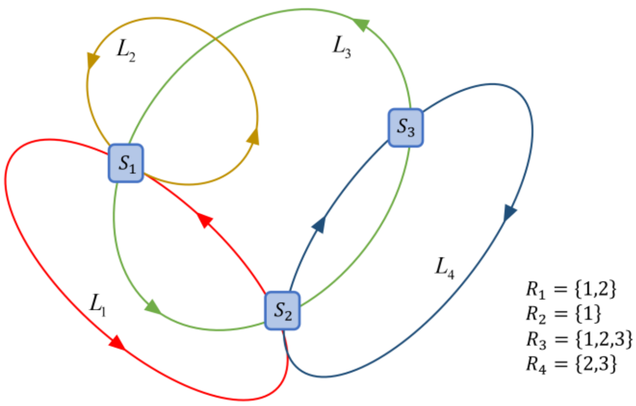

Fig. 6.1 Representation of some lines and eligible stations sites.

Let, for each line L_j the following information be defined:

- The initial energy contents [kWh] of the bus battery, namely $X_j^{init} \cdot E^{CAP}$, where E^{CAP} [kWh] is the capacity of the battery, and X_j^{init} is the initial state of charge;

- The final energy contents [kWh] of the bus battery, namely $X_j^{fin} \cdot E^{CAP}$, where X_j^{fin} is the final state of charge;
- $F_j^{\min}$: minimum *frequency for completion of charging services* [#charg/h]; this is the lower bound on the value of the frequency at which the events corresponding to the completion of charging service take place;
- $F_j^{min,serv}$: minimum *transit frequency* of buses [h^{-1}];
- D_j^{trip} : duration of a trip of a bus [h];
- N_j^{trips} : number of completed trips between two successive recharges;
- T_j^{trips} : time necessary to complete N_j^{trips} trips without interruptions [h].

All parameters listed above are considered fixed and known. In particular, X_j^{init} is evaluated by considering the difference between the state X_j^{fin} and the consumption determined by using the model in [115].

Clearly, the following equalities hold

$$F_j^{\min,serv} = N_j^{trips} F_j^{\min} \qquad j = 1,...,M \tag{6.1}$$

$$T_j^{trips} = N_j^{trips} D_j^{trip} \qquad j = 1,...,M \tag{6.2}$$

Note that E^{CAP}, as well as the other parameters characteristics of the battery, are assumed to be the same for all lines. It is assumed that, for each line, the same minimum transit frequency characterizes all time intervals in which the service must be ensured.

For any charging station (site) S_i, the following (decision) variables are defined:

- n_i^{sock} : number of sockets, that is, the maximum number of vehicles that can be simultaneously charged;
- p_i^{sock} : the maximum power flow through a socket [kW];
- y_i : a binary decision variable that says whether the station is activated ($y_i = 1$) or not ($y_i = 0$).

The maximum power that can be provided by the service station, namely p_i^{tot} [kW], is given by

$$p_i^{tot} = n_i^{sock} p_i^{sock} \qquad i = 1,...,N \tag{6.3}$$

The frequency f_j of the *events* corresponding to the *completion of charging services* for line L_j is a decision variable, too. The value $f_j N_j^{trips}$ provides the actual *transit frequency* of buses on line L_j .

The assignment of lines to stations (one of the issues to be determined) is modeled through the following set of binary decision variables

$$\delta_{i,j} = \begin{cases} 1\ if\ \ L_j\ is\ assigned\ to\ S_i \in R_j \\ 0\ otherwise \end{cases} \qquad j = 1,...,M, i : S_i \in R_j \tag{6.4}$$

Note that, for simplicity, a line is assumed to be *entirely* assigned, for charging service, to a *unique* station. Different formulations with fractional assignments are possible but are not considered in this model.

The model considered for the battery of the EBs is the same proposed in the previous chapter. Moreover, the same assumption on the profile of the power flowing into the battery holds (Fig. 6.2).

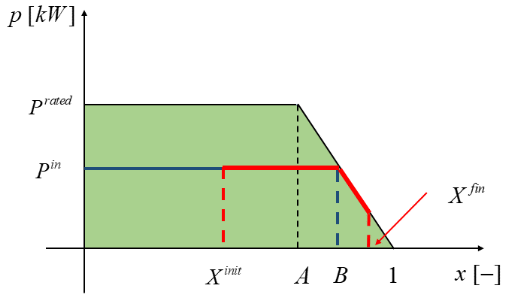

Fig. 6.2 The actual power profile of the battery (red line).

From this model, the only constraints that must be considered in the optimization problem are

$$p_j^{in} \geq D\left(1 - X_j^{fin}\right) \qquad j = 1,...,M \tag{6.5}$$

$$t_j^{ch} = E^{CAP}\left(\frac{\left(1 - \frac{p_j^{in}}{D} - X_j^{init}\right)}{p_j^{in}} - \frac{\ln\frac{D\left(1 - X_j^{fin}\right)}{\left(p_j^{in}\right)}}{D}\right) \qquad j = 1,...,M \tag{6.6}$$

Clearly, the number of charging services completed, over a time horizon of a given length H [h], over the station $S_i \in R_j$, is given by

$$\delta_{i,j}\, f_j\, H \qquad j = 1,...,M \tag{6.7}$$

where f_j (already defined) is the actual frequency of completion of charging services for line L_j.

Then, the overall duration [h] of services for buses of line L_j over the station S_i is

$$\delta_{i,j}\, f_j\, H\, t_j^{ch} \qquad j = 1,...,M, i = 1,...,N \tag{6.8}$$

where the decision variables are the binary variables $\delta_{i,j}$, as well as f_j, and t_j^{ch}.

On this basis, the *overall service time* provided by the station S_i, within time horizon H, is

$$\sum_{j:S_i \in R_j} \delta_{i,j}\, f_j\, H\, t_j^{ch} \qquad i = 1,...,N \tag{6.9}$$

The overall potential service time, within a generic time horizon H, for station S_i is $n_i^{sock} \cdot H$. Thus, the first basic requirement to be satisfied in the planning problem is

$$n_i^{sock} \cdot H \geq \Psi \sum_{j:S_i \in R_j} \delta_{i,j} \, f_j \, H \, t_j^{ch} \qquad i = 1,\ldots,N \qquad (6.10)$$

that is,

$$n_i^{sock} \geq \Psi \sum_{j:S_i \in R_j} \delta_{i,j} \, f_j \, t_j^{ch} \qquad i = 1,\ldots,N \qquad (6.11)$$

where the coefficient $\Psi(\geq 1)$ is introduced to guarantee a certain safety margin of the solution of the planning problem.

Besides, the following constraints must be fulfilled

$$p_j^{in} \leq \sum_{j:S_i \in R_j} \delta_{i,j} \, p_i^{sock} \qquad j = 1,\ldots,M \qquad (6.12)$$

Constraints (6.12) impose that the initial value of the input power for (any vehicle of the) line L_j is lower than or equal to the maximum output power flow for any socket of the station to which the line is assigned.

6.1 The optimal planning problem

In the optimization problem statement, it is assumed that the buses are physically indistinguishable from each other and that each bus is assigned uniquely to a line.

Let n_j^B the number of buses assigned (in the solution of the optimization problem) to line L_j.

The optimization problem whose solution jointly defines the optimum selection of the stations (sites) to be activated, their sizes (in terms of the number of sockets and maximum power for the sockets), along with the assignment of the lines to the stations, and the bus fleet sizing, can be stated as follows.

$$\min \left\{ \begin{array}{l} c^s + \sum_{j=1}^{M} C_j^B \, n_j^B + \sum_{j=1}^{M} C_j^T \, f_j \, T_j^{oper} + \\ \Omega \sum_{j=1}^{M} t\left(p_j^{in}, X_j^{init}, X_j^{fin}\right) f_j \, T_j^{oper} \end{array} \right\} \qquad (6.13)$$

subject to (6.3), (6.5), (6.11), (6.12), along with the following further constraints

$$t_j^{MC} = T_j^{trips} + t_j^{ch} \qquad j = 1,\ldots,M \qquad (6.14)$$

$$f_j = \frac{n_j^B}{t_j^{MC} + t_j^W} \qquad j = 1,\ldots,M \qquad (6.15)$$

$$c^s = \sum_{i=1}^{N} \left(C_i^{act}\, y_i + K_i^1\, n_i^{sock} + K_i^2\, p_i^{sock} \right) \tag{6.16}$$

$$\sum_{i \in R_j} \delta_{i,j} = 1 \qquad j = 1,\ldots,M \tag{6.17}$$

$$\delta_{i,j} \in \{0,1\} \qquad i = 1,\ldots,N,\; j = 1,\ldots,M \tag{6.18}$$

$$y_i \in \{0,1\} \qquad i = 1,\ldots,N \tag{6.19}$$

$$y_i \Pi - p_i^{tot} \geq 0 \qquad i = 1,\ldots,N \tag{6.20}$$

$$n_i^{sock} \leq N_i^{sock,max} \qquad i = 1,\ldots,N \tag{6.21}$$

$$p_i^{sock} \leq P_i^{sock,max} \qquad i = 1,\ldots,N \tag{6.22}$$

$$p_i^{tot} \leq P_i^{tot,max} \qquad i = 1,\ldots,N \tag{6.23}$$

$$p_j^{in} \leq P^{rated} \qquad j = 1,\ldots,M \tag{6.24}$$

$$f_j \geq F_j^{min} \qquad j = 1,\ldots,M \tag{6.25}$$

Remark 1

The objective function is composed of four terms:

- c^s is the cost relevant to the stations.
- $\sum_{j=1}^{M} C_j^B\, n_j^B$ is the cost of the buses.
- $\sum_{j=1}^{M} C_j^T\, f_j\, T_j^{oper}$ is the operational cost of each line.
- $\Omega \sum_{j=1}^{M} t_j^{ch}\, f_j\, T_j^{oper}$ is the cost related to the overall time needed for recharging each year.

where C_j^B [€/year] the unit cost (per year) for a bus, in general, depending on the line over which it is operating; C_j^T [€/trip] is the cost corresponding to N_j^{trips} of a bus on line L_j; T_j^{oper} [h y^{-1}] the number of operating hours on line L_j in one year; Ω is a tradeoff coefficient [€/h]. Constraints (6.14) define the minimum cycle time t_j^{MC}, i.e., the minimum time interval between two successive charging service completions on line L_j. In (6.15) the overall (average) waiting time for a bus on line L_j, namely t_j^W [h], is introduced in order to express the (actual) charging frequency f_j [h^{-1}]. In constraints (6.16) the cost for the stations c^s [€/year] is defined as a sum of different terms where:

- C_i^{act} [€/year] is the yearly fixed cost of activation related to the presence of station S_i;

- K_i^1 [€/year·#of sockets] is the proportional term of the cost relevant to the number of sockets that are established in station S_i;
- K_i^2 [€/year·kWh] is the proportional term of the cost relevant to the maximum power for each socket for the station S_i.

Constraints (6.17) imply that each line is assigned, as regards the charging service, to one and only one station. Constraints (6.18) and (6.19) just specify that the interested variables are binary. Constraints (6.20) correspond, as usual, to the disjunctive constraints that impose that the station must exist (hence the activation cost must be paid) whenever its maximum power flow p_i^{tot} is different from zero. Π is an arbitrary number very large with respect to the values of the parameters embedded in the problem formalization and to the values that the variables can assume.

Constraints (6.21), (6.22), and (6.23) derive from physical limitations concerning the design of the stations over the eligible sites. The terms appearing on the r. h. s. of these inequalities are just the maximum allowable values for the variables appearing in the l.h.s.

Constraints (6.24) limit the initial charging power for each service.

Constraints (6.25) ensure the required quality of service for the bus lines (in terms of a required minimum frequency). The constraints are expressed in terms of charging frequency (instead of transit frequency) but, of course, this is equivalent to imposing a constraint on the transit frequency, owing to relationship (1).

The considered problem is a mixed-integer nonlinear one, and thus it is characterized by high computational complexity. However, for small/moderate sizes of problem instances, it can be solved in acceptable times (note that this is *planning* problem, that has to be solved *offline*) even by use of commercial mathematical programming tools.

The proposed approach can be summarized as in the Fig. 6.3.

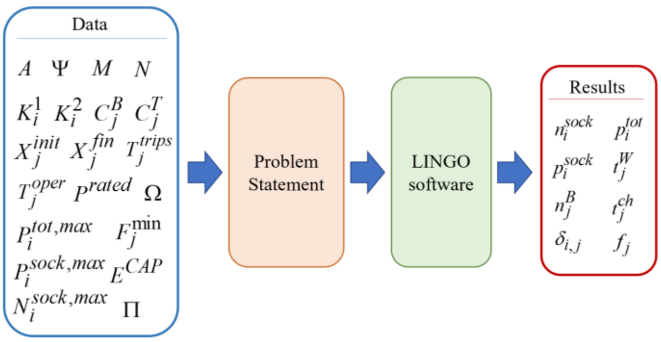

Fig. 6.3 The information flow diagram of the proposed procedure.

It is important to remark that the main effort reported in this paper regards the formalization of the problem: the expression of the cost to be minimized and – more importantly – the constraints to be taken into account.

In particular, among such constraints, a particular relevance characterizes constraints (6.6) that are written referring to a specific nonlinear model of the vehicle batteries.

Remark 2

Note that the logical structure of the optimization problem formalized in this paper may resemble that of the set-partitioning problem, one of the classical problems in the literature concerning combinatorial optimization [116]. Indeed, even in our case, the problem can be seen as that of selecting, among a set of feasible subsets (in this case, corresponding to the stations), a collection of such subsets capable of covering all elements of the overall set considered (such elements correspond to the lines, in our model) without redundancy, that is, ensuring that each element (=each line) is included (=is assigned) to a single selected subset (=each activated station).

However, this similarity is only apparent because, in the proposed optimization model, not only the selection of the sites (i. e., the stations) has to be determined, along with the lines that are assigned to each station, but also the sizing of each of the selected station. This means that, for each station, the number of sockets and the maximum power deliverable by each socket are to be determined. Besides, the initial power at which the charging process for each bus of a certain line starts, and the number of buses traveling on each line is determined by solving the optimization.

Thus, unfortunately, it is impossible to formalize this problem as a set partitioning problem, in which the cost of any feasible subset is computable a priori. For this reason, the well-known and efficient methods to solve the set-partitioning problem cannot be used for the problem considered in this paper.

Remark 3

Given the general formulation of our problem, one could believe that it is quite similar to the so-called nonlinear resource allocation problem (see, for instance, [117] and [118]). In fact, our problem may be viewed as having the purpose of allocating some resources (the charging stations) to jobs (the lines) under some constraints.

However, even this resemblance is only apparent for several reasons. First, the quantities of resources assigned to the various jobs are not the only decision variables in our problem. It is not easy in our case to speak of a quantity of resources assigned to a given line since the total sizes of the resources to be shared (i.e., in our case, for each resource, the number of sockets and their maximum power) are themselves issues to be determined by the solution of the optimization problem. Besides, the charging process for each line (that is, the initial charging power) itself is something to be determined by solving the problem. Finally, the problem-solution also determines the number of buses for each line (of course, affects the service request, from each line to the resource to which it is assigned).

6.2 Application to a case study

This section applies the proposed approach to a specific case study, providing a detailed presentation of the results.

The electric power consumption of an electric bus is retrieved by using a model presented in [119]. In particular, all aspects affecting the vehicles' dynamic are considered, such as the forces acting on the vehicle during departure and movement (which give rise to a waste of energy), and the energy recovery in the downward stroke and in the braking phases, which is peculiar of electric buses.

The following features influence the electricity consumed by an electric bus:

- the total mass of the bus that includes the curb mass and the loaded cargo;
- the gradient of the terrain, since proceeding uphill requires a higher energy amount than traveling on flat terrain or downhill;
- the characteristics of the electric drive, i.e., the efficiencies due to the energy conversion and power electronics;
- the travel speed that affects the rolling and aerodynamic resistance.

This section considers the first instance as a basic case study, and the results are analyzed in detail. Then, the results obtained for case studies of higher dimensions are briefly discussed to analyze the performance of the method from the computational viewpoint.

Moreover, some results regarding a sensitivity analysis performed varying the battery size, and the minimum service frequency will be presented.

6.2.1 The basic instance

The first instance is relevant to an instance with three (N=3) available sites and twelve lines (M=12). The data come from the public transportation company AMT which operates in the Genoa area.

The data relevant to this instance are reported in Table 6.1,Table 6.2, and Table 6.3.

Table 6.1 Data for the first instance

Symbol	**Quantity**	**Unit**
N	3	-
M	12	-
E^{CAP}	600	kWh
Ψ	1.2	-
P^{rated}	80	kWh
Π	500	-

Ω	5	€/h
A	0.8	-
$C_j^B \quad \forall j$	20000	€/y
$C_j^T \quad \forall j$	150	€/trip
$T_j^{oper} \quad \forall j$	7000	h/y

Table 6.2 Data relevant to sites $S_i, i = 1, \dots, 3$ (First Instance).

i	$N_i^{sock,max}$ **[#]**	$P_i^{sock,max}$ **[kW]**	$P_i^{tot,max}$ **[kW]**	K_i^1 **[€/year·#of sockets]**	K_i^2 **[€/year·kWh]**
1	10	100	1000	1000	10
2	10	100	1000	1000	9
3	10	100	1000	1100	11

Table 6.3 Data relevant to lines $L_j, j = 1, \dots, 12$ (First Instance).

j	X_j^{init}	X_j^{fin}	T_j^{trips} **[h]**	$F_j^{\min}$ **[h^{-1}]**
1	0.40	0.90	5	0.2
2	0.50	0.95	5	0.2
3	0.40	0.90	5	0.25
4	0.50	0.85	5	0.25
5	0.40	0.90	5	0.25
6	0.45	0.95	5	0.25
7	0.40	0.90	5	0.2
8	0.50	0.95	5	0.2
9	0.40	0.90	5	0.2
10	0.50	0.85	5	0.2
11	0.40	0.90	5	0.2
12	0.45	0.95	5	0.2

The optimization problem has been solved (finding an optimal solution) by use of Lingo [113] with an Intel Corei7-6500U, 3.5 GHz processor. It turns out that this instance of the Mixed-Integer Nonlinear Problem (MINLP) formalized in this chapter is characterized by 54 integer variables and 114 continuous variables, along with 123 constraints (of which 47 are nonlinear). The runtime needed to obtain an optimal result has been equal to 36 seconds. The results are reported in Table 6.4 and Table 6.5.

Table 6.4 Results for Sites $S_i, i = 1, \dots, 3$ (First Instance).

i	n_i^{sock} **[-]**	p_i^{tot} **[kW]**	p_i^{sock} **[kW]**

1	4	320	80
2	9	720	80
3	0	0	0

As it is provided in Table 6.4, the solution of the problem leads to the installation of 13 sockets between site 1 and 2. More specifically, 4 sockets are installed in station 1 and 9 in station 2. Station 3 is not activated at all.

Table 6.5 Results for lines $L_j, j = 1, \ldots, 12$ (First Instance).

j	t_j^{ch} **[h]**	n_j^B **[-]**	t_j^W **[h]**
1	4.04	2	0.96
2	4.33	2	0.67
3	4.04	3	2.96
4	2.68	2	0.32
5	4.04	3	2.96
6	4.70	3	2.30
7	4.04	2	0.96
8	4.33	2	0.67
9	4.04	2	0.96
10	2.68	2	2.32
11	4.04	2	0.96
12	4.70	2	0.30

From Table 5.5 it is possible to observe that at least 2 buses are necessary for each line.

An important performance index is the utilization factor u_i of station S_i that is defined as the fraction

$$u_i = \frac{\begin{array}{c} Overall\ working\ time\ of\ a\ socket \\ in\ S_i\ during\ a\ time\ interval\ H \end{array}}{H} \tag{6.26}$$

that is equivalent to

$$u_i = \frac{\sum_{j:S_i \in R_j} \delta_{i,j}\, f_j\, t_j^{ch}}{n_i^{sock}} \qquad i = 1, \ldots, N \tag{6.27}$$

This performance indicator (always lower than or equal to 1) allows to evaluate the criticality or the stress level of a station, as well as its possible poor utilization.

In this case study, the value assumed by u_i is 0.83 in site 1 and 0.78 in site 2, which can be considered satisfactory values.

6.2.2 Analysis of computational requirements

A further campaign has been carried out to evaluate the capability of the proposed approach to cope with instances having higher dimensions. However, it has not always been possible for large dimension instances to obtain an optimal solution in a reasonable computing time. Nevertheless, during the program's execution, the used solver provides current upper and lower bounds for the optimal cost. Thus, even when the time required to obtain an optimal solution is quite long, the run can be stopped whenever the gap between the upper and lower bounds is sufficiently low. In this case, the current best feasible solution found is retained as the problem's solution. This corresponds to a common practice in optimization applications and may also be justified by considering that instance data are affected by some imprecision that may be comparable with the inaccuracy due to the acceptance of a suboptimal solution. It must be reminded that this is a planning problem whose solution must be determined offline. Thus the allowable runtime can be adjusted in order to achieve a maximum level of suboptimality of the solution that is retained when the run is stopped.

Table 6.6 reports the computational performances obtained in connection with 9 instances of increasing dimension. The information provided for each instance includes the total number of constraints, the number of nonlinear constraints (NL constraints), the number of integer variables, and the time needed to reach an acceptable (relative) value of the Δ^{GAP} between the upper and lower bounds for the optimal costs.

The Δ^{GAP} is defined as

$$\Delta^{GAP} = \frac{J^{curr} - J^{LB}}{J^{LB}} \cdot 100 \tag{6.28}$$

where J^{curr} is the value of the objective function for the current best feasible solution found, and J^{LB} is the current lower bound determined by the software tool.

Table 6.6 Instances comparison

Inst.	**N**	**M**	**Constr.**	**NL Constr.**	**Int. Var.**	**Time [s]**	Δ^{GAP} **[%]**
1	3	12	123	47	54	0.1	2.13
2	3	13	131	50	58	2	2.15
3	3	14	139	53	62	3	2.40
4	3	15	147	56	66	3	2.37
5	4	12	130	50	68	8	2.30
6	4	13	138	53	73	16	2.21
7	4	14	146	56	78	36	0.62

8	4	15	154	59	83	36	2.10
9	5	16	169	65	106	84	2.22

It appears that, in general, the higher the dimension of the instance (that is, the values *N* and *M*), the longer the time necessary to find a satisfactory solution. Note that, for any of the considered case instances, the solver was able to attain a satisfactory solution within a short time interval. By the way, for the first three instances, an optimal solution was attained in less than 2 minutes.

Chapter 7
Conclusions and Future Developments

The progressive shift from traditional vehicles to EVs is considered as one of the key measures to achieve the objective of a significant reduction in the emission of pollutants, especially in urban areas. In this thesis, attention has been focused on applying control and optimization methods and approaches to energy systems in which EVs are integrated, with specific reference to planning and scheduling decision problems. An interdisciplinary approach is considered because the optimal management of EVs and charging stations (CSs) is a decision problem across different disciplines: transportation and logistics, scheduling, and smart grids. In smart grids, energy production and storage systems are usually scheduled by an EMS to minimize costs, power losses, and CO2 emissions while satisfying energy demands. When CSs are connected to a smart grid, EVs served by CSs represent an additional load to the power system to be satisfied and an additional storage system in the case V2G technology is enabled. However, the load generated by EVs is deferrable. In this case, it can be thought as a process in which there are machines (CSs) that serve customers/products (EVs) based on release time, due date, deadline, energy request, like it happens in manufacturing systems. In this thesis, two kinds of approaches have been used to deal with the optimal scheduling of EVs. Firstly, attention is focused on the formalization of a discrete-time optimization problem in which fossil fuel production plants, storage systems, and renewables are considered to satisfy the grid's electrical load. The discrete-time formalization can use forecasting for renewables and loads without data elaboration. On the other side, a huge number of decision variables are present, making the optimization problem hard to solve through commercial optimization tools. Secondly, the same decision problems have been faced through a discrete-event formalization.

Summing up the results obtained with the two approaches it is possible to compare them. In particular, Scenario I (Section 5.4.1) utilize the same data of the discrete time case study (Section 4.5). The two results have a difference in the overall cost but also in the computational time. In the discrete time model the overall cost is 340.12€ and the run time is 33 s. In the discrete event model, the cost is 355.05€ and the run time is less then 2 s. This huge difference necessarily linked to the number of variables in the two problems. In fact, the number of variables in the discrete time approach depends on the length the discretization interval, in the discrete event model, as highlighted, it depends on the number of EVs. The main drawback of this approach is certainly to be searched in the loss of precision for the solution. It cannot be stated a-priori that the solution will be worse in terms of cost (even if it happens in this instance), but it is straightforward to say that, by definition, considering the average values of the power flows over “longer” time intervals, the actual power profile will not be perfectly represented. Even in the case of the optimization approach described in Chapter 5, the continuous power profiles are obtained only by introducing some assumptions.

It must be denoted that the proposed approach has some limitations and could be improved. The main limit could be found in using a polynomial approximation which cannot always fit the forecasted power's real values, especially if the order is low, but increasing the order would lead to a high computational burden. Another limitation is the absence of the V2G operation mode, which, in this model, would lead to a too complex formulation with too many binary variables. Certainly, a further improvement to this approach could be the use of a combination of the two models (i.e., discrete events and discrete time models) in order to take advantage of their main feature, trying to reduce the number of variables with the discrete event model and then obtaining a detailed solution with the discrete time model. When dealing with EVs, it is necessary to consider other issues that influence the scheduling, i.e., the optimal location of charging stations, and the assignment of users to CSs. For this reason, Chapter 6 is relevant to a planning problem with charging stations placement and line assignment.

In particular, a novel optimization problem has been introduced to define the service infrastructure for charging a fleet of EBs in a public transportation system. The infrastructure (location of the charging stations, the number of sockets, and maximum power for each station and each socket) is determined jointly with the assignment of lines to charging stations and bus fleet sizing (for each line). The formalization of the problem is based on economic cost minimization while guaranteeing a certain quality of service (a minimum service frequency specified for each line). The objective function is defined assuming that the overall system operates periodically and is intended to provide the specifications for the framework's design over which a detailed operational scheduling procedure can then be developed. Another novelty of the paper is the detailed modeling of the nonlinear charging characteristic of the EB's battery. The proposed problem has been solved by applying a mathematical programming software tool. The results obtained refer to a series of case studies that correspond to a real instance, with some possible variations about it. These results show that in this way, it is possible to obtain, within a reasonable computing time, an optimal solution, or at least a suboptimal solution whose distance from the optimal one is strictly upper bounded. A possible future research direction is developing a multiobjective optimization approach, in which economic cost and quality of service are considered as different objective functions to be minimized. Finally, a further research direction is to analyze the possibility of developing a detailed scheduling procedure for the bus recharging process jointly with the service scheduling of the buses (i.e., the timetabling of the various trips during the day).

Of course, other topics should be mentioned that are worthy of investigation in the planning and management of EVs. In fact, they not only influence the management of power and energy systems but also the one of sustainable transportation and mobility systems. This is the reason why it is mandatory to couple different networks and integrate different disciplines such as traffic systems, autonomous vehicles, electrical systems, transportation networks and logistics. Some approaches have been studied during the Ph.D. activity some are currently under investigation.

Appendix

Optimization problems

An optimization problem is characterized by three main components: decision variables, objective function, and constraints. Decision variables are those entities that represent the decisions of a specific decision problem (for example power produced by some production plant, the number and the size of charging stations in a territory, the path of a vehicle, etc.). The objective function represents the target (or the key performance indicators) of the decision problem to be minimized or maximized (like for example costs, revenues, emissions, temperature and state of charge levels); it should be a function of the decision variables and it is generally an algebraic equation. Constraints represent restrictions such as the size of production plants, emission levels from regulation, etc. An optimization problem is generally expressed by:

$$\min_{x} f(x) \tag{XXIX}$$

s.t.

$$h(x) = 0 \tag{XXX}$$

$$g(x) \leq 0 \tag{XXXI}$$

where $x \in \mathbb{R}^n$ is the decision variable vector, $f(x): \mathbb{R}^n \to \mathbb{R}$ is the objective function to be minimized, $h(x): \mathbb{R}^n \to \mathbb{R}^{n_E}$ are the functions for the equality constraints and $g(x): \mathbb{R}^n \to \mathbb{R}^{n_I}$ for the inequality constraints.

It is important to note that:

- A feasible solution is any $x \in \mathbb{R}^n$ that respects constraints (XXX)-(XXXI).
- If a feasible solution minimizes (XXIX), it is an optimal solution, which then provides the objective function optimal value.
- Minimizing $f(x)$ is equivalent to maximizing $-f(x)$.

Example: Linear optimization problem

A LP problem is a mathematical programming problem in which functions f, $\underline{g}$ and $\underline{h}$ are all linear functions (or affine functions) of the vector $\underline{x}$ of the decision variables. An affine function is a linear function plus a constant. Any LP problem can be put in the *standard form*

$$\max \quad x_0 = \underline{c}^T \underline{x} \tag{XXXII}$$

s.t.

$$A\underline{x} = \underline{b} \tag{XXXIII}$$

$$\underline{x} \geq 0 \tag{XXXIV}$$

where

$\underline{x} \in R^n$
$\underline{c}^T \in R^n$
$\underline{b} \in R^m$
$\dim[A] = m \cdot n$

besides, it is supposed that m<n and that *rank [A] =m.*

Note that $\underline{c}^T$, $A, \underline{b}$ are the known parameters of the optimization problem.

Remark 1.1.

The justification for the above claim of the generality of the standard form is relatively easy. Any linear inequality constraint may be put into an equality form by introducing additional non-negative auxiliary variables. For example:

$$\begin{aligned} 3x_1 + 2x_2 \leq 5 \quad &\leftrightarrow \quad \begin{cases} 3x_1 + 2x_2 + x_3 = 5 \\ x_3 \geq 0 \end{cases} \\ 3x_1 + 5x_2 \geq 7 \quad &\leftrightarrow \quad \begin{cases} 3x_1 + 5x_2 - x_3 = 7 \\ x_3 \geq 0 \end{cases} \end{aligned} \tag{XXXV}$$

Besides, if a variable is unrestricted in sign, it can be represented via two variables restricted in sign

$$x_1 \leq\geq 0 \quad \leftrightarrow \quad \begin{cases} x_1 = x_1^+ - x_1^- \\ x_1^+ \geq 0 \\ x_1^- \geq 0 \end{cases} \tag{XXXVI}$$

Finally, it should be noted that any minimization problem can be put in the form of a maximization problem and vice-versa.

$$\min\,(3x_1 - 5x_2) \quad \leftrightarrow \quad \max\,(-3x_1 + 5x_2) \tag{XXXVII}$$

Regarding the standard form of an LP problem,

- A vector $\underline{x}$ satisfying the matrix equality $A\underline{x} = \underline{b}$ is said to be a solution;
- The solution $\underline{x}$ is said *feasible* if it also satisfies the non-negativity constraint $\underline{x} \geq 0$;
- A feasible solution $\underline{x}^*$ is *optimal* if no other feasible solution $\underline{x}'$ exists such that $\underline{c}^T \underline{x}' > \underline{c}^T \underline{x}^*$ (that is if no better feasible solution exists).

Modeling a dynamic system

A dynamic system is characterized by input ($\mathbf{u}(t)$) and output ($\mathbf{y}(t)$) vectors within an initial time t_0 and a final time t_f and related by equations $\mathbf{y} = \mathbf{g}(\mathbf{u})$ [120]. That is,

$$\begin{aligned} \mathbf{u}(t) &= \left[u_1(t),.....,u_p(t)\right]^T \quad t_0 \leq t \leq t_f \\ \mathbf{y}(t) &= \left[y_1(t),.....,y_m(t)\right]^T \quad t_0 \leq t \leq t_f \end{aligned} \tag{XXXVIII}$$

$$\mathbf{y} = \mathbf{g}(\mathbf{u}) = \left[g_1(u_1(t),....,u_p(t)),........,g_m(u_1(t),....,u_p(t))\right]^T \tag{XXXIX}$$

where $\mathbf{g}(\cdot)$ represents the vector of functions $g_1(\cdot),...,g_m(\cdot)$.

The state of a system at time t_0 is the information required at t_0. Generally, a vector denoted by ***x(t)***, and the components $x_1(t),.....,x_n(t)$ are called *state variables*. The set of equations required to specify the state ***x(t)*** for all $t \geq t_0$ given $x(t_0)$ and the function $\mathbf{u}(t)$, $t \geq t_0$, are called state equations. The following representation based on differential equations for the system state is used:

$$\dot{\mathbf{x}}(t) = \mathbf{f}(\mathbf{x}(t),\mathbf{u}(t),t) \tag{XL}$$

while for the state-space representation the form is

$$\begin{aligned} \dot{\mathbf{x}}(t) &= \mathbf{f}(\mathbf{x}(t),\mathbf{u}(t),t) \qquad x(t_0) = x_0 \\ \mathbf{y}(t) &= \mathbf{g}(\mathbf{x}(t),\mathbf{u}(t),t) \end{aligned} \tag{XLI}$$

A system is linear when it takes the following form:

$$\begin{aligned}\dot{x}(t) &= \mathbf{A}(t)x(t) + \mathbf{B}(t)u(t) \\ y(t) &= \mathbf{C}(t)x(t) + \mathbf{D}(t)u(t)\end{aligned} \tag{XLII}$$

where **A, B, C, D** represent model parameters.

The system can be also expressed by a discrete-time formalization. That is,

$$\begin{aligned}x(\mathrm{k}+1) &= \mathbf{A}(\mathrm{k})x(\mathrm{k}) + \mathbf{B}(\mathrm{k})u(\mathrm{k}) \\ y(\mathrm{k}) &= \mathbf{C}(\mathrm{k})x(\mathrm{k}) + \mathbf{D}(\mathrm{k})u(\mathrm{k})\end{aligned} \tag{XLIII}$$

where k represents the time counter.

It is important to note that in a discrete-time formalization, time intervals are equal in length and that control variables are assumed to be constant over the length of time. The state equations can be inserted as constraints in a general optimization problem in which the objective function depends on the state and control variables.

Finally, a system can also be represented by a discrete event approach. In this case, the state and control variables change when an event occurs. Figure 1 reports this particular case that should be modeled appropriately; this book details the application to EVs' scheduling.

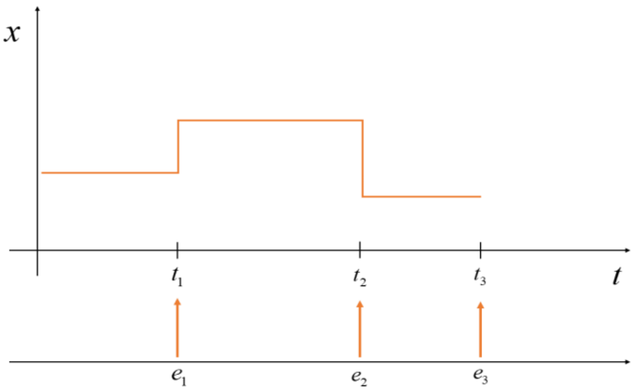

Fig. I Discrete event case

References

[1] B. Nykvist and M. Nilsson, “Rapidly falling costs of battery packs for electric vehicles,” *Nature Climate Change*, vol. 5, no. 4, 2015, doi: 10.1038/nclimate2564.

[2] Z. Chen, N. Guo, X. Li, J. Shen, R. Xiao, and S. Li, “Battery pack grouping and capacity improvement for electric vehicles based on a genetic algorithm,” *Energies*, vol. 10, no. 4, 2017, doi: 10.3390/en10040439.

[3] A. König, L. Nicoletti, D. Schröder, S. Wolff, A. Waclaw, and M. Lienkamp, “An Overview of Parameter and Cost for Battery Electric Vehicles,” *WEVJ*, vol. 12, no. 1, p. 21, Feb. 2021, doi: 10.3390/wevj12010021.

[4] A. Sakti, J. J. Michalek, E. R. H. Fuchs, and J. F. Whitacre, “A techno-economic analysis and optimization of Li-ion batteries for light-duty passenger vehicle electrification,” *Journal of Power Sources*, vol. 273, 2015, doi: 10.1016/j.jpowsour.2014.09.078.

[5] “Lithium-ion Battery Pack Prices Rise for First Time to an Average of $151/kWh,” *BloombergNEF*, Dec. 06, 2022. https://about.bnef.com/blog/lithium-ion-battery-pack-prices-rise-for-first-time-to-an-average-of-151-kwh/ (accessed Feb. 21, 2023).

[6] S. Manzetti and F. Mariasiu, “Electric vehicle battery technologies: From present state to future systems,” *Renewable and Sustainable Energy Reviews*, vol. 51. 2015. doi: 10.1016/j.rser.2015.07.010.

[7] C. Iclodean, B. Varga, N. Burnete, D. Cimerdean, and B. Jurchiş, “Comparison of Different Battery Types for Electric Vehicles,” in *IOP Conference Series: Materials Science and Engineering*, 2017. doi: 10.1088/1757-899X/252/1/012058.

[8] H. S. Das, M. M. Rahman, S. Li, and C. W. Tan, “Electric vehicles standards, charging infrastructure, and impact on grid integration: A technological review,” *Renewable and Sustainable Energy Reviews*, vol. 120, p. 109618, Mar. 2020, doi: 10.1016/j.rser.2019.109618.

[9] J. R. Woo, H. Choi, and J. Ahn, “Well-to-wheel analysis of greenhouse gas emissions for electric vehicles based on electricity generation mix: A global perspective,” *Transportation Research Part D: Transport and Environment*, vol. 51, pp. 340–350, 2017, doi: 10.1016/j.trd.2017.01.005.

[10] L. Raykin, M. J. Roorda, and H. L. MacLean, “Impacts of driving patterns on tank-to-wheel energy use of plug-in hybrid electric vehicles,” *Transportation Research Part D: Transport and Environment*, vol. 17, no. 3, pp. 243–250, 2012, doi: 10.1016/j.trd.2011.12.002.

[11] B. Zhou *et al.*, “Real-world performance of battery electric buses and their life-cycle benefits with respect to energy consumption and carbon dioxide emissions,” *Energy*, vol. 96, no. 2016, pp. 603–613, 2016, doi: 10.1016/j.energy.2015.12.041.

[12] W. Choi, E. Yoo, E. Seol, M. Kim, and H. H. Song, “Greenhouse gas emissions of conventional and alternative vehicles: Predictions based on energy policy analysis in South Korea,” *Applied Energy*, vol. 265, p. 114754, May 2020, doi: 10.1016/j.apenergy.2020.114754.

[13] S. Verma, G. Dwivedi, and P. Verma, “Life cycle assessment of electric vehicles in comparison to combustion engine vehicles: A review,” *Materials Today: Proceedings*, vol. 49, pp. 217–222, Jan. 2022, doi: 10.1016/j.matpr.2021.01.666.

[14] A. Wang, J. Xu, M. Zhang, Z. Zhai, G. Song, and M. Hatzopoulou, “Emissions and fuel consumption of a hybrid electric vehicle in real-world metropolitan traffic conditions,” *Applied Energy*, vol. 306, p. 118077, 2022, doi: https://doi.org/10.1016/j.apenergy.2021.118077.

[15] R. Challa, D. Kamath, and A. Anctil, “Well-to-wheel greenhouse gas emissions of electric versus combustion vehicles from 2018 to 2030 in the US,” *Journal of Environmental Management*, vol. 308, p. 114592, Apr. 2022, doi: 10.1016/j.jenvman.2022.114592.

[16] A. Temporelli, M. L. Carvalho, and P. Girardi, “Life Cycle Assessment of Electric Vehicle Batteries: An Overview of Recent Literature,” *Energies*, vol. 13, no. 11, Art. no. 11, Jan. 2020, doi: 10.3390/en13112864.

[17] F. Arshad *et al.*, “Life cycle assessment of lithium-ion batteries: a critical review,” *Resources, Conservation and Recycling*, vol. 180, p. 106164, 2022.
[18] M. B. Mansur, A. S. Guimarães, and M. Petraniková, “An overview on the recovery of cobalt from end-of-life lithium ion batteries,” *Mineral Processing and Extractive Metallurgy Review*, vol. 43, no. 4, pp. 489–509, 2022.
[19] L. Zhu and M. Chen, “Development of a Two-Stage Pyrolysis Process for the End-Of-Life Nickel Cobalt Manganese Lithium Battery Recycling from Electric Vehicles,” *Sustainability*, vol. 12, no. 21, Art. no. 21, Jan. 2020, doi: 10.3390/su12219164.
[20] G. Harper *et al.*, “Recycling lithium-ion batteries from electric vehicles,” *Nature*, vol. 575, no. 7781, Art. no. 7781, Nov. 2019, doi: 10.1038/s41586-019-1682-5.
[21] J. Neumann *et al.*, “Recycling of Lithium-Ion Batteries—Current State of the Art, Circular Economy, and Next Generation Recycling,” *Advanced Energy Materials*, vol. 12, no. 17, p. 2102917, 2022, doi: 10.1002/aenm.202102917.
[22] H. Bae and Y. Kim, “Technologies of lithium recycling from waste lithium ion batteries: a review,” *Mater. Adv.*, vol. 2, no. 10, pp. 3234–3250, 2021, doi: 10.1039/D1MA00216C.
[23] IEC, “IEC 61851-1 ed2.0: Electric vehicle conductive charging system - Part 1: General requirements,” 2010. http://webstore.iec.ch/webstore/webstore.nsf/Artnum_PK/44636
[24] IEC, “IEC 62196-2 ed1.0: Plugs, socket-outlets, vehicle connectors and vehicle inlets - Conductive charging of electric vehicles,” 2011. http://webstore.iec.ch/webstore/webstore.nsf/Artnum_PK/45683
[25] N. S. Pearre and H. Ribberink, “Review of research on V2X technologies, strategies, and operations,” *Renewable and Sustainable Energy Reviews*, vol. 105, pp. 61–70, 2019.
[26] W. Kempton and J. Tomić, “Vehicle-to-grid power implementation: From stabilizing the grid to supporting large-scale renewable energy,” *Journal of Power Sources*, vol. 144, no. 1, pp. 280–294, 2005, doi: 10.1016/j.jpowsour.2004.12.022.
[27] F. Mwasilu, J. J. Justo, E. K. Kim, T. D. Do, and J. W. Jung, “Electric vehicles and smart grid interaction: A review on vehicle to grid and renewable energy sources integration,” *Renewable and Sustainable Energy Reviews*, vol. 34, pp. 501–516, 2014, doi: 10.1016/j.rser.2014.03.031.
[28] R. Jovanovic and I. S. Bayram, “Scheduling Electric Vehicle Charging at Park-and-Ride Facilities to Flatten Duck Curves,” in *2019 IEEE Vehicle Power and Propulsion Conference (VPPC)*, Hanoi, Vietnam: IEEE, Oct. 2019, pp. 1–5. doi: 10.1109/VPPC46532.2019.8952394.
[29] X. Wu, L. Li, J. Zou, and G. Zhang, “EV-based voltage regulation in line distribution grid,” in *2016 IEEE International Instrumentation and Measurement Technology Conference Proceedings*, May 2016, pp. 1–6. doi: 10.1109/I2MTC.2016.7520568.
[30] X. Wang, Z. Y. He, and J. W. Yang, “Unified strategy for electric vehicles participate in voltage and frequency regulation with active power in city grid,” *IET Generation, Transmission & Distribution*, vol. 13, no. 15, pp. 3281–3291, 2019.
[31] M. M. Islam, X. Zhong, Z. Sun, H. Xiong, and W. Hu, “Real-time frequency regulation using aggregated electric vehicles in smart grid,” *Computers and Industrial Engineering*, vol. 134, no. January 2018, pp. 11–26, 2019, doi: 10.1016/j.cie.2019.05.025.
[32] I. Pavić, T. Capuder, and I. Kuzle, “Value of flexible electric vehicles in providing spinning reserve services,” *Applied Energy*, vol. 157, pp. 60–74, 2015.
[33] A. Dik, S. Omer, and R. Boukhanouf, “Electric Vehicles: V2G for Rapid, Safe, and Green EV Penetration,” *Energies*, vol. 15, no. 3, p. 803, 2022.
[34] G. Trotta, “An empirical analysis of domestic electricity load profiles: Who consumes how much and when?,” *Applied Energy*, vol. 275, p. 115399, Oct. 2020, doi: 10.1016/j.apenergy.2020.115399.
[35] J. D. Rhodes, W. J. Cole, C. R. Upshaw, T. F. Edgar, and M. E. Webber, “Clustering analysis of residential electricity demand profiles,” *Applied Energy*, vol. 135, pp. 461–471, Dec. 2014, doi: 10.1016/j.apenergy.2014.08.111.

[36] J. Hildermeier, J. Burger, A. Jahn, and J. Rosenow, "A Review of Tariffs and Services for Smart Charging of Electric Vehicles in Europe," *Energies*, vol. 16, no. 1, Art. no. 1, Jan. 2023, doi: 10.3390/en16010088.

[37] S. Deilami, A. S. Masoum, P. S. Moses, and M. A. S. Masoum, "Real-time coordination of plug-in electric vehicle charging in smart grids to minimize power losses and improve voltage profile," *IEEE Transactions on Smart Grid*, vol. 2, no. 3, 2011, doi: 10.1109/TSG.2011.2159816.

[38] H. Kikusato *et al.*, "Electric Vehicle Charge-Discharge Management for Utilization of Photovoltaic by Coordination between Home and Grid Energy Management Systems," *IEEE Transactions on Smart Grid*, vol. 10, no. 3, pp. 3186–3197, 2019, doi: 10.1109/TSG.2018.2820026.

[39] S. M. B. Sadati, J. Moshtagh, M. Shafie-khah, and J. P. S. Catalão, "Smart distribution system operational scheduling considering electric vehicle parking lot and demand response programs," *Electric Power Systems Research*, vol. 160, pp. 404–418, Jul. 2018, doi: 10.1016/j.epsr.2018.02.019.

[40] H. Khalkhali and S. H. Hosseinian, "Multi-class EV charging and performance-based regulation service in a residential smart parking lot," *Sustainable Energy, Grids and Networks*, vol. 22, p. 100354, 2020, doi: 10.1016/j.segan.2020.100354.

[41] P. Aliasghari, B. Mohammadi-Ivatloo, M. Alipour, M. Abapour, and K. Zare, "Optimal scheduling of plug-in electric vehicles and renewable micro-grid in energy and reserve markets considering demand response program," *Journal of Cleaner Production*, vol. 186, pp. 293–303, 2018, doi: 10.1016/j.jclepro.2018.03.058.

[42] N. Hashemipour, P. C. del Granado, and J. Aghaei, "Dynamic allocation of peer-to-peer clusters in virtual local electricity markets: A marketplace for EV flexibility," *Energy*, vol. 236, p. 121428, 2021.

[43] T. D. Hutty, A. Pena-Bello, S. Dong, D. Parra, R. Rothman, and S. Brown, "Peer-to-peer electricity trading as an enabler of increased PV and EV ownership," *Energy Conversion and Management*, vol. 245, p. 114634, 2021.

[44] H. Fontenot and B. Dong, "Modeling and control of building-integrated microgrids for optimal energy management – A review," *Applied Energy*, vol. 254, no. July, p. 113689, 2019, doi: 10.1016/j.apenergy.2019.113689.

[45] P. Cappers, C. Goldman, and D. Kathan, "Demand response in US electricity markets: Empirical evidence," *Energy*, vol. 35, no. 4, pp. 1526–1535, 2010.

[46] M. H. Albadi and E. F. El-Saadany, "Demand response in electricity markets: An overview," in *2007 IEEE power engineering society general meeting*, IEEE, 2007, pp. 1–5.

[47] A. Y. Saber and G. K. Venayagamoorthy, "Optimization of vehicle-to-grid scheduling in constrained parking lots," in *2009 IEEE Power & Energy Society General Meeting*, IEEE, 2009, pp. 1–8.

[48] P. N. Ovalle, J. Vuelvas, A. Fajardo, C. A. Correa-Flórez, and F. Ruiz, "Optimal portfolio selection methodology for a demand response aggregator," *Energies*, vol. 14, no. 23, p. 7923, 2021.

[49] H. Hou, Y. Wang, C. Xie, B. Xiong, Q. Zhang, and L. Huang, "A dispatching strategy for electric vehicle aggregator combined price and incentive demand response," *IET Energy Systems Integration*, vol. 3, no. 4, pp. 508–519, 2021.

[50] S. Sharma and P. Jain, "Risk-averse integrated demand response and dynamic G2V charge scheduling of an electric vehicle aggregator to support grid stability," *International Transactions on Electrical Energy Systems*, vol. 31, no. 5, p. e12867, 2021.

[51] J. E. Contreras-Ocaña, M. R. Sarker, and M. A. Ortega-Vazquez, "Decentralized coordination of a building manager and an electric vehicle aggregator," *IEEE Transactions on Smart Grid*, vol. 9, no. 4, pp. 2625–2637, 2016.

[52] J. Huang, Z. Yang, X. Zeng, H. Zou, Y. Tang, and L. Zhang, "Demand Response of Electric Vehicles for Building Integrated Energy System," in *2018 2nd IEEE Conference on Energy Internet and Energy System Integration (EI2)*, IEEE, 2018, pp. 1–5.

[53] L. Miao, "On controlling prioritized discrete event systems with real-time constraints," *Discrete Event Dynamic Systems*, vol. 28, no. 3, pp. 427–447, 2018.

[54] T. A. Costa, P. N. Pena, and R. H. Takahashi, “Sco-concat: a solution to a planning problem in flexible manufacturing systems using supervisory control theory and optimization techniques,” *Journal of Control, Automation and Electrical Systems*, vol. 29, pp. 500–511, 2018.

[55] Q.-S. Jia, J. Wu, Z. Wu, and X. Guan, “Event-based HVAC control—A complexity-based approach,” *IEEE Transactions on Automation Science and Engineering*, vol. 15, no. 4, pp. 1909–1919, 2018.

[56] G. Ferro, F. Laureri, R. Minciardi, and M. Robba, “An optimization model for electrical vehicles scheduling in a smart grid,” *Sustainable Energy, Grids and Networks*, vol. 14, pp. 62–70, 2018, doi: 10.1016/j.segan.2018.04.002.

[57] G. Ferro, R. Minciardi, L. Parodi, and M. Robba, “Discrete event optimization of a vehicle charging station with multiple sockets,” *Discrete Event Dynamic Systems: Theory and Applications*, 2020, doi: 10.1007/s10626-020-00330-0.

[58] G. Ferro, F. Laureri, R. Minciardi, and M. Robba, “A predictive discrete event approach for the optimal charging of electric vehicles in microgrids,” *Control Engineering Practice*, vol. 86, pp. 11–23, May 2019, doi: 10.1016/j.conengprac.2019.02.004.

[59] M. L. Pinedo, *Scheduling*, vol. 29. Springer, 2012.

[60] S. French, “Sequencing and scheduling,” *An Introduction to the Mathematics of the Job-shop*, 1982.

[61] P. Brucker, “Scheduling algorithms,” *Journal-Operational Research Society*, vol. 50, pp. 774–774, 1999.

[62] H. Yang *et al.*, “Operational Planning of Electric Vehicles for Balancing Wind Power and Load Fluctuations in a Microgrid,” *IEEE Transactions on Sustainable Energy*, vol. 8, no. 2, pp. 592–604, Apr. 2017, doi: 10.1109/TSTE.2016.2613941.

[63] F. Kong, Q. Xiang, L. Kong, and X. Liu, “On-line event-driven scheduling for electric vehicle charging via park-and-charge,” in *2016 IEEE Real-Time Systems Symposium (RTSS)*, IEEE, 2016, pp. 69–78.

[64] A. Di Giorgio, F. Liberati, and S. Canale, “IEC 61851 compliant electric vehicle charging control in smartgrids,” in *21st Mediterranean Conference on Control and Automation*, IEEE, 2013, pp. 1329–1335.

[65] A. R. Sparacino, G. F. Reed, R. J. Kerestes, B. M. Grainger, and Z. T. Smith, “Survey of battery energy storage systems and modeling techniques,” in *2012 IEEE Power and Energy Society General Meeting*, IEEE, 2012, pp. 1–8.

[66] A. Seaman, T.-S. Dao, and J. McPhee, “A survey of mathematics-based equivalent-circuit and electrochemical battery models for hybrid and electric vehicle simulation,” *Journal of Power Sources*, vol. 256, pp. 410–423, 2014.

[67] A. Fotouhi, D. J. Auger, K. Propp, S. Longo, and M. Wild, “A review on electric vehicle battery modelling: From Lithium-ion toward Lithium–Sulphur,” *Renewable and Sustainable Energy Reviews*, vol. 56, pp. 1008–1021, 2016.

[68] M. Jongerden and B. Haverkort, “‘Battery modeling,’ Centre for Telematics & Information Technology University of Twente,” TR-CTI, 2008.

[69] A. Shafiei, A. Momeni, and S. S. Williamson, “Battery modeling approaches and management techniques for plug-in hybrid electric vehicles,” in *2011 IEEE vehicle power and propulsion conference*, IEEE, 2011, pp. 1–5.

[70] P. Notten, H. Bergveld, and W. Kruijt, “Battery management systems: design by modeling.” Kluwer Academic Publisher Norwell, 2002.

[71] Y. Wang *et al.*, “A comprehensive review of battery modeling and state estimation approaches for advanced battery management systems,” *Renewable and Sustainable Energy Reviews*, vol. 131, p. 110015, 2020.

[72] M. Zhang and X. Fan, “Review on the state of charge estimation methods for electric vehicle battery,” *World Electric Vehicle Journal*, vol. 11, no. 1, p. 23, 2020.

[73] S. B. Sarmah *et al.*, “A review of state of health estimation of energy storage systems: Challenges and possible solutions for futuristic applications of li-ion battery packs in electric vehicles,” *Journal of Electrochemical Energy Conversion and Storage*, vol. 16, no. 4, p. 040801, 2019.

[74] J. Lin, X. Liu, S. Li, C. Zhang, and S. Yang, "A review on recent progress, challenges and perspective of battery thermal management system," *International Journal of Heat and Mass Transfer*, vol. 167, p. 120834, 2021.

[75] R. Deng, Y. Liu, W. Chen, and H. Liang, "A Survey on Electric Buses - Energy Storage, Power Management, and Charging Scheduling," *IEEE Transactions on Intelligent Transportation Systems*, vol. 22, no. 1, pp. 9–22, 2021, doi: 10.1109/TITS.2019.2956807.

[76] S. Lekshmi and L. P. PS, "Mathematical modeling of Electric vehicles-A survey," *Control Engineering Practice*, vol. 92, p. 104138, 2019.

[77] Z. He, Q. Shi, Y. Wei, J. Zheng, B. Gao, and L. He, "A torque demand model predictive control approach for driving energy optimization of battery electric vehicle," *IEEE Transactions on Vehicular Technology*, vol. 70, no. 4, pp. 3232–3242, 2021.

[78] N. A. El-Taweel, A. Zidan, and H. E. Farag, "Novel electric bus energy consumption model based on probabilistic synthetic speed profile integrated with HVAC," *IEEE Transactions on Intelligent Transportation Systems*, vol. 22, no. 3, pp. 1517–1531, 2020.

[79] H. Basma, C. Mansour, M. Haddad, M. Nemer, and P. Stabat, "Comprehensive energy modeling methodology for battery electric buses," *Energy*, vol. 207, p. 118241, 2020, doi: 10.1016/j.energy.2020.118241.

[80] G. Ferro, M. Paolucci, and M. Robba, "Optimal charging and routing of electric vehicles with power constraints and time-of-use energy prices," *IEEE Transactions on Vehicular Technology*, vol. 69, no. 12, pp. 14436–14447, 2020.

[81] R. Pagany, L. Ramirez Camargo, and W. Dorner, "A review of spatial localization methodologies for the electric vehicle charging infrastructure," *International Journal of Sustainable Transportation*, vol. 13, no. 6, pp. 433–449, 2019.

[82] G. Ferro, R. Minciardi, and M. Robba, "A user equilibrium model for electric vehicles: Joint traffic and energy demand assignment," *Energy*, vol. 198, p. 117299, 2020, doi: 10.1016/j.energy.2020.117299.

[83] M. Hosseini and S. MirHassani, "Selecting optimal location for electric recharging stations with queue," *KSCE Journal of Civil Engineering*, vol. 19, no. 7, p. 2271, 2015.

[84] Y. Xiang, J. Liu, R. Li, F. Li, C. Gu, and S. Tang, "Economic planning of electric vehicle charging stations considering traffic constraints and load profile templates," *Applied Energy*, vol. 178, pp. 647–659, 2016.

[85] G. Ferro, R. Minciardi, L. Parodi, and M. Robba, "Optimal Planning of Charging Stations in Coupled Transportation and Power Networks Based on User Equilibrium Conditions," *IEEE Transactions on Automation Science and Engineering*, vol. 19, no. 1, pp. 48–59, 2021.

[86] C. Wang, F. He, X. Lin, Z.-J. M. Shen, and M. Li, "Designing locations and capacities for charging stations to support intercity travel of electric vehicles: An expanded network approach," *Transportation Research Part C: Emerging Technologies*, vol. 102, pp. 210–232, 2019.

[87] S. Wang, Z. Y. Dong, F. Luo, K. Meng, and Y. Zhang, "Stochastic collaborative planning of electric vehicle charging stations and power distribution system," *IEEE Transactions on Industrial Informatics*, vol. 14, no. 1, pp. 321–331, 2017.

[88] Z. Zhou, H. Sun, and Q. Guo, "Stochastic User Equilibrium in Charging Station Selection Based on Discrete Choice Model," in *IEEE Power and Energy Society General Meeting*, IEEE Computer Society, Dec. 2018. doi: 10.1109/PESGM.2018.8586008.

[89] B. Zhou *et al.*, "Smart home energy management systems: Concept, configurations, and scheduling strategies," *Renewable and Sustainable Energy Reviews*, vol. 61, pp. 30–40, 2016.

[90] S. Sen and V. Kumar, "Microgrid control: A comprehensive survey," *Annual Reviews in control*, vol. 45, pp. 118–151, 2018.

[91] A. Q. Badar and A. Anvari-Moghaddam, "Smart home energy management system–a review," *Advances in Building Energy Research*, vol. 16, no. 1, pp. 118–143, 2022.

[92] F. Delfino, G. Ferro, R. Minciardi, M. Robba, M. M. Rossi, and M. M. Rossi, “Identification and optimal control of an electrical storage system for microgrids with renewables,” *Sustainable Energy, Grids and Networks*, vol. 17, p. 100183, 2019, doi: 10.1016/j.segan.2018.100183.

[93] S. M. Hosseini, R. Carli, and M. Dotoli, “Robust Optimal Energy Management of a Residential Microgrid Under Uncertainties on Demand and Renewable Power Generation,” *IEEE Transactions on Automation Science and Engineering*, vol. 18, no. 2, pp. 618–637, 2021, doi: 10.1109/TASE.2020.2986269.

[94] P. Firouzmakan, R.-A. Hooshmand, M. Bornapour, and A. Khodabakhshian, “A comprehensive stochastic energy management system of micro-CHP units, renewable energy sources and storage systems in microgrids considering demand response programs,” *Renewable and sustainable energy reviews*, vol. 108, pp. 355–368, 2019.

[95] F. Delfino, G. Ferro, M. Robba, and M. Rossi, “An Energy Management Platform for the Optimal Control of Active and Reactive Powers in Sustainable Microgrids,” *IEEE Transactions on Industry Applications*, vol. 55, no. 6, pp. 7146–7156, Nov. 2019, doi: 10.1109/TIA.2019.2913532.

[96] W. Su, J. Wang, and J. Roh, “Stochastic energy scheduling in microgrids with intermittent renewable energy resources,” *IEEE Transactions on Smart grid*, vol. 5, no. 4, pp. 1876–1883, 2013.

[97] R. Carli and M. Dotoli, “A decentralized control strategy for optimal charging of electric vehicle fleets with congestion management,” in *2017 IEEE International Conference on Service Operations and Logistics, and Informatics (SOLI)*, 2017, pp. 63–67. doi: 10.1109/SOLI.2017.8120971.

[98] S. M. Hosseini, R. Carli, A. Parisio, and M. Dotoli, “Robust Decentralized Charge Control of Electric Vehicles under Uncertainty on Inelastic Demand and Energy Pricing,” in *2020 IEEE International Conference on Systems, Man, and Cybernetics (SMC)*, 2020, pp. 1834–1839. doi: 10.1109/SMC42975.2020.9283440.

[99] P. You, Z. Yang, M.-Y. Chow, and Y. Sun, “Optimal cooperative charging strategy for a smart charging station of electric vehicles,” *IEEE Transactions on Power Systems*, vol. 31, no. 4, pp. 2946–2956, 2015.

[100] P. Scarabaggio, R. Carli, A. Parisio, and M. Dotoli, “On Controlling Battery Degradation in Vehicle-to-Grid Energy Markets,” in *2022 IEEE 18th International Conference on Automation Science and Engineering (CASE)*, 2022, pp. 1206–1211. doi: 10.1109/CASE49997.2022.9926729.

[101] M. A. Ortega-Vazquez, “Optimal scheduling of electric vehicle charging and vehicle-to-grid services at household level including battery degradation and price uncertainty,” *IET Generation, Transmission & Distribution*, vol. 8, no. 6, pp. 1007–1016, 2014.

[102] A. Parisio, E. Rikos, and L. Glielmo, “A model predictive control approach to microgrid operation optimization,” *IEEE Transactions on Control Systems Technology*, vol. 22, no. 5, pp. 1813–1827, 2014.

[103] R. Minciardi and M. Robba, “A Bilevel Approach for the Stochastic Optimal Operation of Interconnected Microgrids,” *IEEE Transactions on Automation Science and Engineering*, 2017, doi: 10.1109/TASE.2016.2620150.

[104] S. Bracco, F. Delfino, F. Pampararo, M. Robba, and M. Rossi, “A dynamic optimization-based architecture for polygeneration microgrids with tri-generation, renewables, storage systems and electrical vehicles,” *Energy Conversion and Management*, vol. 96, pp. 511–520, May 2015, doi: 10.1016/j.enconman.2015.03.013.

[105] M. F. Zia, E. Elbouchikhi, and M. Benbouzid, “Microgrids energy management systems: A critical review on methods, solutions, and prospects,” *Applied Energy*, vol. 222, no. May, pp. 1033–1055, 2018, doi: 10.1016/j.apenergy.2018.04.103.

[106] Y. Zhang, N. Gatsis, and G. B. Giannakis, “Robust energy management for microgrids with high-penetration renewables,” *IEEE transactions on sustainable energy*, vol. 4, no. 4, pp. 944–953, 2013.

[107] F. Delfino, G. Ferro, R. Minciardi, M. Robba, M. Rossi, and M. Rossi, “Identification and optimal control of an electrical storage system for microgrids with renewables,” *Sustainable Energy, Grids and Networks*, 2019, doi: 10.1016/j.segan.2018.100183.

[108] L. Zhao, P. Awater, A. Schaefer, C. Breuer, and A. Moser, “Scenario-based evaluation on the impacts of electric vehicle on the municipal energy supply systems,” in *2011 IEEE Power and Energy Society General Meeting*, IEEE, 2011, pp. 1–8.

[109] S. Deilami, A. S. Masoum, P. S. Moses, and M. A. Masoum, “Real-time coordination of plug-in electric vehicle charging in smart grids to minimize power losses and improve voltage profile,” *IEEE Transactions on smart grid*, vol. 2, no. 3, pp. 456–467, 2011.

[110] S. Allard, P. C. See, M. Molinas, O. B. Fosso, and J. A. Foosnæs, “Electric vehicles charging in a smart microgrid supplied with wind energy,” in *2013 IEEE Grenoble Conference*, IEEE, 2013, pp. 1–5.

[111] S. Khemakhem, M. Rekik, and L. Krichen, “A flexible control strategy of plug-in electric vehicles operating in seven modes for smoothing load power curves in smart grid,” *Energy*, vol. 118, pp. 197–208, 2017.

[112] Z. Song, “The evaluation of parameter m in the big m method of linear programming,” in *International Conference on Materials Engineering and Information Technology Applications (MEITA 2015)*, Atlantis Press, 2015, pp. 37–40.

[113] “LINGO™.” 2022. [Online]. Available: https://www.lindo.com/index.php/products/lingo-and-optimization-modeling

[114] G. Ferro, R. Minciardi, L. Parodi, and M. Robba, “Optimal Location and Line Assignment for Electric Bus Charging Stations,” *IEEE Systems Journal*, pp. 1–12, 2023, doi: 10.1109/JSYST.2023.3240364.

[115] F. Delfino, G. Ferro, R. Minciardi, M. Robba, M. Rossi, and M. Rossi, “Identification and optimal control of an electrical storage system for microgrids with renewables,” *Sustainable Energy, Grids and Networks*, vol. 17, Mar. 2019, doi: 10.1016/j.segan.2018.100183.

[116] E. Balas and M. W. Padberg, “Set Partitioning: A survey,” *SIAM Review*, vol. 18, no. 4, 1976, doi: 10.1137/1018115.

[117] P. Y. Yin and J. Y. Wang, “Ant colony optimization for the nonlinear resource allocation problem,” *Applied Mathematics and Computation*, vol. 174, no. 2, pp. 1438–1453, 2006, doi: 10.1016/j.amc.2005.05.042.

[118] P. Y. Yin and J. Y. Wang, “A particle swarm optimization approach to the nonlinear resource allocation problem,” *Applied Mathematics and Computation*, vol. 183, no. 1, pp. 232–242, 2006, doi: 10.1016/j.amc.2006.05.051.

[119] G. Ferro, M. Paolucci, and M. Robba, “Optimal charging and routing of electric vehicles with power constraints and time-of-use energy prices,” *IEEE Transactions on Vehicular Technology*, vol. 69, no. 12, pp. 14436–14447, 2020.

[120] C. G. Cassandras and S. Lafortune, *Introduction to discrete event systems*. 2008. doi: 10.1007/978-0-387-68612-7.